Benders Decomposition-based Global Optimization for Natural Gas and Power Flow Systems

by

Dan Li

A thesis submitted to the
Department of Chemical Engineering
in conformity with the requirements for
the degree of Master of Applied Science

Queen's University
Kingston, Ontario, Canada
April 2016

Abstract

Mixed-integer nonlinear programming (MINLP) framework has been attracting more and more attention since late last century. It can be applied to address various process systems engineering problems, such as process design and operation, large-scale system scheduling, and supply chain management [19, 42]. As a class of the many such problems, integrated design and operation of large-scale energy system is to determine both the network design decisions and the flows in operation to achieve the best expected profit, while meeting the customer demands and product specifications. It is well known that these integrated design and operation problems are nonconvex MINLPs, and therefore inherently difficult for which classical gradient-based optimization methods cannot guarantee an optimal solution. Decomposition-based methods have been used to achieve global optimal solutions for nonconvex MINLPs. One of the popular decomposition-based optimization methods is Benders decomposition. Its extensions, generalized Benders decomposition (GBD) [16] and nonconvex generalized Benders decomposition (NGBD) [27], can guarantee the convergence to a global optimum with mild assumptions.

In this thesis, our primary goal is to incorporate domain reduction into Benders decomposition-based global optimization methods for a class of large-scale energy systems that are MINLP problems with separable structure, which not only ensures a

global optimum but also converges faster than the standard Benders decomposition-based methods and commercial global optimization solvers. The research objective is twofold. One is how to reduce the search domain and feasible region with a minimum amount of computation; to achieve this, the domain reduction methods based on convex nonlinear programming (NLP) relaxations [37] are extended to Benders decomposition-based methods. The other is customization of decomposition-based methods for large-scale energy systems; to demonstrate this, an integrated design and operation of natural gas production network problem that addresses gas flows, pressures and uncertainties is proposed with multi-loop NGBD, a customized Benders decomposition-based method that is faster than the regular method by at least an order of magnitude.

Co-Authorship

The research presented in this thesis is conducted by the author under the supervision of Dr. Xiang Li of the Department of Chemical Engineering, Queen's University.

Both Chapter 2 and 3 have been reorganized and submitted to international journals with co-author Dr. Xiang Li. Materials in Chapter 2 is submitted to Journal of Computers and Chemical Engineering, and materials in Chapter 3 is submitted to Journal of American Institute of Chemical Engineers (AIChE).

Acknowledgments

It brings me great pleasure for an opportunity to work on decomposition-based global optimization, which is the main facet of my research in Queen's University, Canada. For this I deeply indebted to my adviser Dr. Xiang Li for his invaluable enlightenment and outstanding guidance, without him I may never have chance to finish this interesting work. I still remembered the exciting moments we had in summer workshops, where I was motivated by massive inspirations on nonconvex optimization. Thanks to Dr. Xiang Li, I had enjoyable working experiences in Queen's University.

Also, I would like to thank all the professors, staffs and students in Queen's University for their support and encouragement, especially my officemates Ehsan, Hussian, Isaac, Judith, Samuel, Sebastien and Walter (alphabetical order) for making G37 a lively place.

Special thanks to my family, 感谢我的老爸老妈及其他长辈,感谢他们对我一切生活上的支持, 无条件的付出及努力的肯定, 永远爱你们.

Contents

List of Tables

List of Figures

Chapter 1

Introduction

Design and operation of energy systems have been attracting attention in decades. Generally, the models used for design and operation is to optimize certain function f by choosing system decisions x. These decisions, either continuous or discrete, satisfy given mathematical models that are represented by a constraint set X. For design and operation of energy systems, we focus on decisions that are finite dimensional vectors and thus their constraint set is a subset of finite dimensional Euclidean space.

There are two considerations in finding optimal design and operation of energy systems. First, the characters of energy systems must be properly justified via their models. This requires that the set X includes necessary constraints that capture non-trivial system features. For design and operation of energy systems, flow network structure, material balance, energy balance, product quality and demand are considered. Secondly, the resulting problems must be properly formulated, in order to be efficiently solved by optimization methods. The models of energy systems, represented by both linear and nonlinear constraints with continuous or/and discrete decisions, usually lead to nonconvex nonlinear programming (NLP) or mixed-integer nonlinear programming (MINLP) problems, for which local optimization methods

can fail to find and verify global optimal solutions. Also, these models often have large sizes that result from complex energy systems or/and explicit consideration of uncertainties, which further challenge the existing global optimization methods. It is known that the efficiency of classical branch-and-bound-based global optimization methods are affected by the size of problems. If the size of a large-scale nonxonvex problem increases, in the worst case the solution time increases exponentially.

A natural idea to deal with the design and operation of large-scale nonconvex energy systems is to break these nonconvex NLP/MINLP problems into smaller subproblems, which are convex or nonconvex but can be solved efficiently with branch-and-bound-based global optimization. There are two types of decomposition strategies for solving these large-scale nonconvex problems. One is Lagrangian decomposition-based global optimization [12], [9], [6], [24], which is incorporated in a branch-and-bound framework where only a subspace of the problem is partitioned. The other is Benders decomposition-based global optimization [3], [16], [27], which does not require an explicit branch-and-bound procedure but requires certain problem structures. In Benders decomposition-based global optimization, one or multiple nonconvex subproblems need to be solved at each iteration, so the efficiency of optimization relies on how fast each nonconvex subproblems can be solved and how fast the convergence to a global solution can be reached.

It is seen that domain reduction techniques can benefit branch-and-bound-based global optimization, because they can reduce the search domain, which result in tighter convex relaxations and reduced number of nodes that are to be explored in the branch-and-bound search. [42] developed a theoretical global optimization framework based on Lagrangian duality and branch-and-bound search, and it can be customized

to yield a variety of domain reduction techniques in the literature. These domain reduction techniques can be classified into two types. One type extensively utilizes the primal and dual solutions of convex relaxation subproblems to reduce the variable ranges, and it does not require solving extra domain reduction subproblems (unless some sort of probing procedure is needed) [43] [37]. The other type requires solving extra convex optimization subproblems to reduce the variable ranges [30] [44] [7]. In order to distinguish the two types of techniques, we call the former *range reduction calculation* and the latter *bound contraction operation*. While bound contraction operation can usually reduce variable ranges more effectively, it requires much more computing time and therefore cannot be performed so frequent as range reduction calculation do.

In the light of successful integration of domain reduction in branch-and-bound-based global optimization, we are motivated to incorporate domain reduction for Benders decomposition-based global optimization methods, and apply resulting methods to the optimal design and operation of large-scale energy systems.

This thesis considers design and operation of large-scale energy systems as a general class of nonconvex NLP or MINLP problems. These NLP/MINLP problems are required to have separable structures in form of (P0), in order for any decomposition-based algorithms to be practically adopted:

$$\begin{aligned} \min_{x,y_0} \ & f_1(x) + f_2(y_0) \\ \text{s.t.} \ & g_1(x) + g_2(y_0) \leq 0, \\ & x \in X, \ \ y_0 \in Y. \end{aligned} \tag{P0}$$

Here we aim to minimize sum of scalar-valued cost functions f_1 and f_2 with respect to variables x and y_0; g_1 and g_2 are vector-valued functions; and sets X and Y restrict variables x and y_0, respectively. We call variables y_0 complicating variables, given that (P0) can be separated into a number of relatively easy subproblems if these variables are fixed.

For convenience of subsequent discussion, we make the following mild assumption for sets X and Y:

Assumption 1. *Sets X and Y are nonempty and compact.*

Assumption 1 is mild for the models of energy systems, since the bounds of variables can be practically known and the functions that are used to define sets are continuous.

Two objectives of this thesis are presented in Chapters 2 and 3, respectively. Chapter 2 discusses the integration of domain reduction techniques in generalized Bender decomposition (GBD, [16]) and nonconvex generalized Benders decomposition (NGBD, [27]). It is noticed that the concept of domain reduction is applied to logic-based Benders decomposition [21]. In the logic-based Benders decomposition research, domain reduction is achieved by range reduction calculations and limited to mixed-integer linear programming (MILP) problems. Compared with the domain reduction used in logic-based Benders decomposition, Chapter 2 employs the domain reduction techniques for reducing the domain of decomposed nonconvex problems and tightening convex relaxations, and the domain reduction techniques are applied on nonconvex NLP/MINLP problems. In the domain reduction procedure, customized bound contraction operations in reduced space and range reduction calculations for

decomposed nonconvex problems are proposed in this chapter to accelerate the solution of nonconvex subproblems or/and reduce the number of nonconvex subproblems to be solved, for GBD and NGBD. Overall, this is the first attempt in the literature to integrate the domain reduction techniques that have been applied for classical branch-and-bound-based global optimization methods, into GBD and NGBD systematically. Two representative energy system problems, steady-state operation of a natural gas production system, and integrated design and steady-state operation of a mixed Alternating Current and Direct Current (AC-DC) distribution system, are studied and solved with the proposed decomposition methods in this chapter.

Chapter 3 aims to present applications of customized decomposition-based global optimization methods for large-scale energy systems, and here we take an industrial natural gas production system as example. This integrated design and operation problem is cast as a large-scale nonconvex MINLP, and this optimization model describes gas compositions, pressure flow relations, and compressor performances, at different parts of the gas production network. This large-scale nonconvex MINLP cannot be solved by existing decomposition methods efficiently, because each operation subproblem (for each uncertainty realization) is a very challenging nonconvex MINLP. In order to overcome this difficulty, the nonconvex MINLP formulation is reformulated via several steps, and the reformulation procedure is rigorous under mild assumptions. The resulting reformulation has significantly reduced nonconvexity, and its nonconvex part and convex part are separable, allowing efficient solution of each operation subproblem via GBD. It is the first application of GBD to (deterministic) operation problem in process systems engineering. By integrating the classical NGBD and the GBD procedure for solving the operation subproblems, a multi-loop NGBD

method is developed to efficiently solve the proposed optimization model. If the operation problem for a system is decomposable, the integrated design and operation problem (under uncertainty) for the system can be solved by the multi-loop NGBD developed in this chapter.

Chapter 2

On Domain Reduction for Benders Decomposition-based Optimization

In this chapter, we focus on employing domain reduction techniques to Benders decomposition-based global optimization methods that can be applied on large-scale energy systems with the form of (P1). The form (P1) is transmitted from (P0) with the procedure in Appendix A.1.

$$\begin{aligned} \min_{x,y_0} \ & c^{\mathrm{T}}x \\ \text{s.t.} \ & Ax + By_0 \leq d, \\ & x \in X, \\ & y_0 \in Y. \end{aligned} \tag{P1}$$

In (P1), the dimension of vector d is $n_m \times 1$ where m is the number of the constraints in the first group; the dimension of matrices A and B are $n_m \times n_x$ and $n_m \times n_{y_0}$, respectively; the set $X = \{x \in \Omega \subset \mathbb{R}^{n_x} \mid \psi(x) \leq 0\}$ is defined with vector-valued function $\psi : \Omega \to \mathbb{R}^{m_\psi}$ that only contains nonlinear constraints, the set $Y = \{y_0 \in$

$\Phi \subset \mathbb{R}^{n_{y_0}} \mid \varphi(y_0) \leq 0\}$ is defined with vector-valued function $\varphi : \Phi \to \mathbb{R}^{m_\varphi}$. Here complicating variables y_0 are also linking variables, and $Ax + By_0 \leq d$ contain all linear constraints in the problem, including those link x and y_0 and those contain only x.

Obviously, Problem (P1) can be further reformulated into the following form, by introducing extra continuous variables y:

$$\begin{aligned} \min_{x,y,y_0} \ & c^{\mathrm{T}}x \\ \text{s.t.} \ & y - y_0 = 0, \\ & Ax + By \leq d, \\ & x \in X, \\ & y_0 \in Y. \end{aligned} \tag{P}$$

In this reformulation, the constraints that link y_0 and other variables become linear equality constraints that are free from any problem parameters. We call these constraints linking constraints in this chapter. In the section 2 we will show that (P) is a better formulation for Benders decomposition-based optimization, and therefore this formulation will be considered for the rest of the chapter.

Remark 1. *(x^*, y_0^*) is an optimal solution of* Problem (P0) *if and only if (x^*, y_0^*) is an optimal solution of* Problem (P1)*; (x^*, y_0^*) is an optimal solution of* Problem (P1) *if and only if (x^*, y_0^*, y_0^*) is an optimal solution of* Problem (P)*.*

The remaining part of this chapter is organized as follows. Section 1 presents a motivating example that shows the principle of domain reduction for nonconvex

problems. Section 2 introduces the classical GBD method and discusses why reduced variable domain can benefit GBD, and then two bound contraction operations are developed and incorporated in GBD for improved solution efficiency. Section 3 introduces the standard NGBD method in the context of a multi-scenario version of problem formulation, and develops customized bound contraction operations and range reduction calculations for NGBD. Section 4 demonstrates the benefits of the proposed domain reduction methods for GBD and NGBD, through two optimization problems for energy systems. We finish this chapter with a summary in section 5.

2.1 Domain Reduction: A Motivating Example

Domain reduction is achieved via both bound contraction operations and range reduction calculations through convex relaxation problems of the original nonconvex problem. For a simple nonconvex optimization problem in Figure (2.1), we are to minimize the nonconvex function $f(x)$ over the constraint set $x \in [x^{LO}, x^{UP}]$ and aim to reduce the bound of x by pushing up its lower bound x^{LO}. In this figure, a convex underestimating function is denoted as $u_f(x)$, a known upper bound is denoted as UB, obtained lower bound is denoted as LB, and a marginal value for the convex relaxation problem is denoted as λ.

Domain reduction of this problem can be understood in both bound contraction operation and range reduction calculation perspectives. For bound contraction operation, it contracts the lower bound of x by solving the convex problem which minimizes x over the constraint set $\{x \mid x \in [x^{LO}, x^{UP}], u_f(x) \leq \text{UB}\}$, where $u_f(x) \leq \text{UB}$ is a cut that can restrict the initial feasible interval $[x^{LO}, x^{UP}]$. The obtained lower bound of x then becomes x^{BC} in the figure. It is clear that the portion of domain $[x^{LO}, x^{BC}]$

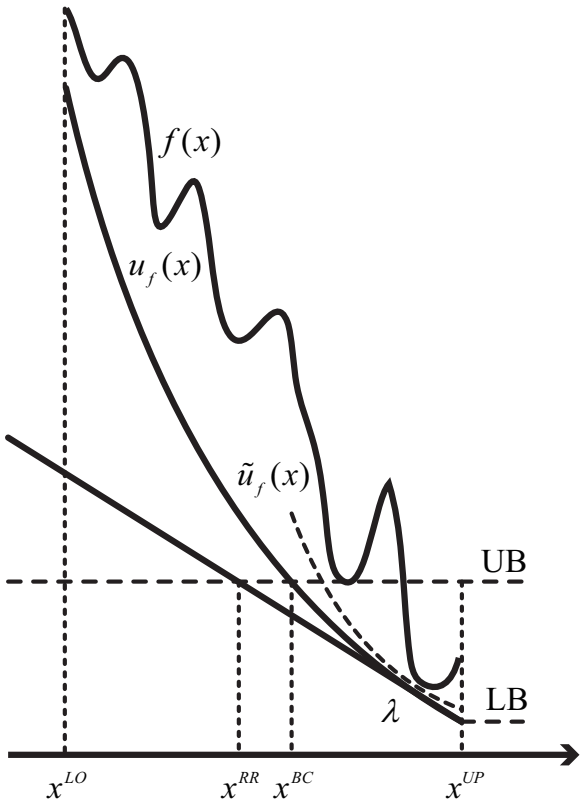

Figure 2.1: A motivating example of domain reduction.

is cut off by bound contraction operation, and the resulting new convex relaxation will be function $\widetilde{u}_f(x)$ over the new domain of the original nonconvex problem, which is $[x^{BC}, x^{UP}]$.

Another technique, range reduction calculation, does not explicitly rely on the solution of extra convex optimization problem but only rely on calculation of bounds directly. With the obtained dual information λ, it can be seen that the new lower bound can be achieved via $x^{RR} = x^{\mathrm{UB}} - (\mathrm{UB} - \mathrm{LB})/\lambda$. Then the portion of domain $[x^{LO}, x^{RR}]$ can be cut off, and the resulting domain is $[x^{RR}, x^{UP}]$. It's known that bound contraction operation can usually achieve tighter bounds than range reduction calculation can do [44].

2.2 Integrating Domain Reduction in GBD

In this section, we discuss the integration of domain reduction in GBD. For GBD to be applicable, Problem (P) needs to satisfy the following assumption:

Assumption 2. *Function ψ (that is used to define set X) is convex on Ω.* Problem (P) *satisfies Slater's condition* [5] *if y_0 is fixed to a point in Y for which* Problem (P) *is feasible.*

Remark 2. Assumption 2 *implies that, after fixing y_0 to any feasible value,* Problem (P) *becomes a convex optimization problem that holds strong duality* [5].

2.2.1 Introduction to GBD

GBD decomposes Problem (P) into primal problems and relaxed master problems, through projection, dualization, relaxation and restriction [16]. In each GBD iteration, upper bound and lower bound of the problem are updated with the solution of a primal problem and a relaxed master problem. The finite ϵ-convergence of GBD has been established for the case in which all functions in the problem are linear (and then GBD is reduce to the classical Benders decomposition) and the case in which all points in Y is feasible for Problem (P).

Figure 2.2 shows the algorithmic flowchart of GBD. At a GBD iteration k, the

following primal problem, derived by fixing $y_0 = y_0^{(k)}$ in Problem (P), is solved:

$$\begin{aligned} obj_{\text{GBDPP}^{(k)}} = \min_{x,y} \ & c^{\mathrm{T}}x \\ \text{s.t.} \ & y - y_0^{(k)} = 0, \\ & Ax + By \leq d, \\ & x \in X. \end{aligned} \tag{GBDPP^k}$$

where $obj_{\text{GBDPP}^{(k)}}$ denotes the optimal objective value of (GBDPP^k). For convenience, we represent the optimal objective value of a problem this way for all problems in this chapter. If $obj_{\text{GBDPP}^{(k)}}$ is lower than the current upper bound UB_{GBD}, then it will become the new upper bound. From the strong duality of (GBDPP^k), its optimal solution implies that:

$$\text{Objective value of Problem (P)} \geq obj_{\text{GBDPP}^{(k)}} - \left(\lambda^{(k)}\right)^T \left(y_0 - y_0^{(k)}\right),$$

where $\lambda^{(k)}$ includes Lagrangian multipliers of the linking constraints in (GBDPP^k). The following set T^k is also generated after obtaining the solution of (GBDPP^k):

$$T^k = \{j \in \{1, ..., k\} : \text{Problem (GBDPP}^j\text{) is feasible}\}.$$

This set includes indices of iterations at which an optimality cut has been generated.

Remark 3. *Lagrangian multipliers for a smooth convex or linear optimization problem are returned by most optimization solvers (e.g., CONOPT [8], SNOPT [17] and CPLEX [22]) together with the optimal solution. Therefore, no extra calculation is needed for obtaining Lagrangian multipliers.*

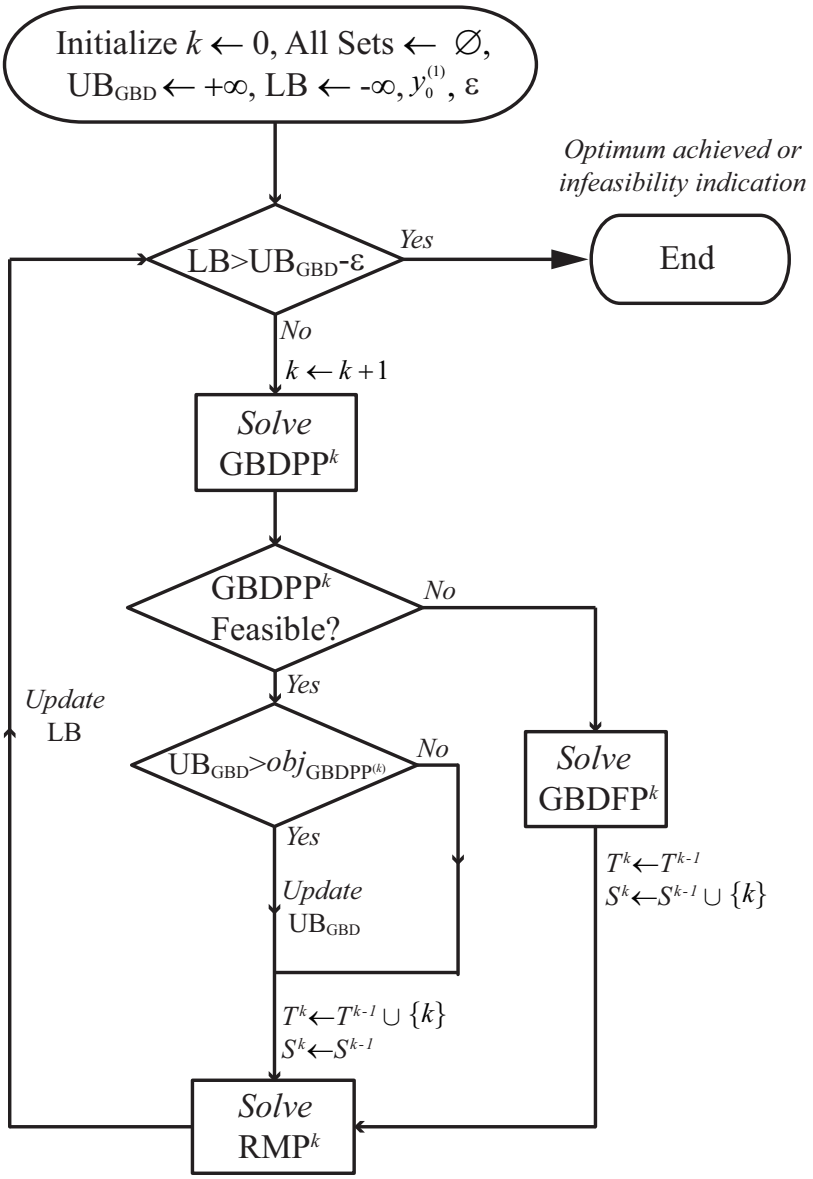

Figure 2.2: The algorithmic framework of GBD.

If Problem (GBDPP^k) is infeasible, the following GBD feasibility problem (GBDFP^k) is solved instead:

$$\begin{aligned} obj_{\text{GBDFP}^{(k)}} = \min_{x,y,v^+,v^-} \ & \left\| v^+ + v^- \right\| \\ \text{s.t. } & y - y_0^{(k)} = v^+ - v^-, \\ & Ax + By \leq d, \\ & x \in X, \ \ v^+, \ v^- \geq 0, \end{aligned} \tag{GBDFP^k}$$

where $\|\cdot\|$ means a norm function, v^+ and v^- are nonnegative slack variable vectors. Problem (GBDFP^k) is convex and satisfies Slater's condition (following Assumption 2), so it holds strong duality. As a result, all feasible points of Problem (P) have to satisfy the following feasibility cut:

$$0 \geq obj_{\text{GBDFP}^{(k)}} - \left(\lambda^{(k)}\right)^T \left(y_0 - y_0^{(k)}\right),$$

where $\lambda^{(k)}$ includes Lagrange multipliers for the linking constraints in (GBDFP^k). And the following index set for feasibility cuts is also generated:

$$S^k = \{j \in \{1, ..., k\} : \text{Problem (GBDPP}^j\text{) is infeasible}\}.$$

According to the already generated optimality and feasibility cuts, we can construct the following relaxed master problem at iteration k:

$$
\begin{aligned}
obj_{\mathrm{RMP}^{(k)}} = \min_{\eta, y_0} \quad & \eta \\
\text{s.t.} \quad & \eta \geq obj_{\mathrm{GBDPP}^{(j)}} - \left(\lambda^{(j)}\right)^T \left(y_0 - y_0^{(j)}\right), \ \forall j \in T^k, \\
& 0 \geq obj_{\mathrm{GBDFP}^{(j)}} - \left(\lambda^{(j)}\right)^T \left(y_0 - y_0^{(j)}\right), \ \forall j \in S^k, \\
& y_0 \in Y^k.
\end{aligned}
\tag{RMP^k}
$$

In the classical GBD method, $Y^k = Y$ for all iterations, but later on we will show that this set can be reduced at each iteration if domain reduction is integrated. Clearly, Problem (RMP^k) lower bounds Problem (P). After solving (RMP^k), the obtained optimal objective value $obj_{\mathrm{RMP}^{(k)}}$ will become the current lower bound LB, and the obtained y_0 values will be used to construct the primal problem for the next iteration.

Note that if the index set $T^k = \emptyset$, Problem (RMP^k) is unbounded; in this case, a feasibility relaxed master problem (FRMP^k) is solved instead, and the formulation of this problem is provided in Appendix A.2.1. GBD relies on the situation that Problems (RMP^k) and (FRMP^k) can be usually solved to ϵ-optimality by state-of-the-art global optimization solvers, such as BARON [38] and ANTIGONE [32]. If Problem (RMP^k) or (FRMP^k) is infeasible, then Problem (P) is infeasible as well.

2.2.2 Comparison of (P) and (P1) for GBD

In this chapter we consider two different formulations (P1) and (P) of Problem (P0), and here we are to show formulation (P) considered in this chapter is better than formulation (P1) in the sense that (P) may generate stronger Benders cuts for the relaxed master problem. We adopt the concepts related to "Pareto-optimal" cuts

from [29] in order to facilitate the discussion. We discuss only the optimality cuts from both formulations, but similar results can be readily obtained for feasibility cuts.

For convenience of the following discussion, we consider two different formulations S and W of a decomposable problem (DP). For the resulting formulations (DP^S) and (DP^W), they are different in the sense that their optimal objective values are equal, but the number of non-linking variables, linking constraints and constraints that only contain non-linking variables, are different.

Consider an optimization problem (DP) with formulation S:

$$\begin{aligned} \min_{x^S,\, y_0} \quad & (c^S)^T x^S \\ st. \quad & A^S x^S + B^S y_0 \leq d^S, \\ & x^S \in X^S, \\ & y_0 \in Y. \end{aligned} \tag{DP^S}$$

The Benders optimality cuts for (DP^S) can be written as:

$$\eta \geq \min_{x^S \in X^S} \; L^S(\lambda, x^S, y_0), \quad \forall \lambda \geq 0,$$

where $L^S(\lambda, x^S, y_0) = (c^S)^T x^S + \lambda^T (A^S x^S + B^S y_0 - d^S)$.

Also, consider Problem (DP) with another formulation W:

$$\begin{aligned} \min_{x^W,\, y_0} \quad & (c^W)^T x^W \\ st. \quad & A^W x^W + B^W y_0 \leq d^W, \\ & x^W \in X^W, \\ & y_0 \in Y. \end{aligned} \tag{DP^W}$$

And the Benders optimality cuts for (DP^W) are:

$$\eta \geq \min_{x^W \in X^W} \; L^W(\mu, x^W, y_0), \quad \forall \mu \geq 0,$$

where $L^W(\mu, x^W, y_0) = (c^W)^T x^W + \mu^T (A^W x^W + B^W y_0 - d^W)$.

Definition 1. *A Benders cut for* (DP^S), $\eta \geq \min_{x^s \in X^s} \; L^S(\lambda, x^S, y_0)$, *is said to equal to a Benders cut for* (DP^W), $\eta \geq \min_{x^w \in X^w} \; L^W(\mu, x^W, y_0)$, *if the right-hand-sides of the two cuts are equal for all* $y_0 \in Y$.

Definition 2. *A Benders cut for* (DP^S), $\eta \geq \min_{x^s \in X^s} \; L^S(\lambda, x^S, y_0)$, *is said to dominate a Benders cut for* (DP^W), $\eta \geq \min_{x^w \in X^w} \; L^W(\mu, x^W, y_0)$, *if for all* $y_0 \in Y$, $\min_{x^s \in X^s} \; L^S(\lambda, x^S, y_0) \geq \min_{x^w \in X^w} \; L^W(\mu, x^W, y_0)$, *and the inequality is strict for at least one* $y_0 \in Y$.

Definition 3. *A Benders cut for* (DP^S) *is said to be unmatched with respect to formulation* (DP^W), *if there is no cut for* (DP^W) *that equals to or dominates it.*

Definition 4. *Formulation* (DP^S) *is said to be cut richer than formulation* (DP^W), *if* (DP^S) *has at least one Benders cut that is unmatched with respect to* (DP^W), *but* (DP^W) *does not have any cuts that are unmatched with respect to* (DP^S).

Remark 4. *According to the above definitions, a cut richer formulation is a better formulation for* GBD, *because it is likely to yield stronger Benders cuts that boost the convergence.*

The next proposition states the condition in which (DP^S) can have a strong Benders cut that (DP^W) does not have.

Proposition 1. *Formulation* (DP^S) *has a Benders cut that is unmatched with respect to formulation* (DP^W)*, if*

$$\max_{\lambda \geq 0} \min_{y_0 \in Y, x^S \in X^S} L^S(\lambda, x^S, y_0) > \max_{\mu \geq 0} \min_{y_0 \in Y, x^W \in X^W} L^W(\mu, x^W, y_0).$$

Proof. Let λ^* is optimal for the Lagrangian dual of (DP^S), then

$$\min_{y_0 \in Y} \min_{x^S \in X^S} L^S(\lambda^*, x^S, y_0) > \max_{\mu \geq 0} \min_{y_0 \in Y, x^W \in X^W} L^W(\mu, x^W, y_0).$$

□

So $\forall \tilde{\mu} \geq 0$, if $\tilde{y}_0 \in Y$ is optimal for the Lagrangian dual of (DP^W), then

$$\begin{aligned}
\min_{x^S \in X^S} L^S(\lambda^*, x^S, \tilde{y}_0) &\geq \min_{y_0 \in Y} \min_{x^S \in X^S} L^S(\lambda^*, x^S, y_0) \\
&> \max_{\mu \geq 0} \min_{y_0 \in Y, x^W \in X^W} L^W(\mu, x^W, y_0) \\
&\geq \min_{y_0 \in Y, x^W \in X^W} L^W(\tilde{\mu}, x^W, y_0) \\
&= \min_{x^W \in X^W} L^W(\tilde{\mu}, x^W, \tilde{y}_0).
\end{aligned}$$

Therefore, the Benders cut $\eta \geq \min_{x^S \in X^S} L^S(\lambda^*, x^S, y_0)$ for (DP^S) is unmatched with respect to formulation (DP^W).

Proposition 1 implies that a formulation with a smaller Lagrangian dual gap is a better formulation for GBD. The next proposition states that the Lagrangian dual gap of (P) cannot be larger than that of (P1).

Proposition 2. *The optimal objective value of the following Lagrangian dual problem*

of (P),

$$\max_{\lambda} \min_{Ax+By\leq d,\, x\in X,\, y_0\in Y} c^T x + \lambda^T (y - y_0),$$

is greater than or equal to the optimal objective value of the following Lagrangian dual problem of (P1),

$$\max_{\mu\geq 0} \min_{x\in X,\, y_0\in Y} c^T x + \mu^T (Ax + By_0 - d).$$

Proof. According to Theorem 1(d) in [15], the optimal objective value of the Lagrangian dual of (P) is equivalent to that of the following relaxation of (P):

$$\begin{aligned} \min_{x,y,y_0} \quad & c^T x \\ s.t. \quad & y - y_0 = 0, \\ & (x, y, y_0) \in conv\{(x, y, y_0) \in X \times \mathbb{R} \times Y \mid Ax + By \leq d\}, \end{aligned} \tag{PR}$$

where $conv\{\cdot\}$ denotes the convex hull of a set. Similarly, the optimal objective value of the Lagrangian dual of (P1) is equivalent to that of the following relaxation of (P1):

$$\begin{aligned} \min_{x,y_0} \quad & c^T x \\ s.t. \quad & Ax + By_0 \leq d, \\ & (x, y_0) \in conv\{X \times Y\}. \end{aligned} \tag{P1R}$$

Note that (P1R) can be equivalently reformulated as

$$\begin{aligned} \min_{x,y,y_0} \quad & c^T x \\ s.t. \quad & y - y_0 = 0, \\ & Ax + By \leq d, \\ & (x, y, y_0) \in conv\{X \times \mathbb{R} \times Y\}. \end{aligned} \tag{P1Ra}$$

The feasible set of (PR) is:

$$F_{PR} = F_1 \cap conv\{F_2 \cap F_3\},$$

where $F_1 = \{(x, y, y_0) \mid y - y_0 = 0\}$, $F_2 = \{(x, y, y_0) \mid Ax + By \leq d\}$, $F_3 = X \times \mathbb{R} \times Y$. The feasible set of (P1Ra) is:

$$F_{P1Ra} = F_1 \cap F_2 \cap conv\{F_3\}.$$

Since set F_2 is convex,

$$conv\{F_2 \cap F_3\} \subseteq conv\{F_2\} \cap conv\{F_3\} = F_2 \cap conv\{F_3\},$$

so $F_{PR} \subseteq F_{P1Ra}$, and the optimal objective value of (PR) is greater than or equal to that of (P1Ra) or (P1R). This completes the proof. □

Proposition 2 implies that formulation (P) may be better than formulation (P1). The next proposition states that (P1) cannot be better than (P).

Proposition 3. *There is no Benders cut for* (P1) *that is unmatched with respect to*

(P).

Proof. Consider an arbitrary Benders cut of (P1R) for a multiplier $\tilde{\mu}$:

$$\eta \geq \min_{x \in X} \; c^T x + \tilde{\mu}^T (Ax + By_0 - d).$$

$\forall y_0 \in Y$, the right-hand-side of the cut satisfies:

$$\begin{aligned}
&\min_{x \in X} \; c^T x + \tilde{\mu}^T (Ax + By_0 - d) \\
=& \min_{x \in X, y \in \mathbb{R}} \; c^T x + \tilde{\mu}^T (Ax + By - d) + \tilde{\mu}^T B(y_0 - y) \\
\leq& \min_{x \in X, y \in \mathbb{R}, Ax + By \leq d} \; c^T x + \tilde{\mu}^T (Ax + By - d) + \tilde{\mu}^T B(y_0 - y) \\
\leq& \min_{x \in X, y \in \mathbb{R}, Ax + By \leq d} \; c^T x + \tilde{\mu}^T B(y_0 - y) \\
=& \min_{x \in X, y \in \mathbb{R}, Ax + By \leq d} \; c^T x + \tilde{\lambda}(y_0 - y). \qquad (\tilde{\lambda} = \tilde{\mu}^T B)
\end{aligned}$$

Therefore, this Benders cut of (P1R) cannot be unmatched with respect to (P). This completes the proof. □

According to the previous definitions and proposition, we have the following comparison result for (P) and (P1).

Theorem 1. *Formulation* (P1) *cannot be cut richer than formulation* (P)*. Formulation* (P) *is cut richer than formulation* (P1) *if its Lagrangian dual gap is smaller than that of* (P1)*.*

Proof. The first statement directly follows from Proposition 3 and Definition 4. For the second statement, if Lagrangian dual gap of formulation (P) is smaller than that of (P1), then by Proposition 1, Proposition 3 and Definition 4 the statement is true. □

2.2.3 Domain Reduction for GBD

It is well-known that domain reduction can benefit the branch-and-bound search because it can tighten convex relaxations and reduce the number of nodes to be explored. For GBD, domain reduction is beneficial for the solution of the relaxed master problem (RMP^k), if (RMP^k) is nonconvex and solved by the branch-and-bound search. In addition, domain reduction may reduce set Y at each iteration by removing the feasible points in Y that cannot be better than the incumbent solution (and this is why we use Y^k instead of Y in (RMP^k)). A diminished Y can contribute to reduced Lagrangian dual gap, and potentially generate stronger Benders cuts according to previous subsection. If the Lagrangian dual gap becomes zero when Y is sufficiently diminished, the GBD procedure can terminate once an optimal solution is found [40].

Here we consider bound contraction operation for domain reduction. Although bound contraction requires extra computing time for solving extra convex subproblems, it can significantly reduce the time for solving nonconvex problem (RMP^k) especially when (RMP^k) is highly nonconvex. Figure 2.3 shows the algorithm flowchart for the GBD integrated with bound contraction operations. The solution procedure for bound contraction subproblems is highlighted with the gray box in the figure.

After the upper bound of the problem, namely $\mathrm{UB}_{\mathrm{GBD}}$, is updated at an iteration k, we can calculate the tightest range for a variable $y_{0,i}$ by solving the following

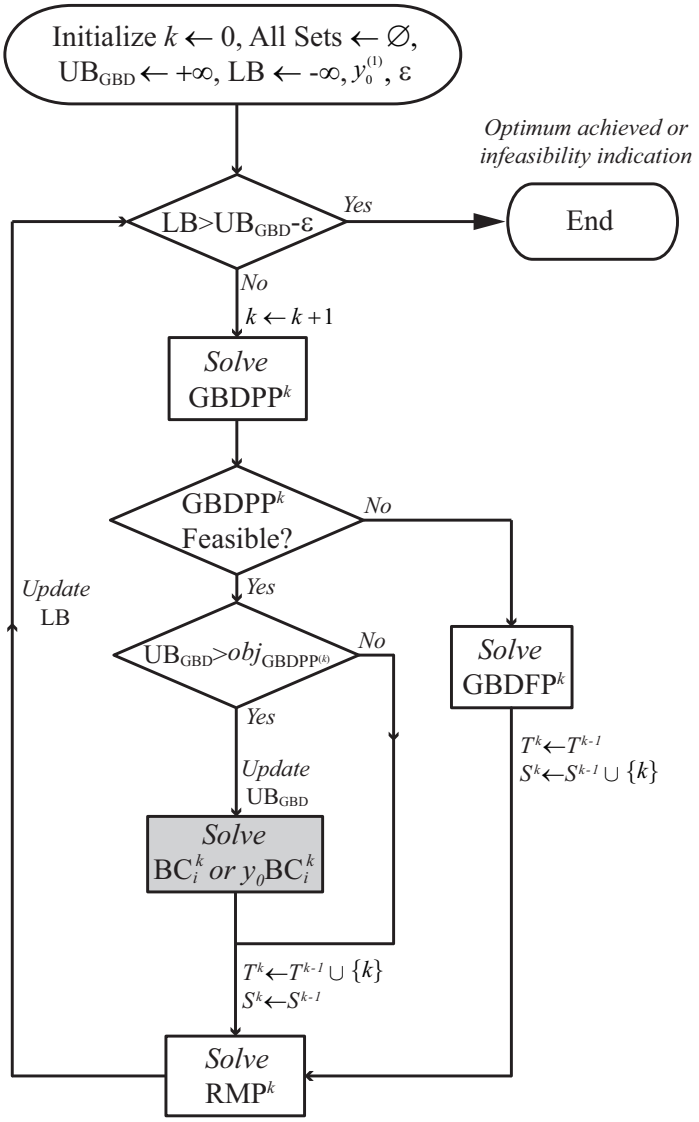

Figure 2.3: The algorithmic framework of GBD with domain reduction.

subproblems:

$$\begin{aligned} \min_{x,\, y,\, y_0} \backslash \max \quad & y_{0,i} \\ s.t. \quad & y - y_0 = 0, \\ & Ax + By \leq d, \\ & x \in X, \quad y_0 \in Y^k, \\ & c^T x \leq \mathrm{UB}_{\mathrm{GBD}}. \end{aligned} \tag{BC\_NC$_i^k$}$$

The last constraint in the problem is to exclude points that lead to inferior solutions of the incumbent one. When the objective is minimized, the problem yields a lower bound for $y_{0,i}$, and when the objective is maximized, the problem yields an upper bound for $y_{0,i}$. If $y_{0,i}$ is an integer variable, the obtained lower bound will be rounded to the the smallest integer above it and the obtained upper bound will be rounded to largest integer below it .

Since Problem (BC_NC$_i^k$) is as difficult as the original problem (P), so it is usually relaxed into the following bound contraction problem:

$$\begin{aligned} \min_{x,\, y,\, y_0} \backslash \max \quad & y_{0,i} \\ s.t. \quad & y - y_0 = 0, \\ & Ax + By \leq d, \\ & x \in X, \quad y_0 \in \hat{Y}^k, \\ & c^T x \leq \mathrm{UB}_{\mathrm{GBD}}, \end{aligned} \tag{BC$_i^k$}$$

where $\hat{Y}$ stands for the convex relaxation of Y. Solving Problem (BC$_i^k$) can still be

time consuming, especially when the dimension of variable x is large (such as those come from scenario-based stochastic programming) and set X is defined by many nonlinear (but convex) constraints. This motives the construction of an easier bound contraction problem. Consider the following convex bound contraction problem defined on the y_0 subspace:

$$\begin{aligned} \min_{y_0} \backslash \max \quad & y_{0,i} \\ \text{s.t.} \quad & \mathrm{UB}_{\mathrm{GBD}} \geq obj_{\mathrm{GBDPP}^{(j)}} - \left(\lambda^{(j)}\right)^T \left(y_0 - y_0^{(j)}\right), \quad \forall j \in T^k, \\ & 0 \geq obj_{\mathrm{GBDFP}^{(j)}} - \left(\lambda^{(j)}\right)^T \left(y_0 - y_0^{(j)}\right), \quad \forall j \in S^k, \\ & y_0 \in \hat{Y}^k. \end{aligned} \tag{$y_0\mathrm{BC}_i^k$}$$

Theorem 2. *The range of y_0 obtained from* Problem (BC_i^k) *is tighter than or equal to that from* Problem ($y_0\mathrm{BC}_i^k$).

Proof. We prove this by showing that any y_0 that is feasible for (BC_i^k) is also feasible for ($y_0\mathrm{BC}_i^k$).

First, according to strong duality of Problem (GBDPP^k) and Problem (GBDFP^k), Problem ($y_0\mathrm{BC}_i^k$) can be reformulated as:

$$\begin{aligned} \min_{y_0} \backslash \max \quad & y_{0,i} \\ \text{s.t.} \quad & \mathrm{UB}_{\mathrm{GBD}} \geq \min_{Ax+By\leq d, x\in X} c^T x + \left(\lambda^{(j)}\right)^T (y - y_0), \quad \forall j \in T^k, \\ & 0 \geq \min_{\substack{Ax+By\leq d, x\in X \\ \upsilon^+,\upsilon^-\geq 0}} ||\upsilon^+ + \upsilon^-|| + \left(\lambda^{(j)}\right)^T \left(y - y_0 - \upsilon^+ + \upsilon^-\right), \quad \forall j \in S^k, \\ & y \in \hat{Y}^k. \end{aligned} \tag{$y_0\mathrm{BCa}_i^k$}$$

Second, reformulation ($y_0\text{BCa}_i^k$) can be restricted by adding an infinite number of cuts, as:

$$
\begin{aligned}
&\min_{y_0} \backslash \max \quad y_{0,i} \\
&\text{s.t.} \quad \text{UB}_{\text{GBD}} \geq \min_{Ax+By\leq d, x\in X} c^T x + \lambda^T (y - y_0), \quad \forall \lambda, \\
&\qquad 0 \geq \min_{\substack{Ax+By\leq d, x\in X \\ \upsilon^+,\upsilon^-\geq 0}} ||\upsilon^+ + \upsilon^-|| + \lambda^T \left(y - y_0 - \upsilon^+ + \upsilon^-\right), \quad \forall \lambda, \\
&\qquad y_0 \in \hat{Y}^k.
\end{aligned}
\tag{MBC$_i^k$}
$$

Finally, we are to prove that any y_0 that is feasible for (BC$_i^k$), say $\tilde{y}_0 \in \hat{Y}^k$, is also feasible for (MBC$_i^k$). $\tilde{y}_0$ feasible for (BC$_i^k$) means that, $\exists x \in X$, $y(=\tilde{y}_0)$ such that:

$$y - \tilde{y}_0 = 0, \quad Ax + By \leq d, \quad c^T x \leq \text{UB}_{\text{GBD}},$$

which implies that

$$\text{UB}_{\text{GBD}} \geq \min_{\substack{y-\tilde{y}_0=0, \\ Ax+By\leq d, x\in X}} c^T x.$$

According to the strong duality,

$$\text{UB}_{\text{GBD}} \geq \max_{\lambda} \min_{Ax+By\leq d, x\in X} c^T x + \lambda^T (y - \tilde{y}_0).$$

Therefore, $\tilde{y}_0$ satisfies the first group of constraints in (MBC$_i^k$). $\tilde{y}_0$ feasible for (BC$_i^k$)

also means that the optimal objective value of the following problem is zero:

$$\begin{aligned} \min_{x,y,v^+,v^-} \quad & ||v^+ + v^-|| \\ s.t. \quad & y - \tilde{y}_0 = v^+ - v^-, \\ & Ax + By \leq d, \\ & x \in X, \quad v^+, v^- \geq 0. \end{aligned}$$

According to the weak duality of the problem,

$$0 \geq \max_{\lambda} \min_{\substack{Ax+By\leq d, x\in X \\ v^+,v^-\geq 0}} ||v^+ + v^-|| + \lambda^T \left(y - y_0 - v^+ + v^-\right),$$

so $\tilde{y}_0$ is also feasible for the second group of constraints of (MBC_i^k). Therefore, $\tilde{y}_0$ is feasible for (MBC_i^k) and this completes the proofs.

□

Remark 5. *The bound contraction problem* ($y_0\mathrm{BC}_i^k$)*, although not as tight as* (BC_i^k)*, can have a much smaller size than* (BC_i^k) *and therefore much easier to solve, unless a large number of cuts are included in the problem (which implies that a large number of iterations are needed for the convergence of* GBD*). Due to the integration of domain reduction, the number of* GBD *iterations needed is not likely to be large.*

2.3 Integrating Domain Reduction in NGBD

If the set X in Problem (P) is nonconvex, then Assumption 2 is not satisfied, and the GBD procedure given in the previous section usually fails to converge to a solution because the upper bounding subproblems do not hold strong duality. Surely we can

extract the "nonconvex variables" in x and include them in y_0 for GBD to be valid, but this way the size of the relaxed master problem (RMP^k) may be overly large and solving (RMP^k) at each iteration may become impractical.

In this section, we consider a multi-scenario version of Problem (P), which usually cannot be practically solved by GBD:

$$\begin{aligned} \min_{\substack{y_0,y_1,\dots,y_s,\\ x_1,\dots,x_s}} \ & \sum_{h=1}^{s} c_h^{\mathrm{T}} x_h \\ \text{s.t.} \ & y_h - y_0 = 0, \quad \forall h \in \{1,\dots,s\}, \\ & A_h x_h + B_h y_h \le d_h, \quad \forall h \in \{1,\dots,s\}, \\ & x_h \in X_h, \quad \forall h \in \{1,\dots,s\}, \\ & y_0 \in Y, \end{aligned} \tag{PS}$$

where h indexes different scenarios that may come from explicit consideration of uncertainty parameters or time periods. Many engineering design or operation problems can be cast as Problem (PS), but global optimization for this problem is very challenging as the size of the problem can be very large when a large number of scenarios are included. Here we restrict our discussion to problems where y_0 are integer variables, which usually represent design decisions that cannot be modeled as continuous variables (e.g., network structure, equipment size). Therefore, we impose the following assumption on Problem (PS).

Assumption 3. *The elements of compact nonconvex set Y are integers.*

With this assumption, Problem (PS) can be solved to global optimality by NGBD. In this section, we discuss how domain reduction can be integrated in NGBD to improve solution efficiency.

2.3.1 Introduction to NGBD

The basic idea of NGBD is to construct a sequence of lower bounding problems through convex relaxation, such that all the lower bounding problems satisfy Assumption 2 and can be readily solved by GBD. The solutions of the lower bounding problems give values of vector y_0 (called integer realizations), which can be used to construct an upper bounding problem. In the standard NGBD procedure [27], the following lower bounding problem is solved via GBD:

$$
\begin{aligned}
&\min_{\substack{y_0,y_1,\ldots,y_s\\ x_1,\ldots,x_s,\\ q_1,\ldots,q_s,}} \sum_{h=1}^{s} c_h^{\mathrm{T}} x_h \\
&\text{s.t. } y_h - y_0 = 0, \quad \forall h \in \{1,...,s\}, \\
&\quad \hat{A}_h x_h + \hat{B}_h y_h + \hat{F}_h q_h \le \hat{d}_h, \quad \forall h \in \{1,...,s\}, \\
&\quad (x_h, q_h) \in \hat{X}_h, \quad \forall h \in \{1,...,s\}, \\
&\quad y_0 \in Y, \\
&\quad \sum_{i \in I_1^j} y_{0,i} - \sum_{i \in I_0^j} y_{0,i} \le |I_1^j| - 1, \ \ \forall j \in R^k.
\end{aligned}
\tag{LBP^k}
$$

In this problem, superscript k indexes all previous GBD iterations used to solve the lower bounding problems. The extra variables q_h come from the need of constructing smooth convex relaxations, e.g., through McCormick relaxation [31], [33]. The first group of constraints in (LBP^k) are linking constraints. The second group of constraints in (LBP^k) includes two parts. The first part is the second group of constraints in the original problem (PS), i.e., $A_h x_h + B_h y_h \le d_h, \ \forall h \in \{1,...,s\}$. The second part is linear constraints generated from the convex relaxation procedure, and these constraints can be written as $\bar{A}_h x_h + F_h q_h \le \bar{d}_h, \ \forall h \in \{1,...,s\}$. The resulting

matrices $\hat{A}_h$, $\hat{B}_h$ and $\hat{F}_h$ and vector $\hat{d}_h$ can be redefined and the set $\hat{X}_h$ is a convex relaxation of set X_h that removes constraints $\bar{A}_h x_h + F_h q_h \leq \bar{d}_h$.

$$\hat{A}_h = \begin{pmatrix} A_h \\ \bar{A}_h \end{pmatrix}, \quad \hat{B}_h = \begin{pmatrix} B_h \\ 0 \end{pmatrix}, \quad \hat{F}_h = \begin{pmatrix} 0 \\ F_h \end{pmatrix}, \quad \hat{d}_h = \begin{pmatrix} d_h \\ \bar{d}_h \end{pmatrix}.$$

The last group of constraints are standard integer cuts [1] that are used to exclude inter realizations that have been generated in the previous NGBD iterations, and these integer cuts are needed to prevent GBD from generating an integer realization multiple times [27]. The index set R^k includes indices of all previous GBD iterations, $I_1^j = \{i \in \{1, ..., n_{y_0}\} \ : \ y_{0,i}^{(j)} = 1\}$, $I_0^j = \{i \in \{1, ..., n_{y_0}\} \ : \ y_{0,i}^{(j)} = 0\}$, and $|\cdot|$ means the cardinality of a set.

The GBD subproblems used for solving the lower bounding problems (LBP^k) are given in Appendix A.2.2. Note that the GBD primal problems (GBDPP) and the GBD feasibility problems (GBDFP) for (LBP^k) can be naturally decomposed over scenarios, so the size of each decomposed primal or feasibility subproblem is independent of the number of scenarios. This is the major benefit of GBD for solving (LBP^k). The optimal objective values of the GBD relaxed master problems are valid lower bounds for (PS), so they can be used to update the current highest lower bound for (PS) (represented by LB in the chapter).

Remark 6. *If* Problem (LBP^k) *is constructed through a standard convex relaxation approach, it may not satisfy the Slater condition requirement stated in* Assumption 2. *In this case, the constraints in* Problem (LBP^k) *that annul the Slater condition can be further outer approximated* [10] *into linear constraints, and the resulting problem is still a valid lower bounding problem.*

Fixing y_0 to a constant $y_0^{[\,l\,]}$ in (PS) results in an upper bounding problem called primal problem. The primal problem can be decomposed over the scenarios and each decomposed primal subproblem can be written as:

$$\begin{aligned} obj_{\mathrm{PP}_h}(y_0^{[\,l\,]}) = \min_{x_h} \ & c_h^{\mathrm{T}} x_h \\ \text{s.t.} \ & A_h x_h + B_h y_0^{[\,l\,]} \leq d_h, \\ & x_h \in X_h, \end{aligned} \tag{PP_h^l}$$

where the superscript l indexes the integer realizations used for constructing primal subproblems. Note that the first and the second groups of constraints in (PS) are combined in (PP_h^l). There is no need to separate the constraints in (PP_h^l) because we do not require their Lagrange multipliers for NGBD. Although Problem (PP_h^l) is nonconvex, its size is independent of the number of scenarios and is smaller than the size of (PS), so the solution time for solving all the necessary subproblems (PP_h^l) is smaller than that for solving original Problem (PS) by at least an order of magnitude, and these subproblems can usually be solved to ϵ-optimality by state-of-the-art global optimization solvers, such as BARON [38] and ANTIGONE [32]. The sum of the optimal objective values of the primal subproblems, $obj_{\mathrm{PP}^{(l)}} = \sum_{h=1}^{s} obj_{\mathrm{PP}_h}(y_0^{[\,l\,]})$, is a valid upper bound for (PS), so it can be used to update the current lowest upper bound of (PS) (represented by UB in the chapter).

Remark 7. *When solving a primal subproblem* (PP_h^l) *in* NGBD*, an upper bound for the problem,* UB_h^l*, can be added in the problem to accelerate the solution. This upper bound can be estimated by* $\mathrm{UB}_h^l = \mathrm{UB} - \sum_{i=1}^{h-1} obj_{\mathrm{PP}_i}(y_0^{[\,l\,]}) - \sum_{j=h+1}^{s} obj_{\mathrm{GBDPP}_j}(y_0^{[\,l\,]})$*, according to* Proposition 3.6 *in* [27].

Figure 2.4 shows the algorithmic framework of NGBD. The part included in the big dashed box is the GBD loop for solving the lower bounding problems, and the subproblems solved at each GBD iteration is indexed by k. The other part is for construction and solution of the primal subproblems, and each iteration is indexed by l. $y_0^{[l]}$ is selected from the integer realizations that have been generated in the previous GBD iterations, according to the following rule:

$$y_0^{[l]} = y_0^{(k^*)}, \quad k^* = \arg\min_{j \in T^k \setminus U^l} \sum_{h=1}^{s} obj_{\text{GBDPP}_h}(y_0^{(j)}),$$

where "$[\cdot]$" for a superscript means that the superscript is to index the primal problems and, "$(\cdot)$" for a superscript means that the superscript is to index the GBD iterations. Set T^k includes all previous generated integer realizations for which the GBD primal subproblems are feasible, and set U^l includes all integer realizations that have been selected for constructing (PP_h^l). If $obj_{\text{GBDPP}_h}(y_0^{[l]}) \geq \text{UB}$, then the primal subproblems will not be solved for $y_0 = y_0^{[l]}$ as their solutions cannot be better than the incumbent solution.

Note that we use tolerance ϵ_G for the GBD loop, and tolerance ϵ for the overall NGBD algorithm. ϵ_G needs to be significantly smaller than ϵ for convergence to an ϵ-optimal solution [27]. In practice we usually choose ϵ_G to be one order of magnitude smaller than ϵ. The discussion of tolerance criteria for algorithms and subproblems has been done in the literature [27].

2.3.2 Domain Reduction for NGBD

As NGBD extends GBD via convex relaxation, the performance of NGBD for Problem (PS) relies heavily on the quality of convex relaxations. The tighter the convex

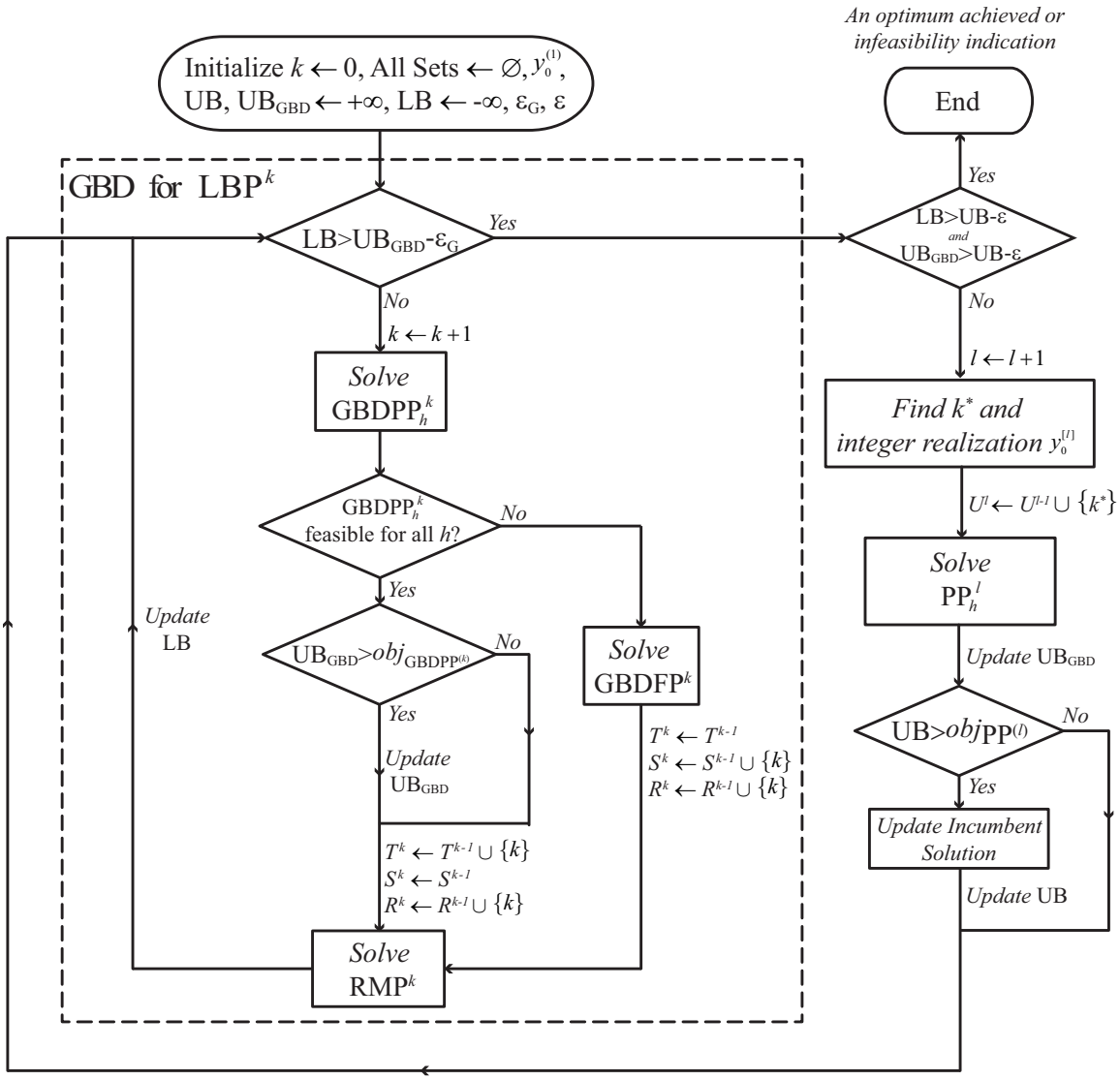

Figure 2.4: The algorithmic framework of NGBD.

relaxations are, the closer the lower bounding problem is to the original problem and therefore usually fewer number of primal subproblems need to be solved in NGBD. With domain reduction, the bounds of variables can be reduced and then tighter convex relaxations can be constructed. And the reduced variable bounds can also benefit the solution of the nonconvex primal subproblems and GBD relaxed master problems. In this section, we discuss how to integrate domain reduction systematically in NGBD.

Figure 2.5 shows the proposed algorithmic framework for NGBD with domain reduction. The two gray boxes highlight the two domain reduction operations added into NGBD. The gray box near the bottom highlights the bound contraction operation, which is performed only when UB has been improved since the last bound contraction operation. These domain reduction operations are indexed by a different superscript r. Therefore, the updated NGBD procedure includes three sub-sequences of operation, i.e., GBD iterations, integer realization enumeration of primal subproblems, and domain reduction operations, which are indexed by k, l, r, respectively. The gray box near the top highlights the extra range reduction calculations performed before solving the primal subproblems.

Updated NGBD subproblems

Due to the frequent change of the variable bounds during the NGBD procedure, the form of each NGBD subproblem needs to be updated. The updated form of the lower

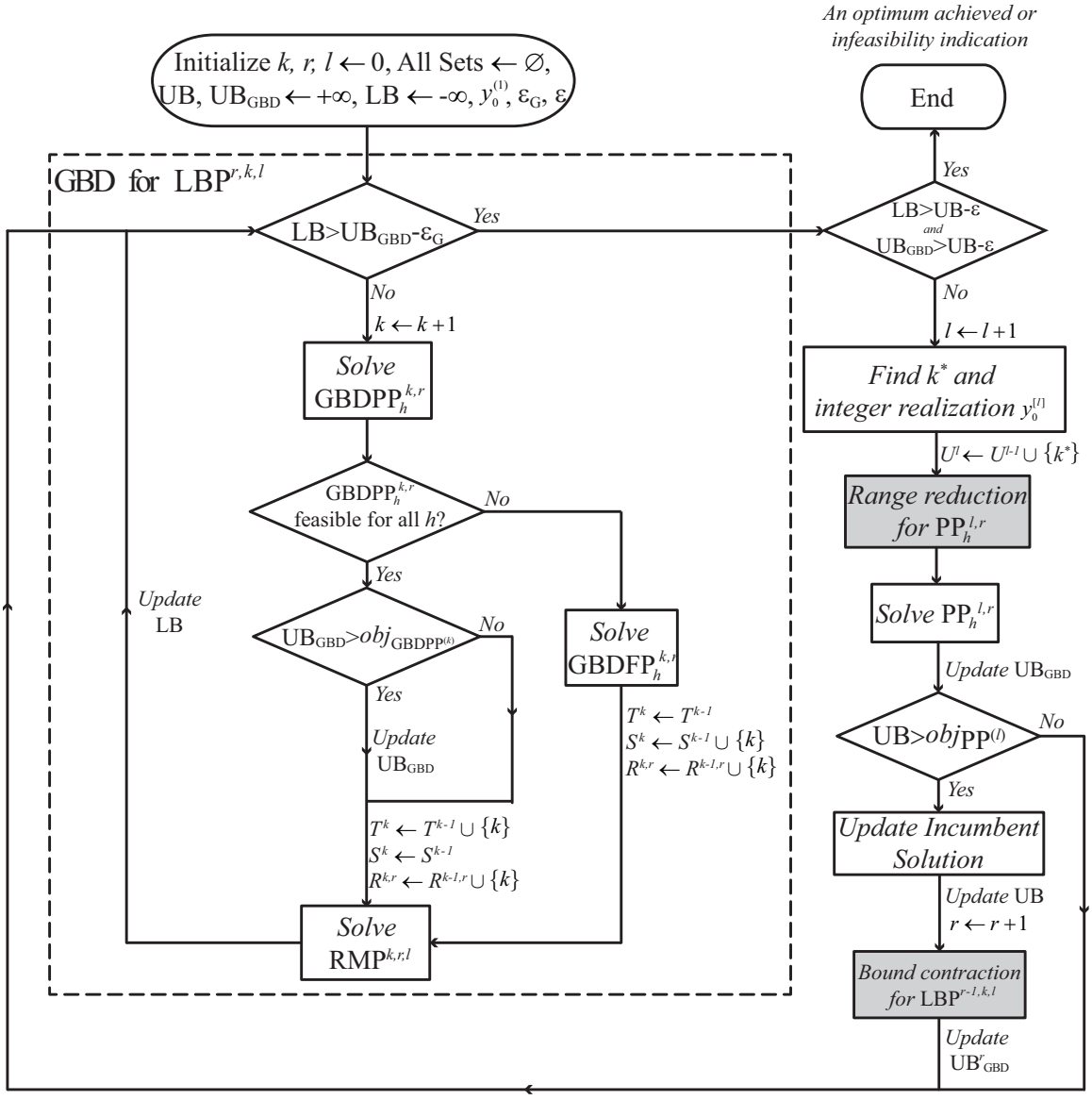

Figure 2.5: The algorithmic framework of NGBD with domain reduction.

bounding problem is:

$$
\begin{aligned}
&\min_{\substack{y_0,y_1,...,y_s\\ x_1,...,x_s,\\ q_1,...,q_s,}} \sum_{h=1}^{s} c_h^{\mathrm{T}} x_h \\
&\text{s.t. } y_h - y_0 = 0, \quad \forall h \in \{1,...,s\}, \\
&\qquad \hat{A}_h^r x_h + \hat{B}_h y_h + \hat{F}_h^r q_h \le \hat{d}_h^r, \quad \forall h \in \{1,...,s\}, \\
&\qquad (x_h, q_h) \in \hat{X}_h^r, \quad \forall h \in \{1,...,s\}, \\
&\qquad y_0 \in Y^r, \\
&\qquad \sum_{i \in I_1^j} y_{0,i} - \sum_{i \in I_0^j} y_{0,i} \le |I_1^j| - 1, \ \ \forall j \in R^{k,r} \cup U^l.
\end{aligned}
\tag{LBP^{r,k,l}}
$$

In this formulation, some coefficients for the second group of constraints are now dependent on bound contraction index r, as the changed convex relaxations influence these coefficients. Set $\hat{X}^r$ is also dependent on r and Y^r as well if bound contraction for y_0 is also performed. The integer cuts included also differ from those in (LBP^k). With these cuts we exclude (a) the integer realizations generated in GBD since the last time UB is updated and bound contraction is performed (and their indices are included in $R^{k,r}$), and (b) the integer realizations that have been used for constructing the primal subproblems. We do not exclude the integer realizations generated before the last bound contraction operation (except for those have been used to construct the primal subproblems), because those integer realizations are generated from less tight convex relations. The GBD subproblems for solving (LBP^{r,k,l}) are provided in Appendix A.2.3.

The updated form of the primal subproblems is:

$$\begin{aligned} obj_{\mathrm{PP}_h}(y_0^{[\,l\,]}) = \min_{x_h} \ & c_h^{\mathrm{T}} x_h \\ \text{s.t.} \ & A_h^{r,l} x_h + B_h y_0^{[\,l\,]} \le d_h^{r,l}, \\ & x_h \in X_h. \end{aligned} \tag{$\mathrm{PP}_h^{l,r}$}$$

Here the coefficients of the linear constraints are dependent on not only r, but also l, because extra range reduction calculations (which will be explained later) are performed before solving the primal subproblems. In order to construct ($\mathrm{PP}_h^{l,r}$), $y^{[\,l\,]}$ is selected from the integer realizations generated since the last domain reduction operation (except those have been used for ($\mathrm{PP}_h^{l,r}$)), according to the following rule:

$$y_0^{[\,l\,]} = y_0^{(k^*)}, \quad k^* = \underset{j \in R^{k,r} \setminus U^l}{\arg\min} \sum_{h=1}^{s} obj_{\mathrm{GBDPP}_h(y_0^{(j)})}.$$

Bound contraction problem

Following the domain reduction idea for GBD (that has been explained in Section 2), we can solve the following convex bound contraction subproblem for each variable whose range is to be reduced:

$$\begin{aligned} \min_{\substack{y_0,y_1,\ldots,y_s \\ x_1,\ldots,x_s,q_1,\ldots,q_s,}} \backslash \max \ & x_{h,i} \ \text{ or } \ y_{h,i} \\ \text{s.t.} \ & y_h - y_0 = 0, \quad \forall h \in \{1,...,s\}, \\ & \hat{A}_h^r x_h + \hat{B}_h y_h + \hat{F}_h^r q_h \le \hat{d}_h^r, \quad \forall h \in \{1,...,s\}, \\ & (x_h, q_h) \in \hat{X}_h^r, \quad \forall h \in \{1,...,s\}, \\ & y_0 \in \hat{Y}^r, \ \sum_{h=1}^{s} c_h^{\mathrm{T}} x_h \le \mathrm{UB}. \end{aligned} \tag{$\mathrm{BC}_{h,i}^r$}$$

Note that we perform domain reduction for y_0 by solving bound contraction problems for y_h instead of y_0. Since we know that $y_0 = y_h$, $\forall h$, then the bounds on y_0 can be updated as

$$y_{0,i}^L = \text{ceil}\left(\max_h\{y_{h,i}^L\}\right), \quad y_{0,i}^U = \text{floor}\left(\min_h\{y_{h,i}^U\}\right),$$

where ceil$(\cdot)$ is the function that maps a real value to the smallest following integer and floor$(\cdot)$ is the function that maps a real value to the largest previous integer.

We do not consider here the bound contraction problem on the y_0 subspace (that is proposed in Section 2 for GBD), because this reduced space problem is not so tight as the above full space bound contraction problem, and therefore cannot reduce as many as possible the nonconvex primal subproblems to be solved.

Problem ($\text{BC}_{h,i}^r$) are convex NLPs or LPs which can be readily solved by most of the existing optimization solvers. However, when the number of scenarios (s) is large, the number of variables for which ($\text{BC}_{h,i}^r$) needs to be solved and the size of each ($\text{BC}_{h,i}^r$) become large, and the total time for the bound contraction operations may be overly large compared to the time for solving other NGBD subproblems. Therefore, we propose to solve the following bound contraction problem instead:

$$\begin{aligned}
&\min_{x_h,q_h,y_h} \backslash \max \; x_{h,i} \;\text{ or }\; y_{h,i} \\
&\text{s.t. } obj_{\text{GBDPP}^{(j)}} \leq \text{UB} + \left(\sum_{\omega=1}^{s}(\lambda_\omega^{(j)})^T\right)\left(y_h - y_0^{(j)}\right) \\
&\qquad\qquad + (\kappa_h^{(j)})^T(\hat{A}_h^r x_h + \hat{B}_h y_h + \hat{F}_h^r q_h - \hat{d}_h^r), \quad \forall j \in J^{k,r}, \qquad (\text{subBC}_{h,i}^{r,k}) \\
&\quad \hat{A}_h^r x_h + \hat{B}_h y_h + \hat{F}_h^r q_h \leq \hat{d}_h^r, \\
&\quad (x_h, q_h) \in \hat{X}_h^r, \\
&\quad y_h \in \hat{Y}^r.
\end{aligned}$$

In this problem, for optimizing a variable for scenario h, only variables in this scenario is included in the problem (while variables for all scenarios are included in ($\mathrm{BC}^r_{h,i}$)). The first group of constraints are called bound contraction cuts or BC cuts, and they are included to strengthen ($\mathrm{subBC}^{r,k}_{h,i}$). For these cuts, set $J^{k,r}$ includes GBD iteration indices in $R^{k,r}$ at which the GBD primal problem is feasible. The optimal objective value, Lagrange multipliers, and the y_0 values of each such feasible GBD primal problem are $obj_{\mathrm{GBDPP}^{(j)}}$, $\lambda_h^{(j)}$ and $\kappa_h^{(j)}$, and $y_0^{(j)}$, respectively. Through the proof of the next proposition, we demonstrate that ($\mathrm{subBC}^{r,k}_{h,i}$) is a valid bound contraction problem.

Proposition 4. *The bound contraction cut does not cut off any optimal solution of* Problem (PS).

Proof. By definition, for each GBD iteration j,

$$obj_{\mathrm{GBDPP}^{(j)}} = \sum_{\omega=1}^{s} obj_{\mathrm{GBDPP}_h(y_0^{(j)})}.$$

According to strong duality of each GBD primal subproblem, for each scenario ω,

$$\begin{aligned} & obj_{\mathrm{GBDPP}_\omega(y_0^{(j)})} \\ = & \min_{(x_\omega,q_\omega)\in\hat{X}^r_\omega,\, y_\omega} c_\omega^T x_\omega + (\lambda_\omega^{(j)})^T(y_\omega - y_0^{(j)}) + (\kappa_\omega^{(j)})^T(\hat{A}^r_\omega x_\omega + \hat{B}_\omega y_\omega + \hat{F}^r_\omega q_\omega - \hat{d}^r_\omega). \end{aligned}$$

So for any $(x_\omega, q_\omega), y_\omega$ that is feasible for the original problem (PS),

$$obj_{\mathrm{GBDPP}_\omega(y_0^{(j)})} \le c_\omega^T x_\omega + (\lambda_\omega^{(j)})^T(y_\omega - y_0^{(j)}) + (\kappa_\omega^{(j)})^T(\hat{A}^r_\omega x_\omega + \hat{B}_\omega y_\omega + \hat{F}^r_\omega q_\omega - \hat{d}^r_\omega).$$

Lump the above inequality for all scenarios, then we get

$$obj_{\text{GBDPP}^{(j)}} \leq \sum_{\omega=1}^{s} c_\omega^T x_\omega + \sum_{\omega=1}^{s} (\lambda_\omega^{(j)})^T (y_\omega - y_0^{(j)}) \\ \sum_{\omega=1}^{s} (\kappa_\omega^{(j)})^T (\hat{A}_\omega^r x_\omega + \hat{B}_\omega y_\omega + \hat{F}_\omega^r q_\omega - \hat{d}_\omega^r). \tag{2.1}$$

For any feasible solution of (PS) that is not inferior than the current incumbent solution,

$$\sum_{\omega=1}^{s} c_\omega^T x_\omega \leq \text{UB},$$

$$(\kappa_\omega^{(j)})^T (\hat{A}_\omega^r x_\omega + \hat{B}_\omega y_\omega + \hat{F}_\omega^r q_\omega - \hat{d}_\omega^r) \leq 0, \quad \forall \omega \in \{1, \cdots, s\}.$$

Therefore, in order to generate a BC cut for a variable in scenario h, we can update equation (2.1) into:

$$obj_{\text{GBDPP}^{(j)}} \leq \text{UB} + \sum_{\omega=1}^{s} (\lambda_\omega^{(j)})^T (y_\omega - y_0^{(j)}) + (\kappa_h^{(j)})^T (\hat{A}_h^r x_h + \hat{B}_h y_h + \hat{F}_h^r q_h - \hat{d}_h^r). \tag{2.2}$$

Note that we drop from the third term of equation (2.1) the parts that are not associated with scenario h. Finally, considering that $y_\omega = y_0$ for all scenarios at the solution, we can change y_ω into y_h for all ω in (2.2). Therefore, (2.2) becomes:

$$obj_{\text{GBDPP}^{(j)}} \leq \text{UB} + \left(\sum_{\omega=1}^{s} (\lambda_\omega^{(j)})^T \right) (y_h - y_0^{(j)}) + (\kappa_h^{(j)})^T (\hat{A}_h^r x_h + \hat{B}_h y_h + \hat{F}_h^r q_h - \hat{d}_h^r). \tag{2.3}$$

Obviously BC cut (2.3) does not cut off an optimal solution of Problem (PS).

□

Remark 8. *In proof of* Proposition 4*, the reformulation of cut* (2.2) *to* (2.3) *relies on*

the special structure of the constraints linking different structures (i.e., $y_h = y_0$). If the original problem was written in form of (P1)*, then this reformulation would not be possible. This shows another advantage of formulation* (P) *for Benders decomposition-based global optimization.*

Remark 9. *It can be seen from the proof of* Proposition 4 *that, the BC cut* (2.3) *is implied by the feasible set of problem* ($\text{BC}^r_{h,i}$)*. Therefore, bound contraction problem* ($\text{subBC}^{r,k}_{h,i}$) *can be viewed as a relaxation of* ($\text{BC}^r_{h,i}$)*.*

Remark 10. *The BC cut can actually contain more nonpositive terms by dualizing nonlinear convex constraints in set $\hat{X}^r_h$. In this way the BC cut is stronger, but it will become nonconvex. Therefore, we only dualize linear constraints for construction of the BC cut.*

Remark 11. *If a bound contraction problem, either* ($\text{BC}^r_{h,i}$) *or* ($\text{subBC}^{r,k}_{h,i}$)*, is infeasible, the corresponding lower bounding problem* ($\text{LBP}^{r,k,l}$) *is infeasible and therefore* NGBD *will stop solving any lower bounding problem by* GBD*.*

Extra range reduction calculations for primal subproblems

When solving a primal subproblem, y_0 is fixed at a constant $y_0^{[\,l\,]}$, then BC cut (2.3) can be reduced to yield a simple way to estimate the bounds for a variable $x_{h,i}$. Specifically, we replace y_h in the cut by constant $y_0^{[\,l\,]}$, and keep in the last term one single constraint that contains $x_{h,i}$ as the only variable and has a nonzero Lagrange multiplier. Let this constraint be $\alpha^r_{h,i}x_{h,i} - d^r_{h,i} \leq 0$ (which is usually just a simple bound on $x_{h,i}$), then the cut becomes:

$$obj_{\text{GBDPP}^{(j)}} \leq \text{UB} + \left(\sum_{\omega=1}^{s}(\lambda^{(j)}_\omega)^T\right)\left(y_0^{[\,l\,]} - y_0^{(j)}\right) + (\kappa^{(j)}_{h,i})(\alpha^r_{h,i}x_{h,i} - d^r_{h,i}),$$

which can be further expressed as:

$$x_{h,i}\begin{cases}\geq \dfrac{obj_{\text{GBDPP}^{(j)}} - \text{UB} - \left(\sum_{\omega=1}^{s}(\lambda_{\omega}^{(j)})^T\right)\left(y_0^{[\,l\,]} - y_0^{(j)}\right) + d_{h,i}^r\kappa_{h,i}^{(j)}}{\alpha_{h,i}^r\kappa_{h,i}^{(j)}}, & \text{if } \alpha_{h,i}^r > 0,\\ \leq \dfrac{obj_{\text{GBDPP}^{(j)}} - \text{UB} - \left(\sum_{\omega=1}^{s}(\lambda_{\omega}^{(j)})^T\right)\left(y_0^{[\,l\,]} - y_0^{(j)}\right) + d_{h,i}^r\kappa_{h,i}^{(j)}}{\alpha_{h,i}^r\kappa_{h,i}^{(j)}}, & \text{if } \alpha_{h,i}^r < 0.\end{cases}$$

Since the BC cut is valid for all $j \in J^{k,r}$, so the $x_{h,i}$ bounds can be updated by the above calculation for all BC cuts.

If with the above calculation the lower bound of a variable is higher than its upper bound, then $y_0 = y_0^{[\,l\,]}$ is either infeasible for Problem (PS) or cannot lead to a solution better than the incumbent solution. Therefore, we do not need to solve the primal subproblems for $y_0 = y_0^{[\,l\,]}$. This can help to reduce the number of nonconvex primal subproblems to be solved in NGBD and therefore reduce the solution time.

2.4 Case Studies

2.4.1 Case Study I: A Natural Gas System

The purpose of this case study is to compare the computational efficiency of three methods: the standard GBD, the proposed GBD with domain reduction integrated, and the monolith approach that solves the problem directly using an optimization solver (without decomposition). The case study problem is an optimal operation problem for an industrial natural gas production system, initially studied in [41], and recently reformulated in [25]. Due to the reformulation, the operation problem can be separated into two parts, one part is a convex pressure-flow relationship model, and

the other is a nonconvex pooling model. The two parts are linked with linear unit conversion constraints. This reformulated operation problem has the structure of (P) and can be readily solved by GBD via viewing the variables in the pooling model as y_0.

This operation problem has 517 variables and 1004 constraints in total. When using GBD to solve the problem, the convex NLP subproblem (GBDPP^k) / (GBDFP^k) has ∼370 variables and ∼740 constaints, and the nonconvex NLP subproblem (RMP^k) / (FRMP^k) have ∼100 variables and more than 270 constraints. The bound contraction problems (BC$_i^k$) and (y_0BC$_i^k$) are LPs. The size of (BC$_i^k$) is similar to that of the original problem, and the size of (y_0BC$_i^k$) is similar to that of (RMP^k). The convex relaxations for constructing bound contraction problems are obtained via the classical McCormick relaxation.

The case study problem was solved on Ubuntu 12.04 with a single 3.40 GHz CPU, 4 GB memory. The problem was formulated on GAMS 24.2.3. Both the monolith approach and the two GBD methods employed BARON 12.7.7 for nonconvex NLP problems. The two GBD methods also employed CONOPT 3.15P for convex NLP problems and CPLEX 12.6 for LP problems. The relative termination tolerance ϵ for optimization was set to be 10^{-3} for all the three methods.

Results and Discussion

Table 2.1 summarizes the computational results with the three methods. The first column of Table 2.1 shows the monolith approach that uses BARON to solve the problem directly. We set up 3600 seconds as the maximum run time for the solver, and BARON terminated at the maximum run with a relative gap of 2.5%. Compared

Table 2.1: Computational results for case study I

Method	Monolith[a]	GBD[b]	GBD[b]	GBD[b]
Bound Contraction Type	-	No BC[c]	y_0BC[d]	BC[e]
Number of RMP[f]	-	47	54	51
Time for RMP[f] (s)	-	436.9	350.9	290.8
Ave. time for one RMP[f] (s)	-	9.3	6.5	5.7
Time for Bound Contraction (s)	-	-	1.0	8.5
Time for GBDPP[g]/GBDFP[h] (s)	-	0.8	0.8	0.7
Total Time (s)	3600 †	437.7	352.7	300.0
Optimality Gap (%)	2.5	< 0.01	< 0.01	< 0.01

† Total time reaches the 3600 s run time limit.
[a] Monolith refers to solving the problem directly using BARON.
[b] GBD refers to generalized Benders decomposition.
[c] No BC refers to no bound contraction operation.
[d] y_0BC refers to bound contraction operation in y_0 subspace that are achieved by solving ($y_0\text{BC}_i^k$).
[e] BC refers to bound contraction operation in full space that are achieved by solving (BC_i^k).
[f] RMP refers to (RMP^k), the relaxed master problem in the GBD procedure.
[g] GBDPP refers to (GBDPP^k), the GBD primal problem.
[h] GBDFP refers to (GBDFP^k), the GBD feasibility problem.

to monolith approach, the standard GBD (shown in the second column of the table) terminated in 437.7 seconds with an optimality gap within the given relative tolerance. The last two columns of the table show the results with the GBD integrated with domain reduction. The third column is with the reduced space bound contraction problem ($y_0\text{BC}_i^k$) and the fourth column with the full space bound contraction problem (BC_i^k). Due to the reduced bounds from bound contraction operations, our proposed GBD methods can solve the nonconvex relaxed master problems (RMPs) more quickly and therefore require less total solution time. Since (BC_i^k) is tighter than ($y_0\text{BC}_i^k$), so it leads to tighter bounds of y_0 and therefore fewer RMPs to solve and faster solution for RMP. On the other hand, (BC_i^k) takes more time to solve.

2.4.2 Case Study II: A Power Flow System

The second case study problem is an integrated design and operation problem for a mixed AC-DC distribution subsystem, which was adapted from a benchmark electricity distribution system of medium office buildings in [14]. Since the problem addresses the operational part for 24 time periods, the problem has a structure of (PS) with y_0 consisting of integer design decisions and h indexing different time periods. Therefore, this problem structure can be exploited by NGBD for an efficient solution. [14] solved the problem using a simplified NGBD approach, in which the lower bounding problems are solved directly with an optimization solver rather than through GBD.

This case study is to compare the computational efficiency of the following six solution approaches:

1. Monolith+BT - This refers to the monolith approach that solves the problem directly using a global optimization solver (BARON). Before sending the problem to BARON, the variables bounds are tightened by solving bound tightening problems (which are essentially problem (BC_i^k) with UB being $+\infty$).

2. F&R-NGBD - This refers to the simplified NGBD method used by [14].

3. F&R-NGBD+BT - This refers to the simplified NGBD method used by [14], with bound tightening problems solved before the start of the NGBD.

4. NGBD - This refers to the standard NGBD.

5. NGBD+BC - This refers to the NGBD with bound contraction problem ($\mathrm{BC}_{h,i}^r$). The size of ($\mathrm{BC}_{h,i}^r$) depends on the number of scenarios (which are time periods in the case study).

6. NGBD+subBC - This refers to the NGBD with bound contraction problem ($\text{subBC}_{h,i}^{r,k}$). The size of ($\text{subBC}_{h,i}^{r,k}$) is independent of the number of scenarios.

In the five NGBD methods, the convex relaxations for constructing lower bounding problems and bound contraction problems are generated through McCormick relaxation and outer linearization of any nonlinear convex functions, as explained in [14]. Therefore the lower bounding problems are MILPs and the bound contraction problems are LPs. The GBD feasibility subproblems minimize the ∞-norm of $\upsilon^+ + \upsilon^-$.

The overall problem is a nonconvex MINLP that has 37,677 variables (in which 57 are binary) and 139,022 constraints. In the NGBD methods, LP subproblems ($\text{GBDPP}_h^{k,r}$) / ($\text{GBDFP}_h^{k,r}$) have ∼1,320 variables and ∼4,620 constaints; MILP subproblems ($\text{RMP}^{k,r,l}$) / ($\text{FRMP}^{k,r,l}$) have 58 variables (in which 57 are binary) and more than 130 constraints; nonconvex NLP problems ($\text{PP}_h^{l,r}$) have ∼1,300 variables and ∼4,500 constaints. The LP bound contraction problem ($\text{BC}_{h,i}^{r}$) have 37,677 variables and 139,023 constraints. The LP bound contraction problem ($\text{subBC}_{h,i}^{r,k}$) has ∼1,380 variables and ∼4,750 constaints,

The case study problem was solved on Ubuntu 12.04 with 10^{-2} relative termination tolerance and three increasingly better computing environments, in order to compare results of proposed methods to ones in the literature:

Environment (a) uses a single 2.40 GHz CPU, 4 GB memory, and the model is formulated on GAMS 24.1.3. The algorithms with this environment employed BARON 12.5.0 for nonconvex MINLP/NLP problems, and CPLEX 12.5.1.0 for MILP/LP problems.

Environment (b) uses a single 2.90 GHz CPU, 4 GB memory, and the model

is formulated on GAMS 24.1.3. The algorithms with this environment employed BARON 12.5.0 for nonconvex MINLP/NLP problems, CPLEX 12.5.1.0 for MILP/LP problems, and this environment is identical with the one in the literature [14].

Environment (c) uses a single 3.40 GHz CPU, 4 GB memory, and the model is formulated on GAMS 24.2.3. The algorithms with this environment employed BARON 12.7.7 for nonconvex MINLP/NLP problems, and CPLEX 12.6 for MILP/LP problems.

Results and Discussion

Table 2.2 summarizes the computational results for comparisons of branch-and-reduce method, NGBD method in the literature [27] and [14], and the proposed methods integrated bound contraction problems ($\mathrm{BC}^{r}_{h,i}$) and ($\mathrm{subBC}^{r,k}_{h,i}$).

The first row in Table 2.2 is the computation result for monolith approach with branch-and-reduce method implemented by BARON in computing environment (a). This large-scale MINLP is clearly so difficult that no solution could be obtained after a reasonable given time.

The second and third row are results from NGBD and NGBD with initial bound tightening in computing environment (b) that reported in [14]. Both methods terminated and the benefits of initial bound tightening procedure was reported. It is seen that integrating bound tightening procedure accelerates the tailored NGBD method that is developed in the same paper, by more than an order of magnitude.

The fourth row is the result for standard NGBD approach both in this chapter and in [27]; and it is implemented in computing environment (a). It can be seen that this method terminates in 61952 seconds, which is faster than tailored NGBD in

[14]. Also, the solution time for nonconvex primal subproblems dominate the time for NGBD. During NGBD procedure, 23 primal subproblems returned feasible solution or indicated infeasibility due to the exceed of 30 minutes time-out limit for each primal subproblem.

The fifth and sixth row are results for proposed methods that integrated bound contraction problems ($\mathrm{BC}^{r}_{h,i}$) and ($\mathrm{subBC}^{r,k}_{h,i}$). Both of them are solved in computing environment (a). The NGBD that integrates full bound contraction problems takes significantly longer time than standard NGBD, since each bound contraction problem has the same problem size as original problem and the algorithm cannot terminate within given tolerance in 400000 seconds. Compared to the standard NGBD and NGBD integrated full bound contraction problems, NGBD that incorporates decomposed bound contraction problems spends shorter time than the other solving methods, and all primal subproblems are efficiently solved by global optimization solver BARON. It is also seen that the number of primal subproblems that are solved in the proposed method with ($\mathrm{subBC}^{r,k}_{h,i}$) is much smaller than the standard NGBD.

The last row is a result for proposed methods that integrated bound contraction problems ($\mathrm{subBC}^{r,k}_{h,i}$) in computing environment (c), in order to give a reference of comparisons between the proposed method in this chapter and the results in literatures. The result with faster CPU indicates that the proposed method could return a global optimum within a much shorter time than results given in literature.

2.5 Summary

This chapter integrated domain reduction techniques for Benders decomposition-based global optimization methods. We took standard GBD and NGBD as examples

Table 2.2: Computational results for case study II

Method	Total Time (s)	Time for PP_h (s)	Num. of PP_h	CPU GHz	Time for BC^b (s)	UB/LB (MW·h)
Monolith+BT	178665 †	-	-	2.4	-	$+\infty$/768.2
F&R-NGBD	464272	459047	1680	2.9	-	783.9/776.2
F&R-NGBD+BT	27337	20727	1128	2.9	3833	783.9/776.2
NGBD	61952	61692	3360	2.4	-	783.6/775.8
NGBD+BC	407824 †	N/A	N/A	2.4	N/A	787.6/770.0
NGBD+subBC	25451	910	552	2.4	23846	783.6/775.8
NGBD+subBC	16176	847	405	3.4	14907	783.6/775.8

†: Terminated with intermediate information.

that were integrated domain reduction. By incorporating domain reduction techniques via bound contraction operations and range reduction calculations, the performance of Benders decomposition-based global optimization methods were improved. The efficiency of the proposed methods were demonstrated by an operation problem of natural gas production system and an integrated design and operation problem of mixed AC-DC power distribution system.

Chapter 3

Benders Decomposition-based Optimization for Natural Gas System

In this chapter, we consider an industrial natural gas production network. A gas production network usually requires large investment costs, a long lift time, properly justified characters, and satisfaction of the many associated uncertain factors. In order to ensure that the network can provide enough gas products under different uncertainty scenarios while optimizing the expected total profit and achieving the most economic designs, the resulting design and long-term operation problem is a large-scale nonconvex MINLP, which cannot be solved practically by any state-of-the-art optimization solver, and currently existed standard decomposition-based global optimization methods. A customized decomposition-based optimization method, called multi-loop NGBD method, is therefore employed to efficiently solve this problem.

The remaining part of this chapter is organized as follows. First, background of natural gas production system is provided, which justifies the necessary constraints that are needed in its mathematical model. Next, the two-stage stochastic programming model is presented in the context of a real industrial natural gas production

system. Third, the model reformulation procedure is explained step by step, and the structure of the final reformulated model is analyzed. Then the multi-loop NGBD method is developed to exploit the structure of the reformulated model, and its advantage over the classical NGBD and the monolith approach is demonstrated via case study results. The chapter ends with a summary.

3.1 Background

In a natural gas production network, raw natural gases from different gas wells are boosted via compressors, mixed at preprocessing facilities or simple pipeline junctions, and finally gathered at terminal processing plants that produce the final gas products. Preprocessing facilities, typically gas platforms at reservoirs, are used for oil separation and water removal. Oil separation is to separate dissolved natural gas from oil, and water removal (dehydration) is to reduce corrosion and make raw natural gas amenable to transport. Raw natural gases from different reservoirs usually contain different amounts of contaminants (such as CO, N_2, CO_2, H_2S, and water vapor)[34], which can hinder natural gas processing and pollute the environment. Therefore, contents of the contaminants need to be kept below certain thresholds before the gases enter the terminal processing plants. To obtain the desired dry natural gas products (mainly methane), the inlet flow pressure to a preprocessing or a terminal processing facility needs to be within a certain range [11, 20, 23, 35]. Moreover, the whole production network has to be robust against the fluctuation in raw gas compositions and the large variation in demands for the gas products. Ideally, an optimization model should describe gas flow compositions, pressures, and uncertainties explicitly, so that the optimization result can represent realistically feasible and optimal decisions.

3.2 The Optimization Model for Integrated Design and Operation Under Uncertainty

The optimization model is presented for a real and representative industrial natural gas production system, called Sarawak Gas Production System (SGPS). This system was originally studied by [41] for optimal short-term operation, and then by [26] for integrated design and operation through a stochastic pooling model. Figure 3.1 illustrates the superstructure of SGPS. Each ellipse in the figure refers to a gas field modeled as a gas platform, which contains multiple gas wells that are not explicitly showed in the figure but are listed in the Appendix B.1. Each gray circle in the figure refers to remote gas production subnetwork connected to SGPS, and it can also be simplified as a gas platform with available flow rate and inlet pressure ranges. Each rectangle refers to a gas platform, a slug-catcher [41], or a simple pipeline conjunction, at which gas flows are mixed and split. Although a gas platform often involves oil-gas separation and water removal, the platform does not remove major impurities in the gas significantly. The three liquefied natural gas (LNG) plants at the end of the network superstructure, labeled as LNG1, LNG2, and LGN3, purify and convert raw gases into final LNG products. For a LNG plant to work properly, the composition of gas entering the plant needs to satisfy certain specification.

For modeling purpose, the gas production network is viewed as a directed graph (V, E), where V is the set of all vertices and E is the set of all directed edges. The vertices represent gas wells, platforms, pipeline junctions, and terminal LNG plants, and the directed edges represent pipelines connecting two vertices. The proposed optimization model is constructed based on previously published work [26, 41]. It contains

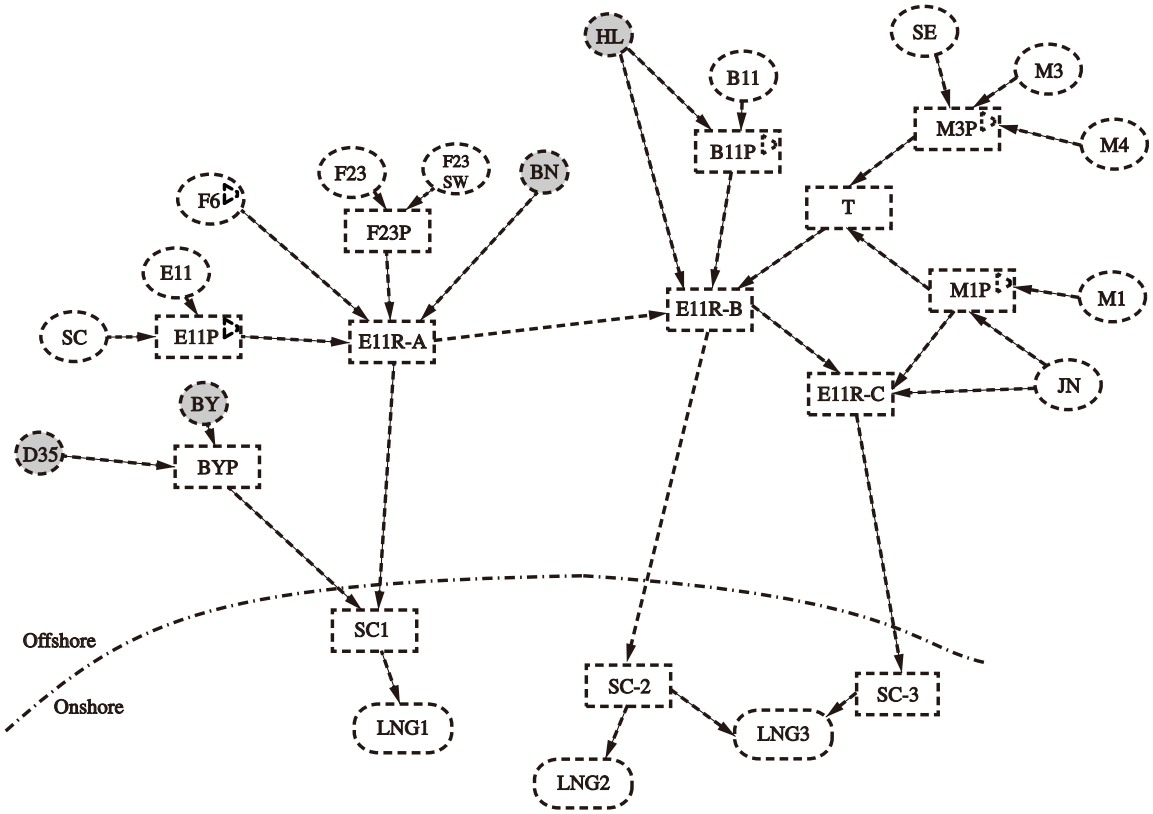

(V, E)	Edges(E)	Vertices(V)				
Units	Pipelines	Gas fields	Gas platforms	Terminal plants	Remote subnetwork	Compressors
Symbols	→	⬭	▭	▭	●	▷

Figure 3.1: The superstructure of Sarawak Gas Production System (SGPS)

a stochastic pooling model [26], which is a two-stage, scenario-based stochastic programming model that describes the topology relationships among the vertices and edges, and the material balances for each major components of the gas flows. It also combines a detailed operation model for each uncertainty scenario based on the work by [41], which describes the relationships between pressures, flows, and energy consumptions in the system. The objective of optimization is to determine the system network structure design that maximize the expected net present value (NPV) of the

system over its life span. Table 3.1 shows all the symbols used in the model. The set elements and parameter values are showed in the Appendix B. Next, each part of the optimization model is presented step by step.

Table 3.1: Descriptions of Symbols

Symbol	Type	Descriptions
E	set	edges in the directed flow graph
E^L	subset of E	edges representing long pipelines
E^W	subset of E	edges connecting wells and platforms
V	set	vertices in the directed flow graph
$\bar{V}$	subset of V	vertices located before compressors
V^C	subset of V	vertices with onsite compressors
V^S	subset of V	vertices representing remote subnetwork
V^T	subset of V	vertices representing terminal plants
V^W	subset of V	vertices representing wells
Ω	set	index set for components in flow
Φ	set	index set for scenarios
CC	superscript	indicator of the capital cost
in	superscript	indicator of the inlet pressures
LB	superscript	indicator of the lower bounds
NPV	superscript	indicator of the net present value
OP	superscript	indicator of the operation cost
out	superscript	indicator of the outlet pressures
q	subscript	index of components
UB	superscript	indicator of the upper bounds
v	superscript	indicator of vertices

Symbol	Type	Descriptions
w	subscript	index of scenarios
f	variable	molar flow rate, $Mmol/day$
s	variable	flow split ratio
y	binary variable	decision variable for development of vertex or edge
C	variable	cost, $Million\$$
P	variable	pressure before pressure regulator on a vertex, bar
$\hat{P}$	variable	pressure after pressure regulator on a vertex, bar
$\bar{P}$	variable	pressure after pressure regulator on an edge, bar
Q	variable	volumetric flow rate, hm^3/day
W	variable	compressor power, MW, $1MW{=}10^6 Watt$
δ	variable	pressure drop due to pressure regular at an edge, bar
Δ	variable	pressure drop due to pressure regular at a vertex, bar
r	parameter	annual discount rate
p	parameter	probability of scenarios
D	parameter	demands of product at terminal plants, $Mmol/day$
F	parameter	flow bounds for edges, $Mmol/day$
K	parameter	composition bounds for terminal plants (%)
M	parameter	the big-M in constraints
U	parameter	component percentage at wells, (%)
Z	parameter	flow bounds for vertices, $Mmol/day$
α	parameter	Darcy's constant, bar^2day^2/hm^6
β	parameter	non-Darcy correction factor, bar^2day^2/hm^6
γ	parameter	power cost, $million\$/(MW \cdot day)$
κ	parameter	coefficients for long pipelines, bar^2day^2/hm^6

Symbol	Type	Descriptions
λ	parameter	well performance coefficients
ν	parameter	coefficient for compression model
π	parameter	reservoir pressure, bar
σ	parameter	compressors capability ratio
ϑ	parameter	well performance coefficients, bar^2day^2/hm^6
ϕ	parameter	unit conversion constant, $hm^3/Mmol$
Γ	parameter	pressure bounds for vertices, bar
Ψ	parameter	bounds for compressor power, MW

3.2.1 The Stochastic Pooling Model

The stochastic pooling model is a two-stage, scenario based stochastic programming model. In this model, the first-stage decisions are network structure design decisions that need to be implemented before the construction of the real physical system. The second-stage decisions are operational decisions on flow rates, which are included to predict the profits of operating the system under different uncertainty scenarios. Each uncertainty scenario is indexed by subscript w. This model consists of the following Eq. (3.1-3.12).

$$\begin{aligned} &f_{j,k,q,w} = s_{j,k,w}\left(\sum_{i\in\{i|(i,j)\in E\}} f_{i,j,q,w}\right), \\ &\forall (j,k) \in \{(j,k)\in E \mid j \notin V^W \cup V^S\}, \quad \forall q \in \Omega, \quad \forall w \in \Phi \end{aligned} \tag{3.1}$$

$$s_{j,k,w} \geq 0, \quad \forall (j,k) \in \{(j,k)\in E \mid j \notin V^W \cup V^S\}, \quad \forall w \in \Phi \tag{3.2}$$

$$\sum_{k\in\{k|(j,k)\in E\}} s_{j,k,w} = 1, \quad \forall j \in V \setminus (V^W \cup V^S \cup V^T) \tag{3.3}$$

$$y_i^v \geq y_{i,j}, \quad \forall (i,j) \in E \tag{3.4}$$

$$y_j^v \geq y_{i,j}, \quad \forall (i,j) \in E \tag{3.5}$$

$$y_i^v \leq \sum_{j \in \{j|(i,j) \in E\}} y_{i,j}, \quad \forall i \in V \setminus V^T \tag{3.6}$$

$$y_j^v \leq \sum_{i \in \{i|(i,j) \in E\}} y_{i,j}, \quad \forall j \in V \setminus (V^S \cup V^W) \tag{3.7}$$

$$y_{i,j} F_{i,j}^{LB} \leq \sum_{q \in \Omega} f_{i,j,q,w} \leq y_{i,j} F_{i,j}^{UB}, \ \ \forall (i,j) \in E, \quad \forall w \in \Phi \tag{3.8}$$

$$y_i^v Z_{i,w}^{LB} \leq \sum_{q \in \Omega} \sum_{j \in \{j|(i,j) \in E\}} f_{i,j,q,w} \leq y_i^v Z_{i,w}^{UB}, \ \ \forall i \in V \setminus V^T, \quad \forall w \in \Phi \tag{3.9}$$

$$y_k^v D_{k,w}^{LB} \leq \sum_{q \in \Omega} \sum_{j \in \{j|(j,k) \in E\}} f_{j,k,q,w} \leq y_{k,k} D_{k,w}^{UB}, \ \ \forall k \in V^T, \ \forall w \in \Phi \tag{3.10}$$

$$\left(\sum_{q \in \Omega} \sum_{j \in \{j|(j,k) \in E\}} f_{j,k,q,w} \right) K_{k,q}^{LB} \leq \sum_{j \in \{j|(j,k) \in E\}} f_{j,k,q,w}, \ \forall k \in V^T, \ \forall q \in \Omega, \ \forall w \in \Phi \tag{3.11}$$

$$\left(\sum_{q \in \Omega} \sum_{j \in \{j|(j,k) \in E\}} f_{j,k,q,w} \right) K_{k,q}^{UB} \geq \sum_{j \in \{j|(j,k) \in E\}} f_{j,k,q,w}, \ \forall k \in V^T, \ \forall q \in \Omega, \ \forall w \in \Phi \tag{3.12}$$

Eq. (3.1-3.3) stand for the material balances for different components (indexed by q) of the gas flows. Eq. (3.1) reflects the fact that different components of gas are split at a vertex with the same ratios (denoted by s). Specifically, the rate of component q in a flow leaving a vertex j equals to the rate of the same component in all flows entering node j times a split fraction for this flow. This relationship is included in the model for all gas flows except those coming out of a starting vertex (i.e., gas wells or remote subnetworks), as the ratios of their components are parameters that are independent of the optimization decisions. Eq. (3.2-3.3) mean that the split fractions

are nonnegative, and the sum of the split fractions of all flows leaving vertex j equals to 1. Note that, Eq. (3.1-3.3) generally introduce nonconvexity, but they can be reduced to a set of linear constraints for a vertex j, if this vertex has only one outlet flow.

Eq.(3.4-3.5) denote topology restriction of the network structure design, they mean that edge (i, j) can be developed only when both vertex i and vertex j are developed. Eq.(3.6-3.7) are introduced to prevent developing a vertex that is not connected to any other vertex. Note that an optimal solution cannot contain an isolated vertex (with certain investment cost) no matter whether Eq.(3.6-3.7) are included in the model, but including these constraints can expedite the solution of the optimization problem.

Eq. (3.8-3.12) pose bounds on the gas flow rates in the pipelines, the total gas flow rates going through a vertex, and component contents of gas in the terminal vertex. When a vertex or edge is not to be developed, the related flow rates are forced to be zero by the bounding constraints.

3.2.2 The Pressure Flow Relationships

Gas flows are driven in the gas production network by pressure differentials, so they are not only restricted by the capacities of gas wells and pipelines, but also restricted by reservoir pressures and pressure rises that can be provided by the compressors. In [26], pressure flow relationships are not considered in the integrated design and operation model, as they can make the optimization model too complicated for practical solution. [41] considers the pressure flow relationships for deterministic operation problems only, and the resulting problem is already very challenging to solve. We

incorporate into our proposed optimization model equations describing the pressure-flow-energy relationships in wells, pipelines and compressors (called well performance, pipeline performance, and compression performance models, respectively), based on the work in [41]. In the next section we will show how reformulation of these equations can lead to a less nonconvex and better structured problem.

Well Performance Model consists of the following Eq. (3.13-3.15). Raw natural gas is corrosive and possibly sticky before going into preprocessing facilities from wells, and a first-principle well performance model can be overly complicated for optimization. Therefore, the well performance is approximated by Eq. (3.13) [41]. In this equation, Darcy's constant $\alpha_{i,w}$ and non-Darcy correction factor $\beta_{i,w}$ reflect in-flow performance, $\vartheta_{i,w}$ and $\lambda_{i,w}$ reflect vertical lift performance, $P^{out}_{i,w}$ and $\pi_{i,w}$ represent tubing head and reservior pressure, $Q_{i,j,w}$ represents volumetric flow rate from well i to a platform j. If the gas well y^v_i is not to be developed, $y_{i,j}$ will be zero and the volumetric gas flow rate in the well will be forced to be zero. With Eq. (3.13), equations (3.14) and (3.15) imply each other so only one of them is needed for optimization. However, they are both included for more efficient global optimization.

$$\alpha_{i,w}Q_{i,j,w} + (\beta_{i,w} + \vartheta_{i,w})Q^2_{i,j,w} = y_{i,j}(\pi^2_{i,w} - \lambda_{i,w}(P^{out}_{i,w})^2), \quad \forall (i,j) \in E^W, \quad \forall w \in \Phi \tag{3.13}$$

$$Q_{i,j,w} \geq 0, \quad \forall (i,j) \in E^W, \quad \forall w \in \Phi \tag{3.14}$$

$$P^{out}_{i,w} \leq \pi_{i,w}, \quad \forall i \in \{i|(i,j) \in E^W\}, \quad \forall w \in \Phi \tag{3.15}$$

Pipeline Performance Model consists of Eq. (3.16-3.17). In a gas pipeline, the gas flow usually includes both gas and liquid phases and there may be mass transfer between the two phases. In order to simplify the model, gas flows are assumed to

contain only gas phase and behave like ideal gas. With these assumptions and under steady-state operation, the pressure flow relationship in a long transmission pipeline that is longer than 20km can be well approximated by Eq. (3.16) [41]. Here $P^{out}_{i,w}$ denotes the pressure at the outlet of vertex i, $P^{in}_{i,w}$ denotes the pressure at the inlet of vertex i, set $E^L \subset E$ includes edges representing long pipelines. This equation also enforces the volumetric flow rate to be zero if the long pipeline is not to be developed. When a pipeline is short (such as one connects a gas well to a gas platform), the pressure drop along the pipeline is usually negligible, so it can be described by Eq. (3.17).

$$y_{i,j}((P^{out}_{i,w})^2 - (P^{in}_{j,w})^2) = \kappa_{i,j} Q^2_{i,j,w}, \quad \forall (i,j) \in E^L, \quad \forall w \in \Phi \tag{3.16}$$

$$y_{i,j}(P^{out}_{i,w} - P^{in}_{j,w}) = 0, \quad \forall (i,j) \in E \setminus E^L, \quad \forall w \in \Phi \tag{3.17}$$

Compression Performance Model consists of Eq. (3.18-3.20). Eq. (3.18) relates the power consumption W with the outlet-inlet pressure ratio and the molar flow rates of gas compressed, where $\sigma_j = 0.121\ MW \cdot day/Mmol$ and $\nu = 1/3$ are the parameters obtained from process data [41], and set $V^C \subset V$ includes vertices having onsite compressors. Eq. (3.19) ensures that the inlet pressure of a compressor is no larger than the outlet pressure. Eq. (3.20) is to bound the power consumption of a compressor and enforce the power consumption to be zero when the gas platform containing the compressor is not to be developed.

$$W_{j,w} - \sigma_j \sum_{i \in \{i|(i,j)\in E\}} \sum_{q \in \Omega} f_{i,j,q,w} \left[\left(\frac{P^{out}_{j,w}}{P^{in}_{j,w}} \right)^{\nu} - 1 \right] = 0, \quad \forall j \in V^C, \quad \forall w \in \Phi \tag{3.18}$$

$$P^{in}_{i,w} \leq P^{out}_{i,w}, \quad \forall i \in V^C, \quad \forall w \in \Phi \tag{3.19}$$

$$y^v_i \Psi^{LB}_i \leq W_{i,w} \leq y^v_i \Psi^{UB}_i, \quad \forall i \in V^C, \quad \forall w \in \Phi \tag{3.20}$$

Other Pressure Constraints are given in Eq. (3.21-3.23). Eq. (3.21) means that there is no pressure rise for a vertex having no onsite compressor. If the vertex is a well, this relationship is already described by Eq. (3.15). Eq. (3.22-3.23) pose bounds on pressures at the inlet of a vertex (excluding the well) and at the outlet of a vertex, respectively.

$$P^{in}_{i,w} \geq P^{out}_{i,w}, \quad \forall i \in V \setminus (V^C \cup V^W), \quad \forall w \in \Phi \tag{3.21}$$

$$y^v_i \Gamma^{in,LB}_{i,w} \leq P^{in}_{i,w} \leq y^v_i \Gamma^{in,UB}_{i,w}, \quad \forall i \in V \setminus V^W, \quad \forall w \in \Phi \tag{3.22}$$

$$y^v_i \Gamma^{out,LB}_{i,w} \leq P^{out}_{i,w} \leq y^v_i \Gamma^{out,UB}_{i,w}, \quad \forall i \in V, \quad \forall w \in \Phi \tag{3.23}$$

3.2.3 Equations for Unit Conversion and the Economic Objective

Molar component flow rates and volumetric total flow rates are used in the stochastic pooling model and in the pressure flow relationship constraints, respectively. The following Eq. (3.24-3.25) link the two types of flow rates, under the ideal gas assumption. ϕ (=42.28 $Mmol/hm^3$) is the unit conversion parameter [41] and $U_{i,q,w}$ is the mole fraction of component q at well or remote subnetwork platform i in scenario w.

$$f_{i,j,q,w} = \phi U_{i,q,w} Q_{i,j,w}, \quad \forall (i,j) \in \{(i,j) \in E \mid i \in V^W \cup V^S\}, \ \forall w \in \Phi \tag{3.24}$$

$$\sum_{q \in \Omega} f_{i,j,q,w} = \phi Q_{i,j,w}, \quad \forall (i,j) \in E, \ \forall w \in \Phi \tag{3.25}$$

The objective of the optimization is to minimize the negative expected NPV of the system over its life span, $C^{(NPV)}$, as defined in Eq. (3.26). $\bar{C}^{(CC)}$ represents the total capital cost, which is calculated using Eq. (3.27), $\bar{C}_w^{(OP)}$ represents the annual operation profit for scenario w, which is calculated using Eq. (3.28), p_w denotes the probability for uncertainty scenario w, L denotes the system life span, and r denotes the annual discount rate.

$$C^{(NPV)} = -\bar{C}^{(CC)} - \sum_{t=1}^{L} \sum_{w} \frac{p_w \bar{C}_w^{(OP)}}{(1+r)^t} \tag{3.26}$$

$$\bar{C}^{(CC)} = \sum_{i \in V} y_i^v C_i^{(v,CC)} + \sum_{(i,j) \in E} y_{i,j} C_{i,j}^{(CC)} \tag{3.27}$$

$$\begin{aligned} \bar{C}_w^{(OP)} = & \sum_{k \in V^T} \left(\sum_{q \in \Omega} \sum_{j \in \{j | (j,k) \in E\}} f_{j,k,q,w} \right) C_{k,w}^{(OP)} \\ & - \sum_{i \in V^W} \left(\sum_{q \in \Omega} \sum_{j \in \{j | (i,j) \in E\}} f_{i,j,q,w} \right) C_{i,w}^{(OP)} \\ & - \sum_{j \in V^C} \gamma_w W_{j,w} \end{aligned} \tag{3.28}$$

3.2.4 The Optimization Model

When considering only the stochastic pooling model, the optimization problem can be stated as:

$$\begin{aligned} \min \quad & C^{(NPV)} \\ s.t. \quad & \text{Eq. } (3.1 - 3.12) \\ & \text{Eq. } (3.26 - 3.28) \end{aligned} \tag{I}$$

This model is relatively easy for global optimization, but may lead to a solution

in which the gas flow rates planned for the operation are not realistic due to the lack of sufficient pressure differential (as will be showed in the case study). Therefore, we propose in this chapter to use the following optimization model that addresses the pressure flow relationships explicitly:

$$\begin{aligned} \min \quad & C^{(NPV)} \\ s.t. \quad & \text{Eq. } (3.1-3.12) \\ & \text{Eq. } (3.13-3.25) \\ & \text{Eq. } (3.26-3.28) \end{aligned} \tag{II}$$

Note that in the right-hand-side of Eq. (3.13), the binary variable $y_{i,j}$ and the expression $(\pi_{i,w}^2 - \lambda_{i,w}(P_{i,w}^{out})^2)$ can be further separated by the well-known big-M method [2], and this reformulation can reduce the nonconvexity of the problem. For simplicity of the subsequent discussion, we do not explicitly present this reformulation here.

Formulation (II) is much more challenging to solve than Formulation (I), because it contains more variables and nonconvex constraints. In order to practically solve the proposed optimization model, we reformulate it in the next section so that: (a) some nonconvex constraints can be rewritten into convex constraints, and (b) the convex and nonconvex parts of the model are separable so that an operation subproblem for a scenario can be solved by a classical decomposition method (such as GBD).

3.3 Reformulation of the Optimization Model

In this section, the proposed optimization formulation (II) is reformulated in three steps. In the first step, we propose to consider the effect of pressure regulators, which

can be readily built in different parts of a gas production network but are omitted in (II). In the second step, it will be seen that, after the inclusion of pressure drop from pressure regulators, some nonlinear equality constraints in formulation (II) (which is nonconvex) can be transformed into nonlinear inequality constraints and some of the reformulated nonlinear inequality constraints are convex. In the third step, the "convex part" of the reformulated nonconvex nonlinear constraints can be separated from its "nonconvex part", under a mild assumption.

3.3.1 Inclusion of Pressure Drops in Pressure Regulators

In Formulation (II), pressures at vertices are uniquely determined by gas flow rates and compressor powers, i.e., there is no flexibility in adjusting the pressures with fixed gas flow rates and compressor powers. This clearly does not represent real gas production systems, as pressure regulators that can provide extra pressure drops are normally installed at different parts of the system. We first consider pressure drop $\Delta_{i,w}$ that is enabled by a pressure regulator near the exit of a gas well i, as illustrated in Figure 3.2. The pressure regulator can reduce the pressure at the end of the well pipeline from $P^{out}_{i,w}$ to $\hat{P}^{out}_{i,w}$, without incurring significant operating cost. Similarly, pressure drop can also be enabled near the exit of a platform (with or without an onsite compressor) by a pressure regulator, as illustrated in Figure 3.3. As a result, the well performance equation (3.13) and the compression performance equation (3.18), can be rewritten as:

$$\begin{aligned} &\alpha_{i,w}Q_{i,j,w} + (\beta_{i,w} + \vartheta_{i,w})Q^2_{i,j,w} = y_{i,j}(\pi^2_{i,w} - \lambda_{i,w}(\hat{P}^{out}_{i,w} + \Delta_{i,w})^2), \\ &\quad \forall (i,j) \in E^W, \quad \forall w \in \Phi \end{aligned} \tag{3.29}$$

$$W_{j,w} - \sigma_j \sum_{i\in\{i|(i,j)\in E\}} \sum_{q\in\Omega} f_{i,j,q,w} \left[\left(\frac{\hat{P}^{out}_{j,w} + \Delta_{j,w}}{P^{in}_{j,w}} \right)^{\nu} - 1 \right] = 0, \quad \forall j \in V^C, \quad \forall w \in \Phi \tag{3.30}$$

In both equations, the pressure after regulator is used instead of the pressure before the regulator. In this way, the outlet pressures of vertices in the model all become pressures after the pressure regulators, and the previous pressure constraints Eq. (3.15), (3.19), (3.21), (3.23) should now be written as:

$$\hat{P}^{out}_{i,w} \leq \pi_{i,w}, \quad \forall i \in V^W, \quad \forall w \in \Phi \tag{3.31}$$

$$P^{in}_{i,w} \leq \hat{P}^{out}_{i,w}, \quad \forall i \in V^C, \quad \forall w \in \Phi \tag{3.32}$$

$$P^{in}_{i,w} \geq \hat{P}^{out}_{i,w}, \quad \forall i \in V \setminus (V^C \cup V^W), \quad \forall w \in \Phi \tag{3.33}$$

$$y^v_i \Gamma^{out,LB}_{i,w} \leq \hat{P}^{out}_{i,w} \leq y^v_i \Gamma^{out,UB}_{i,w}, \quad \forall i \in V, \quad \forall w \in \Phi \tag{3.34}$$

And we should also require that the pressure drop be nonnegative:

$$\Delta_{i,w} \geq 0, \quad \forall i \in V, \quad \forall w \in \Phi \tag{3.35}$$

We can also consider pressure regulators in pipelines. Without loss of generality, assume the pressure regulator in a pipeline is located at the starting vertex of the pipeline, as illustrated in Figure 3.4. $\delta_{i,j,w}$ denotes the pressure drop introduced by the pressure regulator. As a result, the pipeline performance equations (3.16) and (3.17) can be rewritten as:

$$y_{i,j}((\hat{P}^{out}_{i,w} - \delta_{i,j,w})^2 - (P^{in}_{j,w})^2) = \kappa_{i,j} Q^2_{i,j,w}, \quad \forall (i,j) \in E^L, \quad \forall w \in \Phi \tag{3.36}$$

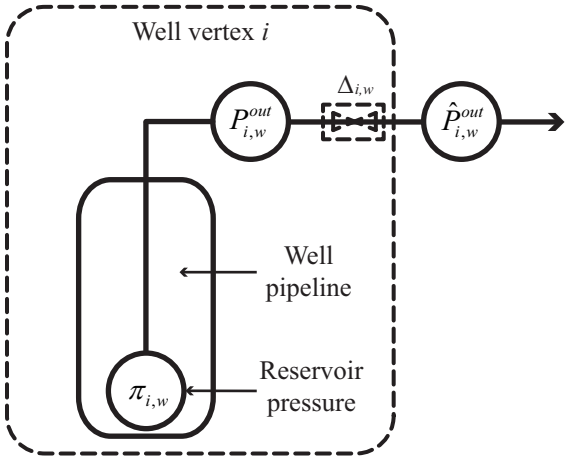

Figure 3.2: Well pipeline with regulator

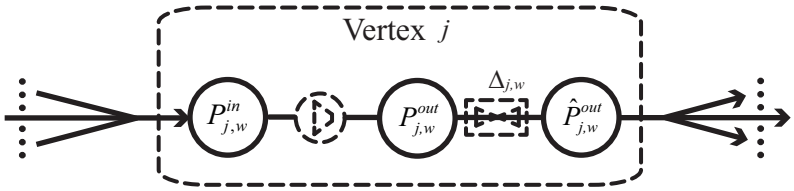

Figure 3.3: Platform with regulator

$$y_{i,j}((\hat{P}^{out}_{i,w} - \delta_{i,j,w}) - P^{in}_{j,w}) = 0, \quad \forall (i,j) \in E \setminus E^L, \quad \forall w \in \Phi \tag{3.37}$$

and the pressure drop and the pressure before the pressure regular have to be non-negative:

$$\delta_{i,j,w} \geq 0, \quad \forall (i,j) \in E, \quad \forall w \in \Phi \tag{3.38}$$

$$\hat{P}^{out}_{i,w} - \delta_{i,j,w} \geq 0, \quad \forall (i,j) \in E, \quad \forall w \in \Phi \tag{3.39}$$

3.3.2 Removal of Pressure Drops

Usually investments and operating costs for pressure regulators are negligible compared to the costs for other major units in a gas production network (such as long pipelines and compressors), so we do not need to include the costs incurred by the

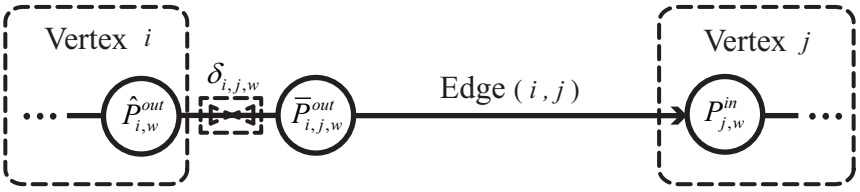

Figure 3.4: Pipeline with regulator

pressure drops in the objective function. As a result, $\Delta_{i,w}$ does not need to be included in the model explicitly, and constraints (3.29), (3.30), (3.35) can be replaced by:

$$\begin{aligned} &\alpha_{i,w}Q_{i,j,w} + (\beta_{i,w} + \vartheta_{i,w})Q^2_{i,j,w} \leq y_{i,j}(\pi^2_{i,w} - \lambda_{i,w}(\hat{P}^{out}_{i,w})^2), \\ &\forall (i,j) \in E^W, \quad \forall w \in \Phi \end{aligned} \tag{3.40}$$

$$W_{j,w} - \sigma_j \sum_{i \in \{i|(i,j)\in E\}} \sum_{q \in \Omega} f_{i,j,q,w} \left[\left(\frac{\hat{P}^{out}_{j,w}}{P^{in}_{j,w}} \right)^{\nu} - 1 \right] \geq 0, \quad \forall j \in V^C, \quad \forall w \in \Phi \tag{3.41}$$

Note that Eq. (3.40) is convex when the binary variable $y_{i,j}$ is fixed (and $y_{i,j}$ can be separated from the quadratic expression by the big-M method). Before the reformulation, Eq. (3.29) is nonconvex with fixed $y_{i,j}$. Therefore, this reformulation reduces the nonconvexity of the optimization model.

Similarly, $\delta_{i,j,w}$ does not need to be included in the model, and constraints (3.36-3.39) can be replaced by:

$$y_{i,j}((\hat{P}^{out}_{i,w})^2 - (P^{in}_{j,w})^2) \geq \kappa_{i,j} Q^2_{i,j,w}, \quad \forall (i,j) \in E^L, \quad \forall w \in \Phi \tag{3.42}$$

$$y_{i,j}(\hat{P}^{out}_{i,w} - P^{in}_{j,w}) \geq 0, \quad \forall (i,j) \in E \setminus E^L, \quad \forall w \in \Phi \tag{3.43}$$

Note that Eq. (3.42) can be written as convex constraints when the binary variable $y_{i,j}$ is fixed. It is obvious when $y_{i,j} = 0$. When $y_{i,j} = 1$, the constraint can be written

as the following second-order cone constraint [28]:

$$\hat{P}^{out}_{i,w} \geq \sqrt{(P^{in}_{j,w})^2 + \kappa_{i,j} Q^2_{i,j,w}}, \quad \forall (i,j) \in E^L, \quad \forall w \in \Phi \tag{3.44}$$

After this step, Formulation (II) can be written into the following optimization formulation:

$$\begin{aligned} \min \quad & C^{(NPV)} \\ s.t. \quad & \text{Eq. } (3.1 - 3.12) \\ & \text{Eq. } (3.14), (3.20), (3.22), (3.24 - 3.25) \\ & \text{Eq. } (3.26 - 3.28) \\ & \text{Eq. } (3.31 - 3.34), (3.40 - 3.43) \end{aligned} \tag{III}$$

The equations in the last row of Formulation (III) are the new equations developed in the two reformulation steps, in place of some constraints in Formulation (II). The operation subproblems of Formulation (III), i.e., the subproblems resulting from fixing the design decision variables y^v_i, $y_{i,j}$, are less nonconvex compared to those of Formulation (II). This is because the well performance and pipeline performance constraints are now convex. However, the compression performance constraint Eq. (3.41) is still highly nonconvex for each $j \in V^C$ and $w \in \Phi$. In addition, these constraints hinder efficient application of decomposition methods for solving each operation subproblem, as the constraint links major variables in the operation problem.

3.3.3 Separation of Flow Rates and Pressures

In order to further reformulate the nasty compression performance constraint (3.41) while preserving the convexity of other pressure related constraints, we make the

following assumption:

Assumption 4. *There are no other compressors between a gas well and a compressor.*

If this assumption is not satisfied for a gas production network but for a subpart of it, the following reformulation procedure can be applied to the subpart of the network.

We define new variables $P_{j,w}^{in,c} \triangleq (P_{j,w}^{in})^2$, $P_{j,w}^{C}$, and rewrite Eq. (3.41) and Eq. (3.32) into:

$$W_{j,w} - \sigma_j \sum_{i \in \{i|(i,j)\in E\}} \sum_{q \in \Omega} f_{i,j,q,w} P_{j,w}^{C} \geq 0, \quad \forall j \in V^C, \quad \forall w \in \Phi \tag{3.45}$$

$$P_{j,w}^{C} \geq (\frac{\hat{P}_{j,w}^{out}}{P_{j,w}^{in}})^{\nu} - 1, \quad \forall j \in V^C, \quad \forall w \in \Phi \tag{3.46}$$

$$P_{j,w}^{C} \geq 0, \quad \forall j \in V^C, \quad \forall w \in \Phi \tag{3.47}$$

and Eq. (3.46) can be further written into

$$(P_{j,w}^{C} + 1)^{2/\nu} \geq \frac{(\hat{P}_{j,w}^{out})^2}{P_{j,w}^{in,c}}, \quad \forall j \in V^C, \quad \forall w \in \Phi \tag{3.48}$$

Note that Eq. (3.48) is convex if $P_{j,w}^{C}$ is fixed [5]. The advantage of Eq. (3.45), (3.47), (3.48) over Eq. (3.41) and (3.32) is that the pressures are separated from the molar flow rates. Following this, we seem to be able to separate the pressure flow relationships (which seem to be convex now) from the stochastic pooling submodel (which is nonconvex). But we need to first examine whether this reformulation can affect other pressure related constraints. Consider a long pipeline connecting the compressor on platform j and an upstream vertex i, as shown in Figure 5. Due to the

inclusion of new variable $\hat{P}^{in,c}_{j,w}$, the pipeline performance constraint Eq. (3.44) needs to be reformulated, and Figure 5 shows three different reformulations. In reformulation (a), the nonconvex constraint $P^{in,c}_{j,w} = (P^{in}_{j,w})^2$ is explicitly included, which destroys the convexity of the pressure related part of the model. In reformulation (b), $P^{in,c}_{j,w}$ is used in place of $(P^{in}_{j,w})^2$, but the constraint becomes nonconvex. In reformulation (c), a new variable $\hat{P}^{out,c}_{i,w} \triangleq (\hat{P}^{out}_{i,w})^2$ is introduced, which leads to a convex constraint.

Reformulation (c) implies that, if we can use $\hat{P}^{out,c}_{i,w}$ instead of $\hat{P}^{out}_{i,w}$ for all the upstream units to a compressor, the pressure part of the model can still be convex. Following this idea, we define a new vertex subset $\bar{V} \subset V$ that includes all vertices which are located before a compressor. According to Assumption 4, the vertices in this subset do not contain a compressor, so the relevant pressure constraints in Formulation (III) are Eq. (3.22), (3.31), (3.33-3.34), (3.40), (3.42-3.43). They now can be rewritten as:

$$y^v_i(\Gamma^{in,LB}_{i,w})^2 \leq P^{in,c}_{i,w} \leq y^v_i(\Gamma^{in,UB}_{i,w})^2, \quad \forall i \in (V^C \cup \bar{V}) \setminus V^W, \quad \forall w \in \Phi \tag{3.49}$$

$$\hat{P}^{out,c}_{i,w} \leq (\pi_{i,w})^2, \quad \forall i \in V^W \cap \bar{V}, \quad \forall w \in \Phi \tag{3.50}$$

$$P^{in,c}_{i,w} \geq \hat{P}^{out,c}_{i,w}, \quad \forall i \in \bar{V} \setminus V^W, \quad \forall w \in \Phi \tag{3.51}$$

$$y^v_i(\Gamma^{out,LB}_{i,w})^2 \leq \hat{P}^{out,c}_{i,w} \leq y^v_i(\Gamma^{out,UB}_{i,w})^2, \quad \forall i \in \bar{V}, \quad \forall w \in \Phi \tag{3.52}$$

$$\begin{gathered}\alpha_{i,w}Q_{i,j,w} + (\beta_{i,w} + \vartheta_{i,w})Q^2_{i,j,w} \leq y_{i,j}(\pi^2_{i,w} - \lambda_{i,w}\hat{P}^{out,c}_{i,w}), \\ \forall (i,j) \in \{(i,j) | (i,j) \in E^W, i \in \bar{V}\}, \quad \forall w \in \Phi\end{gathered} \tag{3.53}$$

$$y_{i,j}(\hat{P}^{out,c}_{i,w} - P^{in,c}_{j,w}) \geq \kappa_{i,j}Q^2_{i,j,w}, \quad \forall (i,j) \in \{(i,j) | (i,j) \in E^L, i \in \bar{V}\}, \quad \forall w \in \Phi \tag{3.54}$$

$$y_{i,j}(\hat{P}^{out,c}_{i,w} - P^{in,c}_{j,w}) \geq 0, \quad \forall (i,j) \in \{(i,j)|(i,j) \in E \setminus E^L, i \in \bar{V}\}, \quad \forall w \in \Phi \tag{3.55}$$

For the vertices that are not included in subset $\bar{V}$, the relevant pressure constraints are unchanged, so:

$$y^v_i \Gamma^{in,LB}_{i,w} \leq P^{in}_{i,w} \leq y^v_i \Gamma^{in,UB}_{i,w}, \quad \forall i \in V \setminus (V^W \cup V^C \cup \bar{V}), \quad \forall w \in \Phi \tag{3.56}$$

$$\hat{P}^{out}_{i,w} \leq \pi_{i,w}, \quad \forall i \in V^W \setminus \bar{V}, \quad \forall w \in \Phi \tag{3.57}$$

$$P^{in}_{i,w} \geq \hat{P}^{out}_{i,w}, \quad \forall i \in V \setminus (V^W \cup V^C \cup \bar{V}), \quad \forall w \in \Phi \tag{3.58}$$

$$y^v_i \Gamma^{out,LB}_{i,w} \leq \hat{P}^{out}_{i,w} \leq y^v_i \Gamma^{out,UB}_{i,w}, \quad \forall i \in V \setminus \bar{V}, \quad \forall w \in \Phi \tag{3.59}$$

$$\begin{gathered} \alpha_{i,w} Q_{i,j,w} + (\beta_{i,w} + \vartheta_{i,w}) Q^2_{i,j,w} \leq y_{i,j}(\pi^2_{i,w} - \lambda_{i,w}(\hat{P}^{out}_{i,w})^2), \\ \forall (i,j) \in \{(i,j)|(i,j) \in E^W, i \in V \setminus \bar{V}\}, \quad \forall w \in \Phi \end{gathered} \tag{3.60}$$

$$y_{i,j}((\hat{P}^{out}_{i,w})^2 - (P^{in}_{j,w})^2) \geq \kappa_{i,j} Q^2_{i,j,w}, \quad \forall (i,j) \in \{(i,j)|(i,j) \in E^L, i \in V \setminus \bar{V}\}, \quad \forall w \in \Phi \tag{3.61}$$

$$y_{i,j}(\hat{P}^{out}_{i,w} - P^{in}_{j,w}) \geq 0, \quad \forall (i,j) \in \{(i,j)|(i,j) \in E \setminus E^L, i \in V \setminus \bar{V}\}, \quad \forall w \in \Phi \tag{3.62}$$

After this reformulation step, the optimization model (III) can be transformed

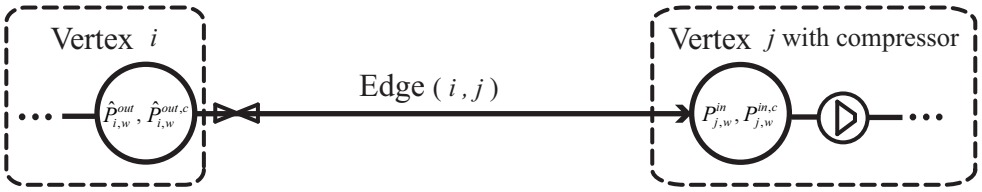

Different reformulations for pipeline performance:

(*a*). $P^{in,c}_{j,w} = (P^{in}_{j,w})^2$, $\hat{P}^{out}_{i,w} \geq \sqrt{(P^{in}_{j,w})^2 + \kappa_{i,j} Q^2_{i,j,w}}$, nonconvex

(*b*). $P^{out}_{i,w} \geq \sqrt{P^{in,c}_{j,w} + \kappa_{i,j} Q^2_{i,j,w}}$, nonconvex

(*c*). $\hat{P}^{out,c}_{i,w} \geq P^{in,c}_{j,w} + \kappa_{i,j} Q^2_{i,j,w}$, convex

Figure 3.5: Pipeline performance reformulations

into the following model:

$$
\begin{aligned}
\min \quad & C^{(NPV)} \\
s.t. \quad & \text{Eq. } (3.1 - 3.12) \\
& \text{Eq. } (3.14), (3.20), (3.24 - 3.25) \\
& \text{Eq. } (3.26 - 3.28) \\
& \text{Eq. } (3.45), (3.47 - 3.48), (3.49 - 3.62)
\end{aligned}
\tag{IV}
$$

3.4 A Customized Global Optimization Method

3.4.1 The Decomposable Structure of Formulation (IV)

This section discusses an efficient global optimization method for solving the proposed optimization formulation (IV) to ϵ-optimality. For convenience of subsequent

discussion, we rewrite Formulation (IV) into the following form:

$$
\begin{aligned}
\min_{x_0, x_1, \cdots, x_s} \quad & \sum_{w=1}^{s} p_w [f_{0,w}(x_0) + f_{1,w}(x_w^{nc}) + f_{2,w}(x_w^c)] \\
s.t. \quad & g_{0,w}(x_0) + g_{1,w}(x_w^{nc}) + g_{2,w}(x_w^c) \leq 0 \ , \quad w = 1, ..., s \\
& x_w^{nc} \in X_w^{nc}, \quad w = 1, ..., s \\
& x_w^c \in X_w^c, \quad w = 1, ..., s \\
& x_0 \in X_0.
\end{aligned}
\tag{P}
$$

Here p_w represents the probability for scenario w. x_0 includes design decisions (i.e., the "y"s in Formulation (IV)) or called first-stage decisions in the context of stochastic programming, and $X_0 \subset \{0,1\}^{n_0}$ is nonempty. $x_w = (x_w^{nc}, x_w^c)$ includes operation decisions, or called second-stage decisions. x_w^{nc} includes the operation decisions involved in nonconvex functions (mostly "s"s, "f"s, "P^C"s and "W"s in Formulation (IV)), which are also called nonconvex variables in this chapter, and set $X_w^{nc} \subset \mathbb{R}^{n_{nc}}$ is nonempty and compact. x_w^c includes the operation decisions only involved in convex functions (i.e., "P"s and "Q"s in Formulation (IV)), which are also called convex variables in this chapter, and $X_w^c \subset R^{n_c}$ is nonempty, compact and convex. Functions $f_{2,w}$, $g_{2,w}$ are convex functions on X_w^c.

Figure 3.6 illustrates the decomposable structure of Problem (P). The first block in Figure 3.6(a) represents the first group of constraints in Formulation (P), which links the design decisions and operation decisions in different scenarios. The second block in Figure 3.6(a) represents the second and third groups of constraints in Formulation (P), which consists of s operation subproblems that are independent of one another. The third block in Figure 3.6(a) represents the last group of constraint in Formulation (P) that restricts the choice of x_0. Intuitively, problem (P) is decomposable in the

sense that it can be separated into a set of operation subproblems via fixing x_0 or dualizing the linking constraints. If each operation subproblem can be solved quickly, then Problem (P) can be solve by either LD (together with explicit branch-and-bound search) or NGBD. Each operation subproblem here is a large nonconvex MINLP for which state-of-the-art global optimization solvers may not be able to solve quickly [41].

Fortunately, due to the reformulation introduced in the last section, each operation problem in Problem (P) also has a decomposable structure, as illustrated by Figure 3.6(b). The operation problem consists of a convex part (i.e., pressure flow submodel), a nonconvex part (i.e., the pooling submodel), and a set of complicating constraints (including unit conversion constraints and compressor constraints (3.48)) that link the convex and the nonconvex parts. Considering that existing state-of-the-art global optimization solvers (such as BARON [38], ANTIGONE [32]) can solve pooling problems very quickly, the operation subproblem may be solved efficiently through a GBD procedure. Following this idea, we show in the next subsection how to develop a variant of NGBD for efficiently solving Problem (P) to ϵ-optimality. The proposed variant of NGBD can be applied not only to Formulation (IV), but also to any other problems that can be written as Problem (P).

3.4.2 The Multi-Loop NGBD Method

NGBD was originally developed for solving problems with the structure shown in Figure 3.6(a). The basic idea is to generate a sequence of upper bounding problem via fixing $x_0 = x_0^l$ at each NGBD iteration l. The upper bounding problem is called **Primal Problem**, which can be naturally decomposed into the following subproblem

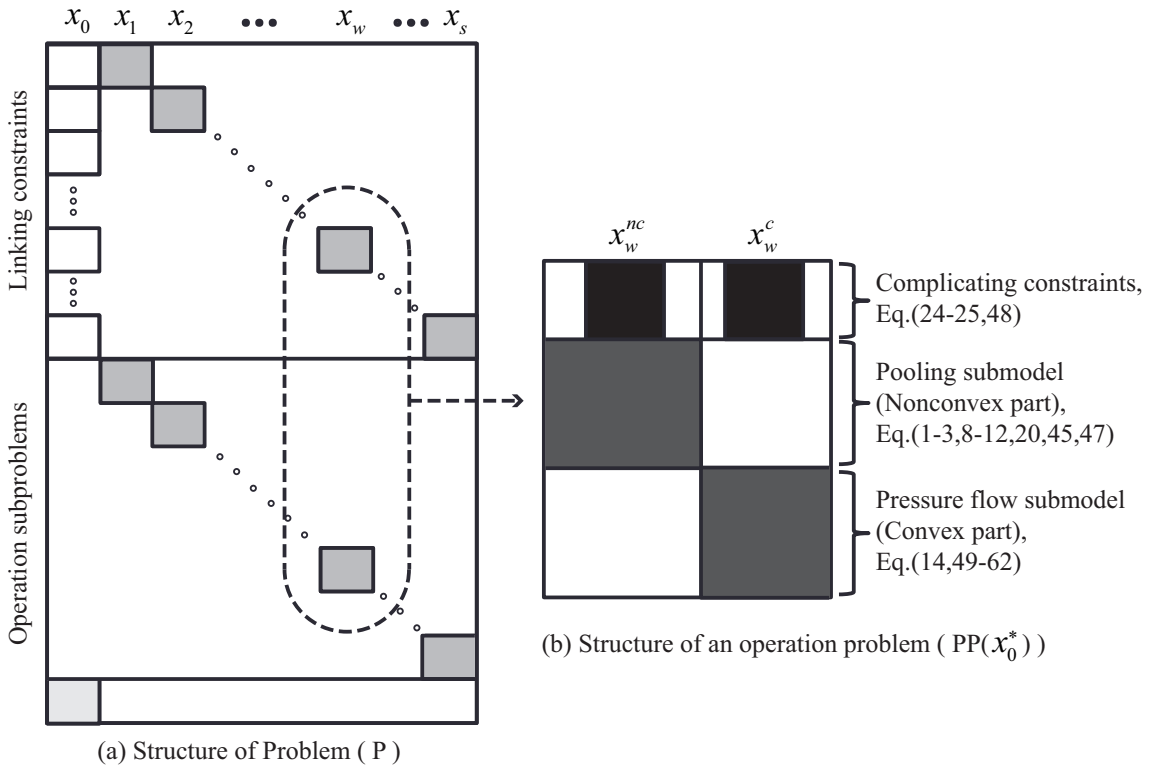

Figure 3.6: The decomposable structure of Problem (P)/Formulation (IV)

for scenario $w = 1, \cdots s$:

$$\begin{aligned} \min_{x_w} \quad & p_w[f_{0,w}(x_0^l) + f_{1,w}(x_w^{nc}) + f_{2,w}(x_w^c)] \\ s.t. \quad & g_{0,w}(x_0^l) + g_{1,w}(x_w^{nc}) + g_{2,w}(x_w^c) \leq 0, \\ & x_w^{nc} \in X_w^{nc}, \\ & x_w^c \in X_w^c. \end{aligned} \tag{PP$_w^l$}$$

On the other hand, a **Lower Bounding Problem** (LBP) is constructed via replacing the nonconvex functions in Problem (P) with their convex relaxations. Problem (LBP) is a large-scale MILP or convex MINLP which can be solved via GBD efficiently, and it is enhanced with an integer cut after each GBD iteration. Therefore,

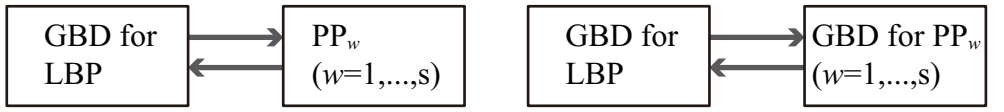

(a) Simplified diagram for single-loop NGBD (b) Simplified diagram for multi-loop NGBD

GBD: Generalized Benders decomposition
LBP: Lower bounding Problem
PP$_w$: Primal subproblem for scenario w

Figure 3.7: Comparison of the two NGBD diagrams

a sequence of lower bounds are generated via the solution of Problem (LBP) over the NGBD iterations. The NGBD algorithm terminates in a finite number of iterations when the upper and lower bounds converge to an ϵ-optimal solution or the infeasibility of the problem is indicated by an infeasible lower bounding problem. Figure 3.7(a) shows a simplified diagram for the standard NGBD algorithm. More details about NGBD subproblems and algorithm can be found in [27]. In this chapter, the standard NGBD algorithm is called single-loop NGBD, as there is only one GBD loop in one NGBD iteration.

For Formulation (IV), a primal subproblem (PP^l_w) is an operation problem for scenario w. As discussed in the previous subsection, each operation problem is further decomposable and can be solved via GBD. Therefore, it is natural to embed another GBD loop in each NGBD iteration, in order to solve the primal subproblems. This leads to a multi-loop NGBD as shown in Figure 3.7(b), which includes 1 GBD loop for Problem (LBP) and s GBD loops for the primal subproblems at each NGBD iteration.

Here we provide more details on the GBD procedure for solving each primal subproblem (PP^l_w). We view x^{nc}_w as the complicating variable, since Problem (PP^l_w) is convex if x^{nc}_w is fixed. Therefore, at each GBD iteration k for solving Problem (PP^l_w),

we fix $x_w^{nc} = x_w^{nc,k}$ to construct an upper bounding problem, called **Benders Primal Problem**, as follows:

$$\begin{aligned} \min_{x_w^c} \quad & p_w[f_{0,w}(x_0^l) + f_{1,w}(x_w^{nc,k}) + f_{2,w}(x_w^c)] \\ s.t. \quad & g_{0,w}(x_0^l) + g_{1,w}(x_w^{nc,k}) + g_{2,w}(x_w^c) \leq 0, \\ & x_w^c \in X_w^c. \end{aligned} \tag{$\text{BPP}_w^{l,k}$}$$

Note that if Problem $\text{BPP}_w^{l,k}$ is a convex NLP, it needs to satisfy some constraint qualification for the GBD algorithm to be valid, as GBD relies on strong duality of each upper bounding problem. The solution of Problem $\text{BPP}_w^{l,k}$ yields an upper bound for Problem (PP_w^l). If Problem $\text{BPP}_w^{l,k}$ is infeasible for $x_w^{nc,k}$, then the following feasibility problem is solved instead:

$$\begin{aligned} \min_{x_w^c, z} \quad & ||z||_1 \\ s.t. \quad & g_{0,w}(x_0^l) + g_{1,w}(x_w^{nc,k}) + g_{2,w}(x_w^c) \leq z, \\ & x_w^c \in X_w^c, \\ & z \geq 0, \end{aligned} \tag{$\text{BFP}_w^{l,k}$}$$

where $||\cdot||_1$ denotes the 1-norm.

After Problem ($\text{BPP}_w^{l,k}$) or ($\text{BFP}_w^{l,k}$) is solved, the following lower bounding problem, called **Benders Relaxed Master Problem**, is solved to yield a lower bound

for Problem (PP_w^l):

$$
\begin{aligned}
\min_{\eta_w, x_w^{nc}} \quad & \eta_w \\
s.t. \quad & \eta_w \geq obj_{\mathrm{BPP}_w^{l,j}} + (f_{1,w}(x_w^{nc}) - f_{1,w}(x_w^{nc,j})) + (\lambda_w^{l,j})^T (g_{1,w}(x_w^{nc}) - g_{1,w}(x_w^{nc,j})), \quad \forall j \in T^k, \\
& 0 \geq obj_{\mathrm{BFP}_w^{l,i}} + (\mu_w^{l,i})^T (g_{1,w}(x_w^{nc}) - g_{1,w}(x_w^{nc,i})), \quad \forall i \in S^k, \\
& x_w^{nc} \in X_w^{nc}, \\
& \mathrm{UBDPP}_w^{l,k} \geq \eta_w, \\
& \mathrm{UB}_w^l \geq \eta_w.
\end{aligned}
\tag{$\mathrm{BRMP}_w^{l,k}$}
$$

The solution of ($\mathrm{BRMP}_w^{l,k}$) yields a lower bound for Problem (PP_w^l), called $\mathrm{LBDPP}_w^{l,k}$; If ($\mathrm{BRMP}_w^{l,k}$) or ($\mathrm{BFP}_w^{l,k}$) is infeasible, then Problem (PP_w^l) is infeasible. In ($\mathrm{BRMP}_w^{l,k}$), the first group of constraints are called optimality cuts. The parameters $obj_{\mathrm{BPP}_w^{l,j}}$ and $\lambda_w^{l,j}$ are the optimal objective value and Lagrange multipliers for subproblem ($\mathrm{BPP}_w^{l,k}$), respectively. Set T^k includes indexes of previous iterations at which subproblem ($\mathrm{BPP}_w^{l,k}$) is feasible. The second group of constraints are called feasibility cuts. The parameters $obj_{\mathrm{FBP}_w^{l,i}}$ and $\mu_w^{l,i}$ are the optimal objective value and Lagrange multipliers for subproblem ($\mathrm{BFP}_w^{l,k}$), respectively. Set S^k includes indexes of previous iterations at which subproblem ($\mathrm{BPP}_w^{l,k}$) is infeasible (and therefore subproblem ($\mathrm{BFP}_w^{l,k}$) is solved). Since Problem ($\mathrm{BRMP}_w^{l,k}$) is nonconvex and its solution time dominates the GBD solution time, we add extra bounding constraints to expedite the solution of Problem ($\mathrm{BRMP}_w^{l,k}$). Two upper bounds are used in the two bounding constraints. $\mathrm{UBDPP}_w^{l,k}$ is the current best upper bound for Problem (PP_w^l), obtained from the best optimal objective value of the previously solved Benders primal problem. This upper bound surely does not exclude an optimal solution of Problem (PP_w^l). UB_w^l is

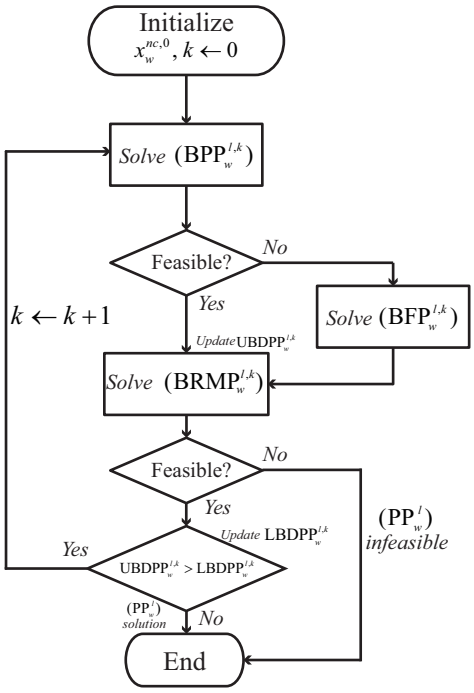

Figure 3.8: Flowchart of GBD for solving (PP_w^l)

obtained from primal problems solved in the previous NGBD iterations, as explained in [27]. This bound can exclude solutions of NGBD primal problem that are worse than the current NGBD upper bound. This upper bound can exclude an optimal solution of Problem (PP_w^l), but not an optimal solution of Problem (P), so it is also a valid bound for the multi-loop NGBD.

Figure 3.8 shows the algorithm flowchart for the customized GBD procedure of solving each NGBD primal subproblem (PP_w^l).

3.5 Case Study

3.5.1 Problem Statement and Implementation

In this case study, we consider an integrated design and operation problem for the SGPS introduced in the second section. In this problem, part of the SGPS is already developed, as shown by the solid lines in Figure 3.9. This existing part includes 5 gas fields (SC, E11, F6, F23SW and F23) that contain 40 wells, 3 remote subnetwork vertices (D35, BY, BN), 4 gas platforms (BYP, E11P, F23P, E11R-A), 1 plant slug catcher (SC-1) , and 1 LNG plant. In order to meet the increased demand, the system is to be expanded, and the superstructure of the part that can be developed for the expansion is showed by the dashed lines in Figure 3.9. This superstructure includes 6 gas fields (B11, SE, M3, M4, M1, JN) that contain 31 wells, 1 remote subnetwork vertex (HL), 5 platforms (B11P, M3P, M1P, E11R-B, E11R-C), 1 pipeline junction (T), 2 plant slug catchers (SC-2, SC-3), and 2 LNG plants. Note that the existing part and potential part of the system include 5 platforms (E11P, F6, B11P, M1P, M3P) that have an onsite compressor. If gas field B11 is to be developed, then platform B11P needs to be developed as well, and vice versa. The same relationship exists between M3 and M3P, M1 and M1P, SC-2 and LNG2, SC-3 and LNG3.

The following assumptions are made for developing the optimization model.

1. If a gas field is to be developed, all wells in the field are to be developed and the fractions of components for gas flows from these wells are the same. With this assumption, there is no pooling effect at each gas field.

2. The total mass loss during gas pre-processing (e.g., water removal, oil/gas separation, etc.) is negligible.

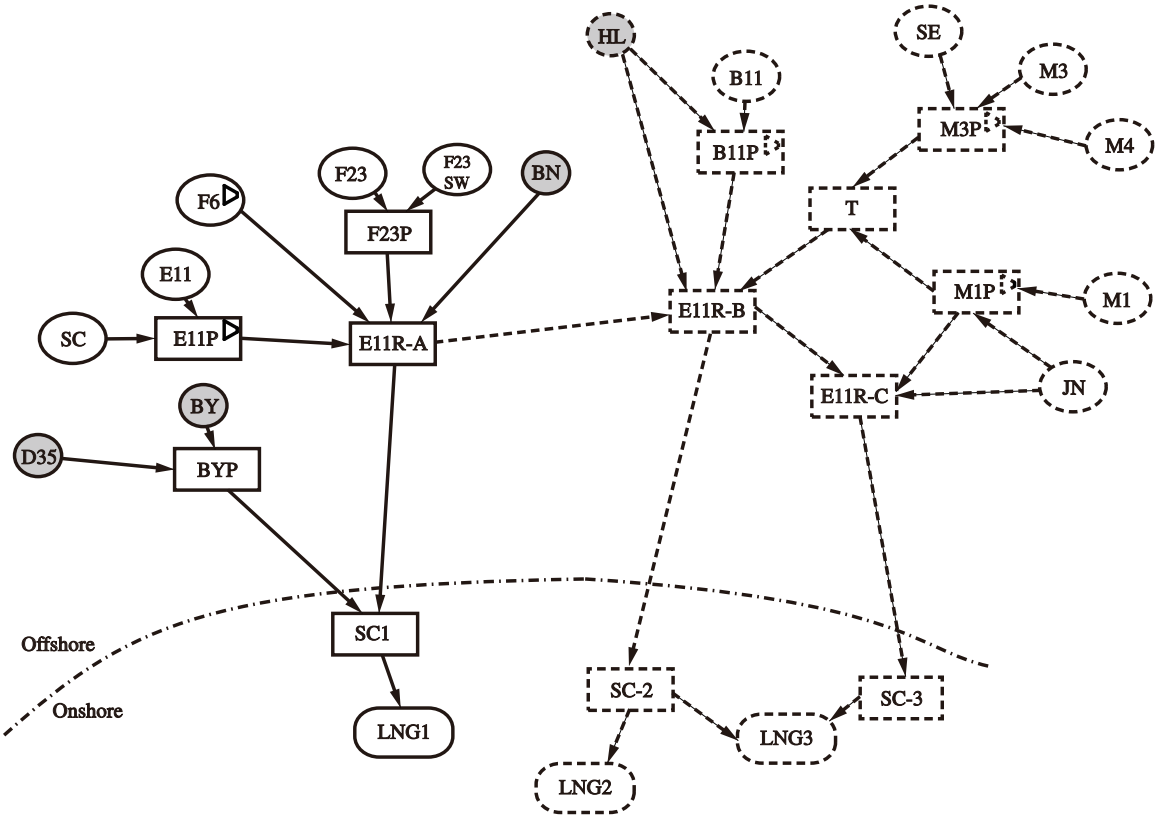

Figure 3.9: The superstructure of Sarawak Gas Production System (SGPS)

3. The pooling subproblem only tracks the CO_2 and H_2S contents in the gas flows, as only bounds on CO_2 and H_2S contents need to be observed.

Many things in natural gas systems, including gas contents at fields, product demands at terminal, infrastructure costs and product prices, can be regard as uncertain parameters in this model. When considering these uncertain parameters together, the way to generate uncertainty scenarios that can efficiently reflect system features is

not trivial and out of the scope of this research. Therefore, one uncertain parameter is considered explicitly in the optimization model, which is the CO_2 content of gas from gas field M1. This parameter is assumed to follow a normal distribution, with the mean $\mu = 5.04$mol% and the standard deviation $\sigma = 0.1$ mol%. A simple scenario sampling rule is used to generate n uncertainty scenarios for the case study:

1. The scenarios are sampled in the 6σ range and the value of x for ith scenario is: $x_i = -3\sigma + \mu + 3\sigma/n + (i-1)6\sigma/n$.

2. The probability of the ith scenario can be calculated by equally dividing interval $[\mu - 3\sigma, \mu + 3\sigma]$ into n subintervals and calculating the probability for each subinterval using cumulative probability distribution function Φ for the standard normal distribution, i.e.,

$$p(x = x_i) = \frac{\Phi(-3\sigma + \mu + 6\sigma i/n) - \Phi(-3\sigma + \mu + 6\sigma(i-1)/n)}{1 - 2\Phi(-3\sigma + \mu)} \tag{3.63}$$

The goal of the optimization is to maximize the expected NPV of the system over the next 25 years, while satisfying the demands for different uncertainty scenarios. Other parameters in this model are provided in the Appendix B.2.

We consider all the four formulations presented in this chapter, Formulations (I-IV), for the case study. Formulation (I), the stochastic pooling model from the literature, does not consider pressure flow relationships. Formulation (II) includes both the pooling submodel and the pressure flow relationships, but it does not include flexible pressure drops that can be provided by pressure regulators. Formulation (III) allows pressure drops from pressure regulators and therefore is more realistic and practical than Formulation (II). Formulation (IV) is a rigorous reformulation of

Formulation (III), which includes separable convex and nonconvex parts that allow further decomposition of the operation subproblems. The rigorous reformulation to Formulation (IV) is possible as the SGPS system satisfies Assumption 1.

All simulations are run on a virtual machine with Ubuntu 12.04, one 3.40GHz CPU core, and 4GB RAM. All problems/subproblems are modeled on using GAMS 24.2.3. The nonconvex MINLP/NLP problems/subproblems are solved with BARON 12.7.7, the convex NLP subproblems are solved with CONOPT 3.15P, and the MILP/LP subproblems are solved with CPLEX 12.6. The termination criteria for decomposition methods is 10^{-2}. The convex relaxations required in single-loop and multi-loop NGBDs are constructed using the standard McCormick approach [31].

3.5.2 Results and Discussion

Computational Results

We first solve the four optimization formulations for the expected value case (i.e., an one-scenario case where the value of the uncertain parameter is its mean value). This problem can be solved by single-loop or multi-loop NGBD. We compare the solution results of single-loop NGBD for the four formulations in Table 3.2. We set a 120-hour time limit for all the problems; for those cannot be solved within this time limit, the best objective value obtained before the termination and the optimality gap are reported in the table. Note that only Formulation (IV) can be solved by multi-loop NGBD, because the operation subproblems in other formulations are not separable in convex and nonconvex variables and GBD cannot be applied for solving these operation subproblems [16].

It can be seen from Table 3.2 that, Formulation (I) can be solved by single-loop

Table 3.2: Computational results for the expected value problem

Formulation	Solution Method	Best obj. (10^9 \$)	Gap	CPU time (hrs)
(I)	Single-loop NGBD	16.1	< 1 %	< 0.001
(II)	Single-loop NGBD	10.5	39.7 %	120
(III)	Single-loop NGBD	14.9	6.4%	120
(IV)	Single-loop NGBD	10.2	57.2%	120
(IV)	Multi-loop NGBD	15.1	< 1%	9.3

NGBD very quickly. However, this formulation ignores the pressure flow relationships and therefore may generate a solution that is unrealistic. We will give further discussion on this later. While Formulation (II-IV) are more realistic than Formulation (I), they cannot be solved to the 10^{-2} tolerance by single-loop NGBD within 120 hours. Formulation (IV) has a better decomposable structure so the multi-loop NGBD is applicable to this formulation; it can be solved with multi-loop NGBD within 10 hours, leading to a solution that is guaranteed to be a global solution with the 10^{-2} tolerance.

In order to further compare the performance of single-loop NGBD and multi-loop NGBD, we solve Formulation (IV) for a case where 9 uncertainty scenarios (sampled using the rule explained before) are explicitly included in the model. The computational results are shown in Table 3.3. It can be seen that the single-loop NGBD cannot solve the problem within 120 hours; at the end of the 120th hour, the gap is still as large as 43.2 % and the expected NPV achieved with the intermediate solution is way worse than the globally optimal expected NPV. Multi-loop NGBD, on the other hand, can return a global optimal solution (a gap smaller than 0.1 %) within 30 hours. The reason for multi-loop NGBD being faster than single-loop NGBD is that the operation subproblems (i.e., Problem (PP_w^l)) are solved via GBD rather

Table 3.3: Computational results for Formulation(IV) with 9 scenarios

Method	Best obj. (billion $)	Gap	Total CPU time (hrs)	CPU Time for PP[a] (hrs)	Num. of PP
Single-loop NGBD	10.2	43.2%	120	120	22
Multi-loop NGBD	15.0	< 0.1 %	29.5	29.5	36

[a] PP refers to primal problem (or equivalently, operation subproblem), which can be decomposed for each scenario w as (PP_w^l)

than directly by BARON. Due to its nice decomposable structure, each operation subproblem can be solved by GBD efficiently.

In order to see why GBD is efficient for the operation subproblems, we show in Table 3.4 computational results for an operation subproblem. In this subproblem, the design decisions x_0 are fixed to the optimal design decisions and the scenario to be considered is the nominal scenario (i.e., the scenario in which the uncertainty parameter takes it mean value). From the table, the monolith approach (i.e., solving the problem by BARON directly) cannot guarantee the global optimal solution within 900s, and the gap at the 900th second is larger than the predefined tolerance 10^{-3}. On the other hand, GBD can return a solution with a gap smaller than the tolerance, using less than 20 seconds. When using GBD, the CPU time is dominated by the time for solving nonconvex relaxed master problems ($\mathrm{BRMP}_w^{l,k}$); each such nonconvex subproblem can be solved much more quickly than the operation problem itself (on average around 0.5 second per subproblem), this is because these subproblems have smaller problem sizes. In fact, the monolith approach generates the optimal solution within a second, but it cannot close the gap and verify the global optimality of the solution quickly, while in the GBD approach the lower bound approaches the optimal objective value quickly although the optimal solution is generated at the termination of the GBD procedure (about the 18th second). Figure 3.10 compares the lower

Table 3.4: Computational Results for an operation subproblem

Method	Best obj. (billion $)	Gap Gap	Total CPU time (seconds)	CPU Time for BRMP[a] (seconds)	Num. of BRMP[a]
Monolith[b]	-15.25	0.16%	900	-	-
GBD	-15.25	< 0.01 %	18.79	18.61	34

[a] BRMP refers to ($BRMP_w^{l,k}$), the relaxed master problem in a GBD procedure for solving a primal problem.
[b] Monolith refers to solving the problem directly using BARON.

bounds generated from the monolith and the GBD approaches over time during the solution procedures.

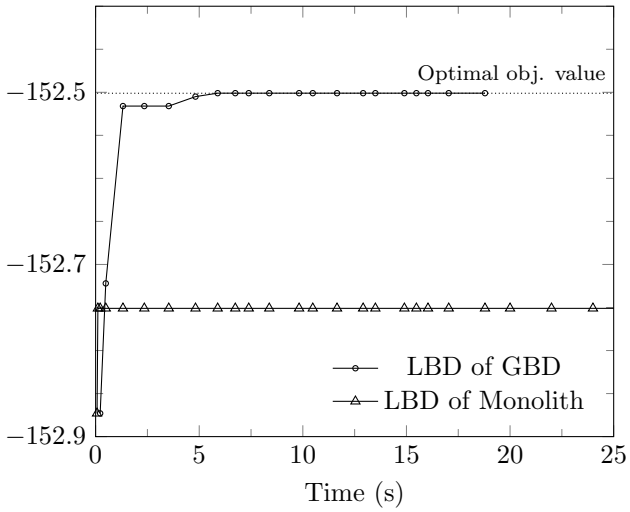

Figure 3.10: Comparison of lower bounds from GBD and the monolith approach

Production Network Structure Design Results

Here we compare the design results from Formulation (I) and Formulation (IV) in order to demonstrate the need for including pressure-flow relationship in the optimization model. Figure 3.11 and Figure 3.12 show the designed SGPS networks from using Formulation (IV) and Formulation (I), respectively. In the former design, gas

fields M3, M1 and JN containing 23 wells in total are developed to supply raw natural gas, while in the latter design only gas field M1 is developed. Although the latter design seems to be more economic as it includes fewer gas fields and platforms, the compressor on platform M1P cannot provide sufficient pressure rise in order to drive 2292 Mmol gas per day to the LNG plants (under the nominal scenario), in order to meet the product demands at the plants. This is the reason why in the former design, only about 1014 Mmol gas per day is planned to be generated from M1, and other raw gas is planned to be generated from M3 and JN.

3.6 Summary

This chapter studied a real industrial natural gas production system with necessary constraints that described gas flow compositions, pressures, and uncertainties. We took step by step model reformulations, analyzed structure of the final reformulated model, and proposed a multi-loop NGBD method to solve the resulted optimization problem. The advantage of proposed model was confirmed via comparing design result to the one obtained from the pooling model that only considered gas flows; and the advantage of proposed multi-loop NGBD method was supported by computational results that were generated from various model formulations and optimization methods.

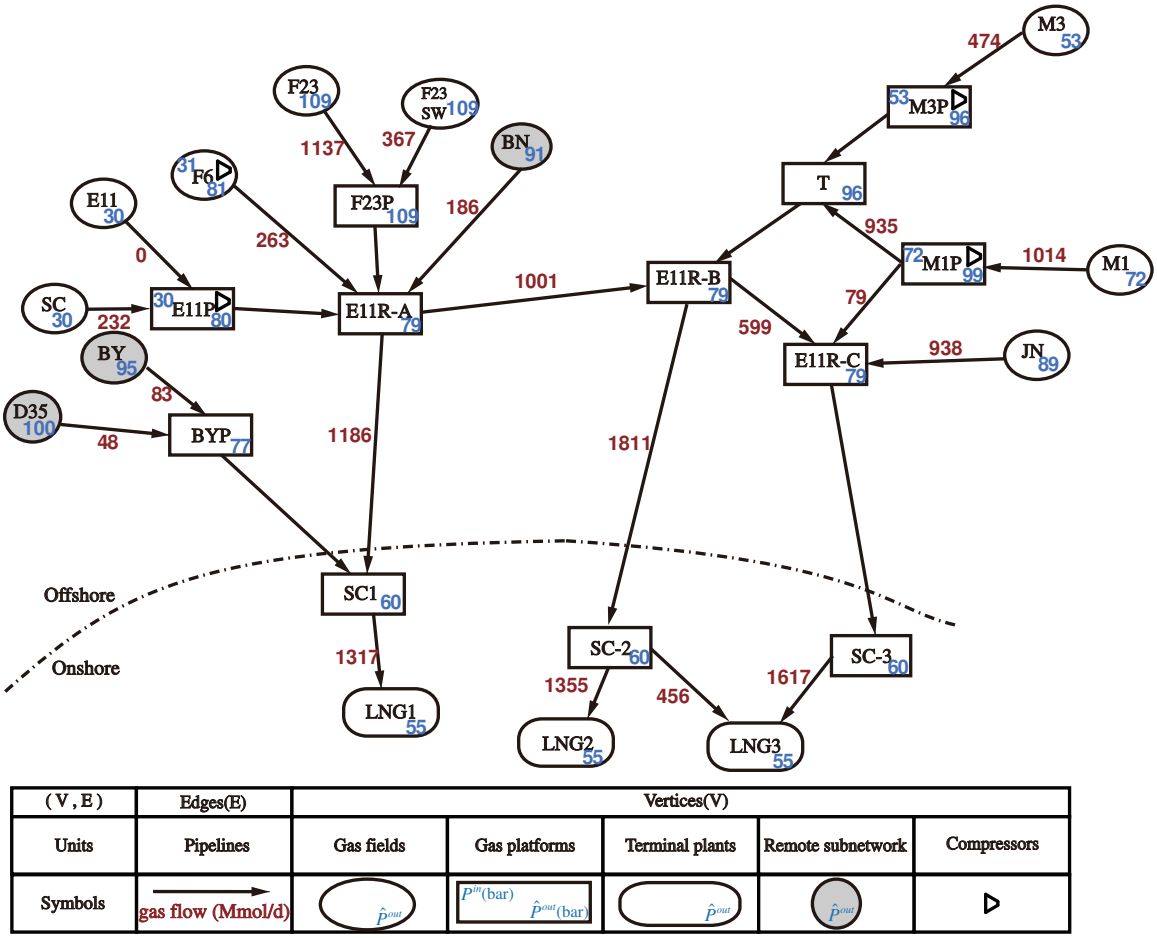

Note: The value near the each vertex is the optimal flow (Mmol/day) under the nominal scenario.

Figure 3.11: The design result with Formulation (IV) including 9 scenarios

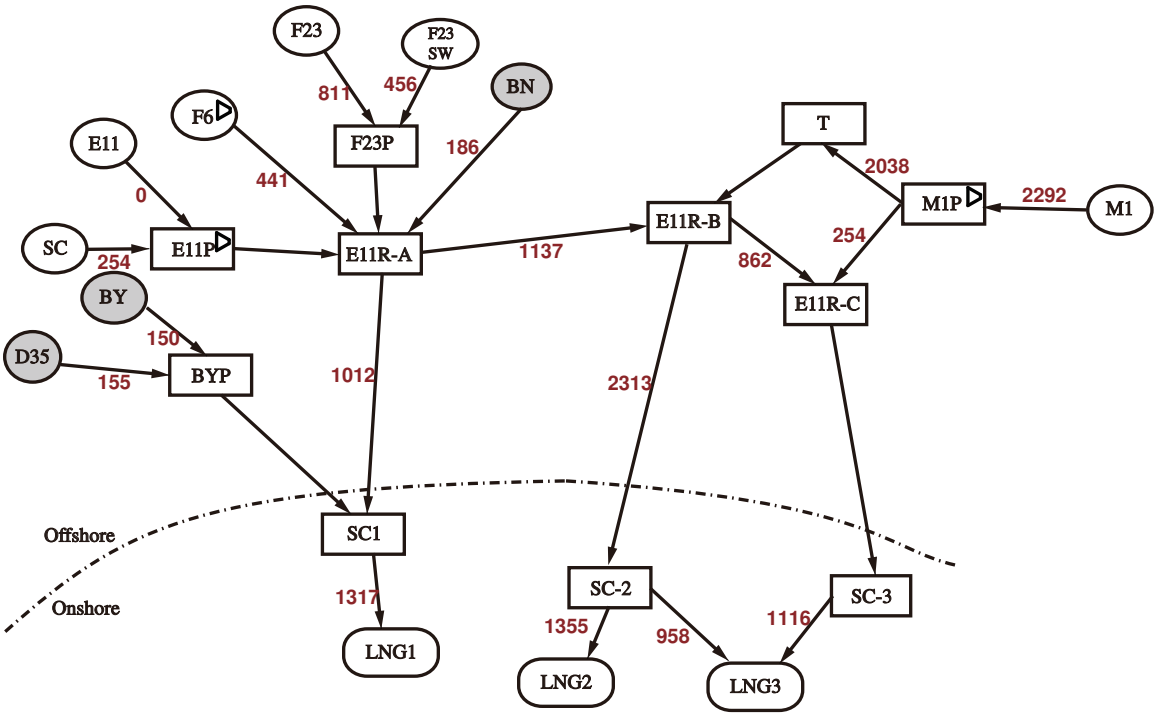

Note: The value near the each vertex is the optimal flow (Mmol/day) under the nominal scenario, and no compressor models are considered.

Figure 3.12: The design result with Formulation (I) including 9 scenarios

Chapter 4

Conclusions

Global optimization for mixed integer nonlinear programs has been applied widely to various engineering problems, ranging from product distribution, infrastructure design to process design and control [4, 13, 18, 36, 39]. Although employing global optimization for design and operation of large-scale energy systems is not uniformly successful, decomposition-based global optimization, fortunately, provides ways to exploit structures of known energy system models and therefore shows potential for efficient solutions. The main achievement of this thesis is the enhancement of Benders decomposition-based global optimization in a general sense, and the application of Benders decomposition-based optimization for representative nonconvex natural gas and power flow systems.

In Chapter 2, domain reduction is applied to two types of Benders decomposition-based global optimization that can solve integrated design and operation of energy system problems with form (P0) and mild assumptions. The first one is known as Generalized Benders Decomposition (GBD) [16], and this method assumes that the set X of Problem (P0) is convex. Then by projecting Problem (P0) on the y_0-space, dualizing and relaxing the projected problem, a sequence of monotone increasing

lower bounds of Problem (P0) is obtained and ϵ-convergence is ensured by strong duality that holds for Problem (P0) with fixed complicating variables. Another one is called Nonconvex Generalized Benders Decomposition (NGBD) [27], and it assumes that the set X is nonconvex, but the compact set Y is discrete. Although needed branch and bound framework for the small decomposed nonconvex problems, this method relies on implicit enumeration to achieve global optimality; and the convergence of the whole algorithm is guaranteed by finiteness of the set Y. Overall, it is the first attempt to develop a systematic framework that employs Domain Reduction to Benders decomposition-based global optimization methods in a general sense. The integration of domain reduction is achieved with specialized techniques, including (a). bound contraction operations in projected y_0-space, which is unique for Benders decomposition-based methods; (b). decomposable and cut enhanced bound contraction operations for convex relaxation tightening; and (c). range reduction calculations for nonconvex subproblems. The effective solutions of two large-scale energy systems demonstrate the advantages of the integration of domain reduction for Benders decomposition-based optimization methods.

In Chapter 3, a two-stage stochastic programming model is proposed for integrated design and operation of natural gas production systems under uncertainty, which describes the material balances for key gas components as well as the pressure flow relationships in gas wells, long and short pipelines, and compressors. This is the first time in the literature that this model is proposed and practically solved for gas production networks. Although the model is proposed for a typical industrial gas production system, most equations developed in this chapter are also valid for other gas production systems. While the importance of considering material balances for key

gas components has been demonstrated in the literature [26], the case study results in this chapter demonstrate the importance of including pressure flow relationships for achieving a realistic optimization result.

In order to solve the large-scale nonconvex MINLP from the proposed model, the model is reformulated in a number of steps such that the model becomes 'more convex' (i.e., the number of nonconvex constraints is reduced) and the convex and nonconvex parts are separable (which enables the application of GBD for operation subproblems). This reformulation is rigorous if a mild assumption on the compressor locations is satisfied, for the whole production network or for a subpart of it. This novel reformulation strategy should also be applicable to other types of networks where pressures play an important role (such as water networks), and it is interesting to generalize the proposed reformulation strategy to other networks in the future.

Since the reformulation allows the further decomposition of the operation subproblems, a variant of NGBD, called multi-loop NGBD method, is developed in this chapter for efficiently solving the proposed reformulated model to global optimality. In the multi-loop NGBD, each primal subproblem (which is an operation subproblem) is solved using GBD rather than using a global optimization solver directly, and it is faster than the standard single-loop NGBD by at least an order of magnitude. This is because each operation subproblem can be solved by GBD much more efficiently. This result indicates that, while GBD has been long considered as an efficient solution approach for multi-scenario problems, it can also be an efficient approach for one-scenario/deterministic optimization problems, such as deterministic optimal operation problems that are very common in chemical engineering practice. Successful application of GBD to a deterministic optimization problem may require

novel reformulation of the optimization model in order to achieve a decomposable structure.

Bibliography

[1] Egon Balas and Robert Jeroslow. Canonical cuts on the unit hypercube. *SIAM Journal on Applied Mathematics*, 23(1):61–69, 1972.

[2] Alberto Bemporad and Manfred Morari. Control of systems integrating logic, dynamics, and constraints. *Automatica*, 35(3):407 – 427, 1999.

[3] Jacques F Benders. Partitioning procedures for solving mixed-variables programming problems. *Numerische mathematik*, 4(1):238–252, 1962.

[4] Lorenz T Biegler and Ignacio E Grossmann. Retrospective on optimization. *Computers & Chemical Engineering*, 28(8):1169–1192, 2004.

[5] Stephen Boyd and Lieven Vandenberghe. *Convex optimization*. Cambridge university press, 2004.

[6] Claus C. Caroe and Rudiger Schultz. Dual decomposition in stochastic integer programming. *Operations Research Letters*, 24(1?2):37 – 45, 1999.

[7] Pedro M. Castro and Ignacio E. Grossmann. Optimality-based bound contraction with multiparametric disaggregation for the global optimization of mixed-integer bilinear problems. *Journal of Global Optimization*, 59(2):277–306, 2014.

[8] Arne Stolbjerg Drud. CONOPT—a large-scale GRG code. *ORSA Journal on Computing*, 6(2):207–216, 1994.

[9] M. Dür and R. Horst. Lagrange duality and partitioning techniques in non-convex global optimization. *Journal of Optimization Theory and Applications*, 95(2):347–369, 1997.

[10] Marco A Duran and Ignacio E Grossmann. An outer-approximation algorithm for a class of mixed-integer nonlinear programs. *Mathematical programming*, 36(3):307–339, 1986.

[11] Salako Abiodun Ebenezer and JS Gudmunsson. Removal of Carbon dioxide from natural gas for LPG production. *Semester project work*, 2005.

[12] M. L. Fisher. The Lagrangian relaxation method for solving integer programming problems. *Management Science*, 27:1–18, 1981.

[13] Christodoulos A Floudas. *Nonlinear and mixed-integer optimization: fundamentals and applications*. Oxford University Press on Demand, 1995.

[14] Stephen M Frank and Steffen Rebennack. Optimal design of mixed AC–DC distribution systems for commercial buildings: A nonconvex generalized Benders decomposition approach. *European Journal of Operational Research*, 242(3):710–729, 2015.

[15] A. M. Geoffrion. *Approaches to Integer Programming*, chapter Lagrangean relaxation for integer programming, pages 82–114. Springer Berlin Heidelberg, Berlin, Heidelberg, 1974.

[16] Arthur M Geoffrion. Generalized Benders decomposition. *Journal of optimization theory and applications*, 10(4):237–260, 1972.

[17] PE Gill, W Murray, and MA Saunders. SNOPT: an SQP algorithm for large-scale constrained optimization. *SIAM Review*, 47:99–131, 2005.

[18] Ignacio E Grossmann. Review of nonlinear mixed-integer and disjunctive programming techniques. *Optimization and engineering*, 3(3):227–252, 2002.

[19] Ignacio E Grossmann and Zdravko Kravanja. *Mixed-integer nonlinear programming: A survey of algorithms and applications*. Springer, 1997.

[20] Erlend Lunde Haugen. Alternative CO_2 removal solutions for the LNG process on an FPSO. 2011.

[21] John N Hooker and Greger Ottosson. Logic-based benders decomposition. *Mathematical Programming*, 96(1):33–60, 2003.

[22] IBM ILOG. V12. 1: Users manual for CPLEX. *International Business Machines Corporation*, 46(53):157, 2009.

[23] Paulina Jaramillo, W Michael Griffin, and H Scott Matthews. Comparative life cycle carbon emissions of LNG versus coal and gas for electricity generation, 2007.

[24] Ramkumar Karuppiah and Ignacio E Grossmann. A Lagrangean based branch-and-cut algorithm for global optimization of nonconvex mixed-integer nonlinear programs with decomposable structures. *Journal of global optimization*, 41(2):163–186, 2008.

[25] Dan Li and Xiang Li. A new optimization model and a customized solution method for natural gas production network design and operation. *AIChE Journal*, 2016. submitted.

[26] Xiang Li, Emre Armagan, Asgeir Tomasgard, and Paul I Barton. Stochastic pooling problem for natural gas production network design and operation under uncertainty. *AIChE Journal*, 57(8):2120–2135, 2011.

[27] Xiang Li, Asgeir Tomasgard, and Paul I Barton. Nonconvex generalized Benders decomposition for stochastic separable mixed-integer nonlinear programs. *Journal of optimization theory and applications*, 151(3):425–454, 2011.

[28] Miguel Sousa Lobo, Lieven Vandenberghe, Stephen Boyd, and Hervé Lebret. Applications of second-order cone programming. *Linear Algebra and its Applications*, 284(1):193 – 228, 1998. International Linear Algebra Society (ILAS) Symposium on Fast Algorithms for Control, Signals and Image Processing.

[29] Thomas L Magnanti and Richard T Wong. Accelerating Benders decomposition: Algorithmic enhancement and model selection criteria. *Operations research*, 29(3):464–484, 1981.

[30] Costas D. Maranas and Christodoulos A. Floudas. Global optimization in generalized geometric programming. *Computers & Chemical Engineering*, 21(4):351–369, 1997.

[31] Garth P McCormick. Computability of global solutions to factorable nonconvex programs: Part I: convex underestimating problems. *Mathematical programming*, 10(1):147–175, 1976.

[32] Ruth Misener and Christodoulos A Floudas. ANTIGONE: Algorithms for continuous/integer global optimization of nonlinear equations. *Journal of Global Optimization*, 59(2-3):503–526, 2014.

[33] A. Mitsos, B. Chachuat, and P. I. Barton. McCormick-based relaxations of algorithms. *SIAM Journal on Optimization*, 20(2):573–601, 2009.

[34] Saeid Mokhatab and William A Poe. *Handbook of natural gas transmission and processing*. Gulf Professional Publishing, 2012.

[35] Pierre Rabeau, Henri Paradowski, and Jocelyne Launois. How to reduce CO_2 emissions in the LNG chain. In *LNG15 International Conference*, 2007.

[36] Hong S Ryoo and Nikolaos V Sahinidis. Global optimization of nonconvex NLPs and MINLPs with applications in process design. *Computers & Chemical Engineering*, 19(5):551–566, 1995.

[37] Hong S Ryoo and Nikolaos V Sahinidis. A branch-and-reduce approach to global optimization. *Journal of Global Optimization*, 8(2):107–138, 1996.

[38] N. V. Sahinidis and M. Tawarmalani. *BARON 9.0.4: Global Optimization of Mixed-Integer Nonlinear Programs,* User's Manual, 2010.

[39] Nikolaos V Sahinidis. Optimization under uncertainty: state-of-the-art and opportunities. *Computers & Chemical Engineering*, 28(6):971–983, 2004.

[40] NV Sahinidis and Ignacio E Grossmann. Convergence properties of generalized benders decomposition. *Computers & Chemical Engineering*, 15(7):481–491, 1991.

[41] A. Selot, L. K. Kuok, M. Robinson, T. L. Mason, and P. I. Barton. A short-term operational planning model for natural gas production systems. *AIChE Journal*, 54(2):495–515, 2008.

[42] Mohit Tawarmalani and Nikolaos V Sahinidis. Global optimization of mixed-integer nonlinear programs: A theoretical and computational study. *Mathematical programming*, 99(3):563–591, 2004.

[43] Lakshman S Thakur. Domain contraction in nonlinear programming: minimizing a quadratic concave objective over a polyhedron. *Mathematics of Operations Research*, 16(2):390–407, 1991.

[44] Juan M Zamora and Ignacio E Grossmann. A branch and contract algorithm for problems with concave univariate, bilinear and linear fractional terms. *Journal of Global Optimization*, 14(3):217–249, 1999.

Appendix A

For Chapter 2

A.1 Reformulation from (P0) to (P1)

Introducing extra variables t_0, t_1 and t_2, and variable vectors t_3 and t_4, we reformulate Problem (P0) into the following one:

$$
\begin{aligned}
\min_{x,y_0,t_0,t_1,t_2,t_3,t_4} \ & t_0 \\
\text{s.t.} \ & t_3 + t_4 \leq 0, \\
& g_1(x) \leq t_3, \\
& g_2(y_0) \leq t_4, \\
& f_1(x) \leq t_1, \\
& f_2(y_0) \leq t_2, \\
& t_1 + t_2 \leq t_0, \\
& x \in X, \ \ y_0 \in Y,
\end{aligned}
\tag{$P0\_a$}
$$

Define new variable vectors $\hat{x} = (x, t_0, t_1, t_3)$ and $\hat{y}_0 = (y_0, t_2, t_4)$, then we can

rewrite Problem ($P0\_a$) into the form ($P0\_b$):

$$\begin{aligned} \min_{x,y_0,t_0,t_1,t_2,t_3,t_4} \quad & t_0 \\ \text{s.t.} \quad & t_3 + t_4 \leq 0, \\ & t_1 - t_0 + t_2 \leq 0, \\ & \hat{x} \in \bar{X}, \;\; \hat{y}_0 \in \bar{Y}, \end{aligned} \tag{$P0\_b$}$$

where $\bar{X} = \{\hat{x} = (x, t_0, t_1, t_3) \mid x \in X, f_1(x) \leq t_1, g_1(x) \leq t_3\}$ and $\bar{Y} = \{\hat{y}_0 = (y_0, t_2, t_4) \mid y_0 \in Y, f_2(y_0) \leq t_2, g_2(y_0) \leq t_4\}$.

Let set $\bar{X}$ be defined by a set of linear and nonlinear constraints of $\hat{x}$ as this:

$$\bar{X} = \{\hat{x} \in \Omega \subset \mathbb{R}^{n_{\hat{x}}} \mid \psi(\hat{x}) \leq 0, \; G\hat{x} \leq w\},$$

where $\psi : \Omega \to \mathbb{R}^{m_\psi}$ is a vector-valued function whose entries are all nonlinear functions of $\hat{x}$. Let $\bar{Y}$ be expressed using functions of $\hat{y}_0$,

$$\bar{Y} = \{\hat{y}_0 \in \Phi \subset \mathbb{R}^{n_{\hat{y}_0}} \mid \varphi(\hat{y}_0) \leq 0\},$$

where $\varphi : \Phi \to \mathbb{R}^{m_\varphi}$ is a vector-valued function that may include both linear and nonlinear functions of $\hat{y}_0$. If we explicitly express the linear constraints in $\bar{X}$ into the

problem, then Problem ($P0\_b$) can be expressed as:

$$\begin{aligned} \min_{x,y_0,t_0,t_1,t_2,t_3,t_4} \ & t_0 \\ \text{s.t.} \ & t_3 + t_4 \leq 0, \\ & t_1 - t_0 + t_2 \leq 0, \\ & G\hat{x} \leq w, \\ & \hat{x} \in \widetilde{X}, \ \ \hat{y}_0 \in \bar{Y}, \end{aligned} \tag{$P0\_c$}$$

where $\widetilde{X} = \{\hat{x} \in \Omega \subset \mathbb{R}^{n_{\hat{x}}} \mid \psi(\hat{x}) \leq 0\}$. We can further express the objective function and the first three linear constraints using $\hat{x}$ and $\hat{y}_0$, as:

$$\begin{aligned} \min_{\hat{x},\hat{y}_0} \ & c^T\hat{x} \\ \text{s.t.} \ & A\hat{x} + B\hat{y}_0 \leq d, \\ & \hat{x} \in \widetilde{X}, \ \ \hat{y}_0 \in \bar{Y}, \end{aligned} \tag{$P0\_d$}$$

where

$$c = \begin{pmatrix} 0 \\ 1 \\ 0 \\ 0 \end{pmatrix}, \quad A = \begin{pmatrix} 0 & 0 & 0 & I \\ 0 & -1 & 1 & 0 \\ & & G & \end{pmatrix}, \quad B = \begin{pmatrix} 0 & 0 & I \\ 0 & 1 & 0 \\ 0 & 0 & 0 \end{pmatrix}, \quad d = \begin{pmatrix} 0 \\ 0 \\ w \end{pmatrix}.$$

The sizes of the identity matrices I and zero matrices/vectors in c, A, B and d are conformable to the sizes of the relevant vectors. The form ($P0\_d$) is the same as Problem (P1) in the thesis.

A.2 Subproblems not provided in the main text

A.2.1 Feasibility relaxed master problem in GBD

For GBD and GBD with domain reduction, their feasibility relaxed master problems have the following form:

$$\begin{aligned} \min_{y_0} \quad & \sum_i y_{0,i} \\ \text{s.t.} \quad & 0 \geq obj_{\text{GBDFP}^{(j)}} - \left(\lambda^{(j)}\right)^T \left(y_0 - y_0^{(j)}\right), \quad \forall j \in S^k, \\ & y_0 \in Y^k. \end{aligned} \tag{FRMP^k}$$

A.2.2 GBD subproblems for standard NGBD

For standard NGBD, the GBD subproblems for solving lower bounding problem (LBP^k) are:

$$\begin{aligned} obj_{\text{GBDPP}_h}(y_0^{(k)}) = \min_{x_h, y_h, q_h} \quad & c_h^{\mathrm{T}} x_h \\ \text{s.t.} \quad & y_h - y_0^{(k)} = 0, \\ & \hat{A}_h x_h + \hat{B}_h y_h + \hat{F}_h q_h \leq \hat{d}_h, \\ & (x_h, q_h) \in \hat{X}_h. \end{aligned} \tag{GBDPP$_h^k$}$$

$$
\begin{aligned}
obj_{\mathrm{GBDFP}_h}(y_0^{(k)}) = \min_{x_h, y_h, q_h, \upsilon^+, \upsilon^-} \ & \left\| \upsilon^+ + \upsilon^- \right\| \\
\text{s.t.} \ & y_h - y_0^{(k)} = \upsilon^+ - \upsilon^-, \\
& \hat{A}_h x_h + \hat{B}_h y_h + \hat{F}_h q_h \leq \hat{d}_h, \\
& (x_h, q_h) \in \hat{X}_h, \ \ \upsilon^+, \ \upsilon^- \geq 0.
\end{aligned}
\tag{GBDFP$_h^k$}
$$

$$
\begin{aligned}
obj_{\mathrm{RMP}^k} = \min_{\eta, y_0} \ & \eta \\
\text{s.t.} \ & \eta \geq obj_{\mathrm{GBDPP}^{(j)}} - \left(\sum_{h=1}^{s} \lambda_h^{(j)} \right)^T \left(y_0 - y_0^{(j)} \right), \quad \forall j \in T^k, \\
& 0 \geq obj_{\mathrm{GBDFP}^{(j)}} - \left(\sum_{h=1}^{s} \lambda_h^{(j)} \right)^T \left(y_0 - y_0^{(j)} \right), \quad \forall j \in S^k, \\
& \sum_{i \in I_1^j} y_{0,i} - \sum_{i \in I_0^j} y_{0,i} \leq |I_1^j| - 1, \ \ \forall j \in R^k \\
& y_0 \in Y.
\end{aligned}
\tag{RMP^k}
$$

$$
\begin{aligned}
\min_{y_0} \ & \sum_i y_{0,i} \\
\text{s.t.} \ & 0 \geq obj_{\mathrm{GBDFP}^{(j)}} - \left(\sum_{h=1}^{s} \lambda_h^{(j)} \right)^T \left(y_0 - y_0^{(j)} \right), \quad \forall j \in S^k, \\
& \sum_{i \in I_1^j} y_{0,i} - \sum_{i \in I_0^j} y_{0,i} \leq |I_1^j| - 1, \ \ \forall j \in R^k \\
& y_0 \in Y.
\end{aligned}
\tag{FRMP^k}
$$

A.2.3 GBD subproblems for NGBD with domain reduction

For the NGBD with domain reduction, the GBD subproblems for solving lower bounding problem ($\mathrm{LBP}^{r,k,l}$) are:

$$
\begin{aligned}
obj_{\mathrm{GBDPP}_h}(y_0^{(k)}) = \min_{x_h, y_h, q_h} \ & c_h^{\mathrm{T}} x_h \\
\text{s.t.} \ & y_h - y_0^{(k)} = 0, \\
& \hat{A}_h^r x_h + \hat{B}_h y_h + \hat{F}_h^r q_h \leq \hat{d}_h^r, \\
& (x_h, q_h) \in \hat{X}_h^r.
\end{aligned}
\tag{$\mathrm{GBDPP}_h^{k,r}$}
$$

$$
\begin{aligned}
obj_{\mathrm{GBDFP}_h}(y_0^{(k)}) = \min_{x_h, y_h, q_h, \upsilon^+, \upsilon^-} \ & \left\| \upsilon^+ + \upsilon^- \right\| \\
\text{s.t.} \ & y_h - y_0^{(k)} = \upsilon^+ - \upsilon^-, \\
& \hat{A}_h^r x_h + \hat{B}_h y_h + \hat{F}_h^r q_h \leq \hat{d}_h^r, \\
& (x_h, q_h) \in \hat{X}_h^r, \ \ \upsilon^+, \ \upsilon^- \geq 0.
\end{aligned}
\tag{$\mathrm{GBDFP}_h^{k,r}$}
$$

$$
\begin{aligned}
obj_{\mathrm{RMP}^{k,r,l}} = \min_{\eta, y_0} \quad & \eta \\
\text{s.t.} \quad & \eta \geq obj_{\mathrm{GBDPP}^{(j)}} - \left(\sum_{h=1}^{s} \lambda_h^{(j)}\right)^T \left(y_0 - y_0^{(j)}\right), \quad \forall j \in T^k, \\
& 0 \geq obj_{\mathrm{GBDFP}^{(j)}} - \left(\sum_{h=1}^{s} \lambda_h^{(j)}\right)^T \left(y_0 - y_0^{(j)}\right), \quad \forall j \in S^k, \\
& y_0 \in Y^r, \\
& \sum_{i \in I_1^j} y_{0,i} - \sum_{i \in I_0^j} y_{0,i} \leq |I_1^j| - 1, \ \ \forall j \in R^{k,r} \cup U^l.
\end{aligned}
\tag{RMP^{k,r,l}}
$$

$$
\begin{aligned}
\min_{y_0} \quad & \sum_i y_{0,i} \\
\text{s.t.} \quad & 0 \geq obj_{\mathrm{GBDFP}^{(j)}} - \left(\sum_{h=1}^{s} \lambda_h^{(j)}\right)^T \left(y_0 - y_0^{(j)}\right), \quad \forall j \in S^k, \\
& y_0 \in Y^r, \\
& \sum_{i \in I_1^j} y_{0,i} - \sum_{i \in I_0^j} y_{0,i} \leq |I_1^j| - 1, \ \ \forall j \in R^{k,r} \cup U^l.
\end{aligned}
\tag{FRMP^{k,r,l}}
$$

Appendix B

For Chapter 3

B.1 Set Definitions for SGPS

This section presents the vertex and edge sets used in the case study, and the elements of these sets.

Table B.1: Set Definitions for SGPS

Definition		
Set	Super Set	Elements
V	-	D35, BY, SC, E11, F6, F23SW, F23, BN, B11, HL, SE, M3, M4, M1, JN, BYP, E11P, F23P, B11P, M3P, M1P, Tpool , E11RA, E11RB, E11RC, SC1, SC2, SC3, LNG1, LNG2, LNG3, B11A, B11B, B11C, B11D, E11A, E11B, E11C, E11D, E11E, E11F, E11G, E11H, E11I, E11J, F23A, F23B, F23C, F23D, F23E, F23F, F23G, F23H, F23I, F23J, F23K, F23L, F23M, F23N, F23SWW, F6A, F6B, F6C, F6D, F6E, F6F, F6G, F6H, F6I, F6J, F6K, F6L, F6M, M1A, M1B, M1C, M1D, M1E, M1F, M1G, M1H, M3A, M3B, M3C, M3D, M3E, M3F, M3G, M3H, M3I, M3J, SCA, SCB, JNA, JNB, JNC, JND, JNE, M4A, M4B, SEA, SEB
$\bar{V}$	V	SC, E11, B11, HL, SE, M3, M4, M1, JN, B11A, B11B, B11C, B11D, E11A, E11B, E11C, E11D, E11E, E11F, E11G, E11H, E11I, E11J, F6A, F6B, F6C, F6D, F6E, F6F, F6G, F6H, F6I, F6J, F6K, F6L, F6M, M1A, M1B, M1C, M1D, M1E, M1F, M1G, M1H, M3A, M3B, M3C, M3D, M3E, M3F, M3G, M3H, M3I, M3J, SCA, SCB, JNA, JNB, JNC, JND, JNE, M4A, M4B, SEA, SEB
V^C	V	F6, M3P, B11P, M1P, E11P
V^S	V	D35, BY,BN, HL
V^T	V	LNG1, LNG2, LNG3

Definition		
Set	Super Set	Elements
V^W	V	B11A, B11B, B11C, B11D, E11A, E11B, E11C, E11D, E11E, E11F, E11G, E11H, E11I, E11J, F23A, F23B, F23C, F23D, F23E, F23F, F23G, F23H, F23I, F23J, F23K, F23L, F23M, F23N, F23SWW, F6A, F6B, F6C, F6D, F6E, F6F, F6G, F6H, F6I, F6J, F6K, F6L, F6M, M1A, M1B, M1C, M1D, M1E, M1F, M1G, M1H, M3A, M3B, M3C, M3D, M3E, M3F, M3G, M3H, M3I, M3J, SCA, SCB, JNA, JNB, JNC, JND, JNE, M4A, M4B, SEA, SEB

Definition		
Set	Super Set	Elements
E	-	(B11A,B11), (B11B,B11), (B11C,B11), (B11D,B11), (E11A,E11), (E11B,E11), (E11C,E11), (E11D,E11), (E11E,E11), (E11F,E11), (E11G,E11), (E11H,E11), (E11I,E11), (E11J,E11), (F23A,F23), (F23B,F23), (F23C,F23), (F23D,F23), (F23E,F23), (F23F,F23), (F23G,F23), (F23H,F23), (F23I,F23), (F23J,F23), (F23K,F23), (F23L,F23), (F23M,F23), (F23N,F23), (F23SWW,F23SW), (F6A,F6), (F6B,F6), (F6C,F6), (F6D,F6), (F6E,F6), (F6F,F6), (F6G,F6), (F6H,F6), (F6I,F6), (F6J,F6), (F6K,F6), (F6L,F6), (F6M,F6), (M1A,M1), (M1B,M1), (M1C,M1), (M1D,M1), (M1E,M1), (M1F,M1), (M1G,M1), (M1H,M1), (M3A,M3), (M3B,M3), (M3C,M3), (M3D,M3), (M3E,M3), (M3F,M3), (M3G,M3), (M3H,M3), (M3I,M3), (M3J,M3), (SCA,SC), (SCB,SC), (JNA,JN), (JNB,JN), (JNC,JN), (JND,JN), (JNE,JN), (M4A,M4), (M4B,M4), (SEA,SE), (SEB,SE), (D35,BYP), (BY,BYP), (SC,E11P), (E11,E11P), (F6,E11RA), (F23SW,F23P), (F23,F23P), (BN,E11RA), (B11,B11P), (HL,B11P), (HL,E11RB), (SE,M3P), (M3,M3P), (M4,M3P), (M1,M1P), (JN,M1P), (JN,E11RC), (BYP,SC1), (E11P,E11RA), (F23P,E11RA), (B11P,E11RB), (M3P,Tpool), (M1P,Tpool), (M1P,E11RC), (Tpool,E11RB), (E11RA,SC1), (E11RA,E11RB), (E11RB,SC2), (E11RB,E11RC), (E11RC,SC3), (SC1,LNG1), (SC2,LNG2), (SC2,LNG3), (SC3,LNG3)

Definition		
Set	Super Set	Elements
E^L	E	(D35,BYP), (BN,E11RA), (HL,B11P), (F6,E11RA), (F23P,E11RA), (B11P,E11RB), (BYP,SC1), (M3P,Tpool), (M1P,Tpool), (Tpool,E11RB), (JN,M1P), (JN,E11RC), (M1P,E11RC), (E11RA,SC1), (E11RB,SC2), (E11RC,SC3)
E^W	E	(B11A,B11), (B11B,B11), (B11C,B11), (B11D,B11), (E11A,E11), (E11B,E11), (E11C,E11), (E11D,E11), (E11E,E11), (E11F,E11), (E11G,E11), (E11H,E11), (E11I,E11), (E11J,E11), (F23A,F23), (F23B,F23), (F23C,F23), (F23D,F23), (F23E,F23), (F23F,F23), (F23G,F23), (F23H,F23), (F23I,F23), (F23J,F23), (F23K,F23), (F23L,F23), (F23M,F23), (F23N,F23), (F23SWW,F23SW), (F6A,F6), (F6B,F6), (F6C,F6), (F6D,F6), (F6E,F6), (F6F,F6), (F6G,F6), (F6H,F6), (F6I,F6), (F6J,F6), (F6K,F6), (F6L,F6), (F6M,F6), (M1A,M1), (M1B,M1), (M1C,M1), (M1D,M1), (M1E,M1), (M1F,M1), (M1G,M1), (M1H,M1), (M3A,M3), (M3B,M3), (M3C,M3), (M3D,M3), (M3E,M3), (M3F,M3), (M3G,M3), (M3H,M3), (M3I,M3), (M3J,M3), (SCA,SC), (SCB,SC), (JNA,JN), (JNB,JN), (JNC,JN), (JND,JN), (JNE,JN), (M4A,M4), (M4B,M4), (SEA,SE), (SEB,SE)
Ω	-	CO_2, H_2S, Other gas components (primarily methane)

Definition		
Set	Super Set	Elements
Φ	-	1, 2, ..., s

B.2 Parameters

B.2.1 Parameters from [41]

Table B.2: CO_2 and H_2S contents at each gas field (U)

Gas fields	CO_2 (mol fraction)	H_2S (mol fraction)
D35	0.72%	0
BY	0.88%	0
SC	0.27%	0
E11	9.23%	1.5e-3%
F6	3.41%	3.8e-3%
F23SW	0.68%	1.0e-3%
F23	1.64%	0.4e-3%
BN	1.45%	0
B11	8.85%	5.2e-2%
HL	1.59%	0
SE	2.43%	0.6e-3%
M3	0.95%	3.6e-3%
M4	2.3%	4.8e-3%
M1	5.04%	3.3e-3%
JN	2.64%	0.3e-3%

Table B.3: Parameters for long pipeline performance

direct edges	$\kappa_{i,j}(bar^2 day^2/hm^6)$
(E11RA, SC1)	2.46
(E11RB, SC2)	6.1
(E11RB, SC3)	7.65
(F6, E11RA	5.33
(F23P, E11RA)	4.4
(B11P, E11RB)	12.78
(HL, B11P)	35.58
(D35, BYP)	3062.62
(BN, E11RA)	97.51
(BYP, SC1)	254.77
(M3P, T)	0.39
(M1P, T)	1.17
(M1P, E11RC)	21.84
(T, E11RB)	2.59
(JN, E11RC)	3.17
(JN, M1P)	3.17

Table B.4: Bounds of outlet pressures (Γ)

Vertex	UB (bar)	LB (bar)
D35	100	1
BY	95	1
SC	165	1
E11	187	1
F6	150	1
F23SW	273	1
F23	273	1
BN	120	1
B11	83	1
HL	150	1
SE	169	1
M3	84	1
M4	84	1
M1	125	1
JN	157	1
BYP	95	1
E11P	187	1
F23P	273	1
B11P	83	1
M3P	150	1
M1P	125	1
Tpool	150	1
E11RA	110	1
E11RB	110	1
E11RC	110	1
SC1	70	60
SC2	70	60
SC3	70	60
LNG1	70	50
LNG2	70	50
LNG3	70	50

Table B.5: Bounds of inlet pressures† for platforms (Γ)

Vertex	UB (bar)	LB (bar)
F6	50	1
B11P	83	20
M3P	169	30
M1P	125	1
E11P	187	1

† If not specified, bounds of inlet and outlet pressures are identical.

Table B.6: Bounds of compressor power (Φ)

Vertex	UB ($MW \cdot day$)	LB ($MW \cdot day$)
F6	22	0.01
B11P	27	0.01
M3P	27	0.01
M1P	20	0.01
E11P	22	0.01

Table B.7: Parameters for each well vertex

$Well_i$	$\pi_i(bar)$	$\alpha_i(bar^2day^2/hm^6)$	$\beta_i(bar^2d^2/hm^6)$	λ_i	$\vartheta_i(bar^2day^2/hm^6)$
B11A	75.39	0.02163	0.00056	3.534	728.5
B11B	78.46	0.02287	0.00056	3.204	678.7
B11C	78.62	0.02266	0.00052	3.628	666.8
B11D	71.45	0.02045	0.00052	3.568	798.7
E11A	54.74	0.616	9.3E-05	2.555	3410
E11B	56.68	0.663	9.9E-05	2.78	3558
E11C	60.05	0.6074	9.1E-05	2.706	3700
E11D	52.69	0.6701	9.8E-05	2.595	3340
E11E	56.15	0.6241	8.9E-05	2.433	3320
E11F	56.5	0.596	9.1E-05	2.525	3255
E11G	48.89	0.5831	9.2E-05	2.603	3661
E11H	59.71	0.6503	9.7E-05	2.648	3567
E11I	56.77	0.6153	8.7E-05	2.558	3224
E11J	54.47	0.6661	8.8E-05	2.362	3745
F23A	247.67	1.591	2.4E-06	1.576	496.2
F23B	231.76	1.658	2.2E-06	1.455	465.3

$Well_i$	$\pi_i(bar)$	$\alpha_i(bar^2day^2/hm^6)$	$\beta_i(bar^2day^2/hm^6)$	λ_i	$\vartheta_i(bar^2day^2/hm^6)$
F23C	266.73	1.603	2.5E-06	1.488	51.12
F23D	227.98	1.72	2.2E-06	1.444	485.4
F23E	244.14	1.521	2.2E-06	1.568	460.7
F23F	245.95	1.522	2.5E-06	1.712	523.6
F23G	265.48	1.54	2.6E-06	1.493	495.3
F23H	226.21	1.735	2.2E-06	1.555	497.1
F23I	271.81	1.699	2.1E-06	1.432	448.5
F23J	252.13	1.703	2.5E-06	1.428	488.8
F23K	235.67	1.734	2.6E-06	1.502	498.1
F23L	266.15	1.543	2.3E-06	1.701	453.6
F23M	252.16	1.515	2.2E-06	1.441	491.5
F23N	264.42	1.633	2.1E-06	1.723	483.3
F23SWW	239.26	1.645	2.4E-06	1.688	489.5
F6A	44.81	0.03673	0.0009	1.613	604.9
F6B	47.11	0.03397	0.00082	1.527	599.3
F6C	41.81	0.03781	0.00098	1.553	570.8
F6D	44.95	0.03344	0.00096	1.654	606.6
F6E	40.47	0.03578	0.00098	1.558	583.5
F6F	40.83	0.04016	0.00082	1.691	646.7
F6G	43.24	0.0377	0.00085	1.622	592.6
F6H	47.84	0.03612	0.00084	1.496	555.3
F6I	46.02	0.03444	0.00095	1.486	663.7
F6J	47.91	0.03644	0.00089	1.627	639.9
F6K	44.49	0.03742	0.00096	1.578	619.5
F6L	44.19	0.0339	0.00091	1.703	588.9

$Well_i$	$\pi_i(bar)$	$\alpha_i(bar^2day^2/hm^6)$	$\beta_i(bar^2day^2/hm^6)$	λ_i	$\vartheta_i(bar^2day^2/hm^6)$
F6M	45.43	0.03568	0.00084	1.676	566.6
M1A	113.51	0.1258	0.00255	1.868	158
M1B	113.81	0.1356	0.00265	1.974	147.6
M1C	102.24	0.1378	0.00269	2.013	172.9
M1D	121.17	0.1303	0.00266	1.761	172.7
M1E	109.27	0.1292	0.00236	1.942	148.3
M1F	107.6	8.472	0.00251	1.78	159.8
M1G	111.87	8.484	0.0025	1.695	161.7
M1H	105.22	8.608	0.00233	1.926	156.6
M3A	69.33	8.948	0.00034	1.482	1090
M3B	82.08	8.026	0.00037	1.621	1215
M3C	78.36	7.784	0.00035	1.539	1048
M3D	73.13	8.51	0.00037	1.53	1076
M3E	79.77	8.074	0.00032	1.642	1209
M3F	80.46	0.1888	0.00038	1.446	1160
M3G	82.3	0.1662	0.00035	1.663	1056
M3H	76.71	0.1816	0.00036	1.617	1193
M3I	79.49	0.1657	0.00034	1.621	1033
M3J	72.1	0.1627	0.00035	1.673	1148
SCA	142.3	0.1818	0.00682	3.638	2285
SCB	146.68	0.1825	0.00702	3.577	2345
JNA	142.21	0.1749	1.50E-07	0.724	780.7
JNB	150.05	0.1824	1.47E-07	0.696	751.8
JNC	145.96	0.1577	1.5E-07	0.684	785.3
JND	129.31	0.1724	1.38E-07	0.729	754.8

$Well_i$	$\pi_i(bar)$	$\alpha_i(bar^2day^2/hm^6)$	$\beta_i(bar^2day^2/hm^6)$	λ_i	$\vartheta_i(bar^2day^2/hm^6)$
JNE	152.84	0.1753	1.42E-07	0.773	732.9
M4A	75.69	0.9924	0.00035	1.573	1143
M4B	81.38	1.054	0.00033	1.484	1219
SEA	153.4	1.05	0.0043	3.515	385.3
SEB	141.22	1.154	0.00457	3.813	384.5

B.2.2 Other parameters used in the thesis

Table B.8: Investment costs for platforms and pipelines ($C^{(v,CC)}$, $C^{(CC)}$)

Unit†	Cost ($Million$\$)
B11	20
HL	520
SE	20
M3	100
M4	20
M1	80
JN	550
B11P	500
M3P	500
M1P	500
E11RB	500
E11RC	500
LNG1	7500
LNG2	9300
(HL, B11P)	80
(B11P, E11RB)	320
(HL, E11RB)	400
(SE, M3P)	16
(M4, M3P)	50
(JN, M1P)	80
(M3P, T)	40
(M1P, T)	40
(T, E11RB)	200
(E11RB, E11RC)	10
(E11RB, SC2)	600
(E11RC, SC2)	420

† If not specified, the investment costs of vertices and edges are negligible.

Table B.9: CO_2 and H_2S percentage upper bounds† at the LNG plants (K^{UB})

Plant	CO_2 (mol fraction)	H_2S (mol fraction)
LNG1	2.8%	0.020%
LNG2	2.8%	0.020%
LNG3	2.8%	0.020%

† The lower bounds of CO_2 and H_2S are all zero.

Table B.10: Power cost

γ	0.0023 ($Million\$/MW \cdot day$)

Table B.11: Bounds of molar flow rate (F, D, Z)

Vertex or edges	UB $(Mmol/day)$	LB $(Mmol/day)$
D35	156	48
BY	150	48
SC	254	0
E11	400	0
F6	997	0
F23SW	456	0
F23	6717	0
BN	186	60
B11	480	0
HL	718	0
SE	637	0
M3	977	0
M4	193	0
M1	2954	0
JN	1105	0
LNG1	1317	838
LNG2	1355	718
LNG3	2074	958
(D35,BYP)	156	48
(BY,BYP)	150	48
(SC,E11P)	254	0
(E11,E11P)	400	0

Vertex or edges	UB ($Mmol/day$)	LB ($Mmol/day$)
(F6,E11R-A)	997	0
(F23,F23P)	1137	0
(F23SW,F23P)	456	0
(BN,E11R-A)	186	60
(HL,B11P)	718	0
(HL,E11R-B)	718	0
(B11,B11P)	480	0
(SE,M3P)	637	0
(M3,M3P)	977	0
(M4,M3P)	193	0
(M1,M1P)	2954	0
(JN,M1P)	1078	0
(JN,E11R-C)	1078	0
(BYP,SC-1)	305	48
(E11P,E11R-A)	654	0
(F23P,E11R-A)	1593	0
(E11R-A,SC-1)	1676	0
(E11R-A,E11R-B)	1137	0
(B11P,E11R-B)	718	0
(M3P,T)	1807	0
(M1P,T)	2634	599
(M1P,E11R-C)	1078	0
(T,E11R-B)	2634	0
(E11R-B,E11R-C)	862	0
(E11R-B,SC-2)	3592	0

Vertex or edges	UB ($Mmol/day$)	LB ($Mmol/day$)
(SC-1,LNG1)	1676	0
(SC-2,LNG2)	2634	0
(SC-2,LNG3)	958	0
(SC-3,LNG3)	2155	0